HEMERYTHRIN. STRUCTURAL DETAILS FROM SPECTROSCOPIC ANALYSES

Andrew Kurt Shiemke
B.A., Kalamazoo College, 1980

A dissertation submitted to the faculty
of the Oregon Graduate Center
in partial fulfillment of the
requirements for the degree
Doctor of Philosophy
in
Chemistry

December, 1985

The dissertation "Hemerythrin. Structural Details from Spectroscopic Analyses" by Andrew Kurt Shiemke has been examined and approved by the following Examination Committee:

[redacted]
Thomas M. Loehr, Thesis Advisor
Professor

[redacted]
Joann Sanders-Loehr
Professor

[redacted]
Michael H. Gold
Professor

[redacted]
Research Assistant Professor
Department of Biological Structure
University of Washington

"Would you tell me, please, which way I ought to go from here?"

"That depends a good deal on where you want to get to," said the Cat.

"I don't much care where ---" said Alice

"Then it doesn't matter which way you go", said the Cat.

"--- so long as I get somewhere," Alice added as an explanation.

"Oh, you're sure to do that," said the Cat, "if you only walk long enough."

Lewis Carroll, "Alice's Adventures in Wonderland", 1887.

"... at the earlier stages of life we think we know everything - or to put it more usefully, we are often unaware of the scope and structure of our ignorance. Ignorance is not just a blank space on a person's mental map. It has contours and coherence, and for all I know rules of operation as well. So as a corollary to writing about what we know, maybe we should add getting familiar with our ignorance."

Thomas Pynchon, "Slow Learner", 1984

ACKNOWLEDGEMENT

I've heard it said that anyone can excel in the proper environment. Although this may be an exaggeration, upon hearing it one is compelled to consider that success is more than the manifestation of one individuals talents. In this instance I'm certain that the environment in which I have lived and worked these last four-plus years has contributed greatly to any success I've experienced. I must thank Thomas Loehr and Joann Sanders-Loehr for providing the stimulating and rewarding environment in which I've worked. I have had the freedom to experiment and learn on my own in addition to the guidance necessary to extract as much from this experience as possible. I consider myself lucky to have known and worked with such fine people as my two preceptors.

I would also like to thank my parents for the atmosphere of objective, intellectual inquiry which pervades their home. I have benefitted greatly from it. Without this enlightened upbringing I doubt that I would have had the ambition to even begin this journey.

And I thank my wife, Kim. Her confidence in my abilities never wavered; her heartwarming nature has overcome my despair on many occasions.

TABLE OF CONTENTS

LIST OF TABLES

LIST OF FIGURES

ABSTRACT

HEMERYTHRIN. STRUCTURAL DETAILS FROM SPECTROSCOPIC ANALYSES.

Andrew Kurt Shiemke, Ph.D.

Oregon Graduate Center, 1985

Supervising Professor: Thomas M. Loehr

The binuclear active site of hemerythrin consists of octahedral iron atoms bridged by an oxo group (O^{2-}). The vibrations of this Fe-O-Fe unit dominate the resonance Raman spectra of most forms of hemerythrin. From the analysis of such spectra, details of the binding site structure of oxy, hydroxomet and methemerythrin have been revealed.

The bound O_2 group of oxyhemerythrin is identified as a hydroperoxide based on shifts of the O-O and Fe-O_2 stretching vibrations in D_2O and $^{18}O_2$. Our discovery of the Fe-O-Fe vibrations of oxyhemerythrin permit the conclusion that the hydroperoxide is bound end-on to a single iron of the binuclear cluster. Deuterium exchange also affects the ν_s(Fe-O-Fe) vibration of oxyhemerythrin, causing a shift from 486 cm^{-1} in H_2O to 490 cm^{-1} in D_2O. The deuterium effect on ν_s(Fe-O-Fe) is unique to oxyhemerythrin and leads to the proposal of an intramolecular hydrogen bond between the oxo bridge and the hydroperoxide ligand. The low frequency of the oxyhemerythrin ν_s(Fe-O-Fe) vibration (486 cm^{-1}) relative to those of the methemerythrins (506-516 cm^{-1}) is also attributed to this hydrogen bond interaction.

In the resonance Raman spectrum of hydroxomethemerythrin two peaks at 492 and 506 cm^{-1} shift to 478 and 491 cm^{-1}, respectively, upon ^{18}O substitution of the bridge, identifying both as ν_s(Fe-O-Fe) vibrations, and indicating the existence of two distinct conformations of the metal center. The low frequency of the 492 cm^{-1} Fe-O-Fe vibration is attributed to an intramolecular hydrogen bond between the oxo bridge and the hydroxide ligand in the cis conformation. The 506 cm^{-1} ν_s(Fe-O-Fe) mode is attributed to the trans conformation which lacks this hydrogen bond. This proposal is supported by the observation of a temperature-dependent equilibrium between the two conformations. The change in concentration can be monitored by the redistribution of intensity between the two ν_s(Fe-O-Fe) modes with the cis species becoming the dominant form as the temperature is reduced. A linear van't Hoff plot over the range 310 to 90 K yields a $\Delta H°$ of -0.4 kcal/mole for the hydrogen bond.

A temperature-dependent effect on the Raman spectrum of unligated methemerythrin is also observed. Below 200 K, a second ν_s(Fe-O-Fe) mode at 490 cm^{-1}, is observed in addition to the 510 cm^{-1} mode, indicating that the metal center may adopt two conformations. The equilibrium between these two conformations is not linear with temperature and is thus attributed to a change in protein conformation which affects the geometry of the ligand binding iron. Our observation of two active site geometries correlates well with a number of reactions of methemerythrin which depend on a change in protein conformation.

CHAPTER I

The Resonance Raman Spectroscopy of Hemerythrin.

An Overview.

To be Published as "Non-Heme Respiratory Proteins".

by Andrew K. Shiemke and Thomas M. Loehr,

Chapter 3, Volume IV of Biological Applications of Raman Spectroscopy,

T. G. Spiro, Ed., in Press 1986

INTRODUCTION

All aerobic organisms utilize oxygen and many of them require respiratory proteins to carry out the binding, transport and storage of O_2. Respiratory proteins can be divided into three classes based on the diverse nature of their oxygen binding sites: hemoglobin, hemerythrin and hemocyanin. The most ubiquitous and most extensively studied are hemoglobin and myoglobin which use a heme prosthetic group (Fe protoporphyrin IX) to bind molecular oxygen. In the non-heme respiratory proteins, hemerythrin and hemocyanin, this function is performed by binuclear iron and copper centers, respectively. The different methods of oxygen binding employed by these respiratory proteins seem well adapted to the living conditions of the organisms in which they are found. Since the hemoglobins and hemocyanins occur in animals which range over large areas, the need to respond to changing external conditions is crucial. Oxygen binding in these proteins is under both homotropic and heterotropic allosteric control.[1,2] Such controls also enable these proteins to respond to the various requirements of different internal tissues, an important factor in their O_2 transport function. The hemerythrins, on the other hand, are found in sedentary creatures and in most cases have neither homotropic nor (natural) heterotropic effectors. The animals which use hemerythrin are generally less advanced than those using hemoglobin or hemocyanin, having a minimal vascular system. Thus hemerythrin acts principally to store molecular oxygen, a function to which it is well suited given the high thermodynamic stability of its oxygen adduct.[3]

For all respiratory proteins, oxygen binding is an oxidative addition process that consists of electron transfer from a reduced metal center in the deoxy form of the protein to the dioxygen molecule in the oxygenated form. In hemoglobin and myoglobin, a single electron is transferred from the ferrous heme with the result that oxygen is bound as superoxide (Equation 1).[1]

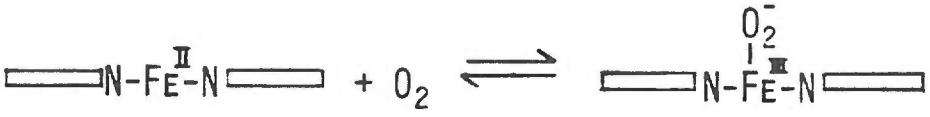

(1)

In both of the non-heme respiratory proteins, the metal ions of the binuclear center act jointly, transferring two electrons thus allowing oxygen to bind as peroxide (Equations 2,3).[2,3]

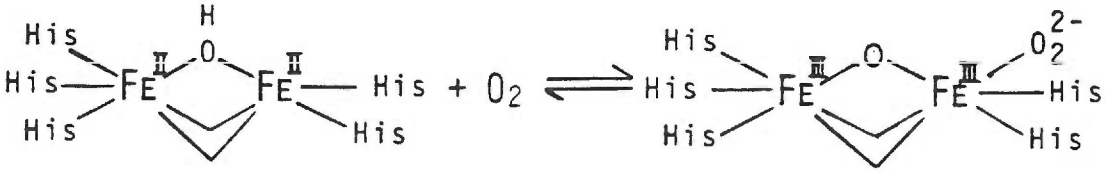

(2)

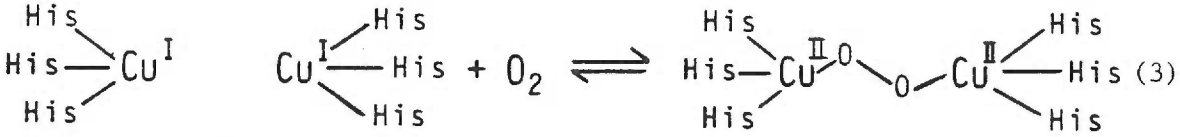

(3)

While colorless in the deoxy state, oxygenation of hemerythrin and hemocyanin causes a dramatic color change to red and blue, respectively. The electronic transitions which are responsible for the color of these proteins also effectively enhance Raman spectra of their binding sites. Resonance Raman spectroscopy of the non-heme respiratory proteins has

been very successful in elucidating the state of the bound dioxygen and its manner of binding. Information on the interaction between the metal centers and other ligands of these proteins has also been forthcoming through this technique. This contrasts with the resonance Raman spectra of the hemoglobins which yield much information on the porphyrin ring but relatively little direct information on metal-ligand interactions.[4]

HEMERYTHRIN

Hemerythrin is found in sipunculids, annelids, priapulids, and brachiopods. The basic protein unit is a single polypeptide chain with a molecular weight of ~13,500 Daltons.[3,5] The protein is most often found as an octamer, but dimers, trimers and tetramers are also known; with one exception these oligomers are non-cooperative.[6] An analogous monomeric O_2 storage protein, myohemerythrin, has also been isolated.[7] In the deoxy state, hemerythrin contains a binuclear ferrous site which binds oxygen in a two Fe per O_2 ratio, resulting in a peroxide-bound, binuclear ferric site. Such a binuclear ferric center is also found in methemerythrin which, although incapable of binding molecular O_2, avidly binds small anions.

A large body of structural information exists from the many x-ray diffraction studies performed on hemerythrin and myohemerythrin.[7,8] The octameric quaternary structure in hemerythrin may be described as a two-layer square doughnut encompassing a large central cavity, with overall D_4 symmetry.[8] The four subunits of each layer are arranged in an end-to-side fashion and the two layers are related through a C_2 rotation. The binuclear iron center of each monomeric unit is held by amino acid

side chains and located between four anti-parallel α-helices. A confacial bioctahedral structure of the binuclear iron cluster is revealed by high resolution studies of oxyhemerythrin, methemerythrin, azidomethemerythrin and azidometmyohemerythrin.[9-12] The three bridging groups, as shown in Figure 1, are carboxylates from Asp and Glu and an oxo (O^{2-}) species derived from solvent. The octahedral geometry of one iron atom is completed by ligation of three histidine nitrogens whereas the other iron is coordinated to two histidine nitrogens and an exogenous ligand.

The strong antiferromagnetic coupling of the irons in the ferric derivatives of hemerythrin ($-J = 134\ cm^{-1}$ for methemerythrin and 77 cm-1 for oxyhemerythrin) is facilitated by the oxo bridge.[13] The magnetic interaction via the oxo bridge also causes the Mössbauer spectra of hemerythrin to have $\Delta Eq > 1.0$ mm/s,[14] whereas monomeric ferric complexes have $\Delta Eq < 1.0$ mm/s.[15] Magnetic coupling of the iron atoms also results in a significant enhancement of the intensity of the metal-based d-d transitions.[16] Additionally, the oxo-bridged binuclear Fe(III) site of hemerythrin is responsible for the intense electronic transitions located between 300 and 400 nm.[14] These have been assigned as $O^{2-} \rightarrow$ Fe(III) charge transfer in origin,[17] and have become increasingly important in the resonance Raman spectroscopy of hemerythrin.[18]

Though oxo-bridged Fe(III) dimers have long been known,[15] only recently have triply-bridged analogs of the hemerythrin binding site been synthesized.[19-21] In these model compounds, the iron atoms are bridged by two carboxylates in addition to the oxo group. The coordination sphere of each metal is completed by a tridentate capping ligand. Under the proper solution conditions, these tribridged complexes assemble

spontaneously, an indication of the intrinsic stability of this structural unit. The magnetic, Mössbauer, and optical spectral properties of the triply-bridged models are completely analogous to those of the ferric hemerythrins. More significant for this review is a comparison between the resonance Raman spectral properties of these models and the methemerythrins. Certain oxo-bridged dimers share with hemerythrin the property that the Fe-O-Fe vibrational modes are strongly enhanced, particularly with UV excitation.

METHEMERYTHRINS

Fe-O-Fe Vibrations. The earliest suggestions that hemerythrin contained an Fe-O-Fe structural unit were based primarily on magnetic susceptibility, Mössbauer and optical spectroscopic measurements of this metalloprotein.[14a] This assumption has recently been confirmed by x-ray crystallography,[9-12] and EXAFS studies,[23] but the first direct evidence for the Fe-O-Fe moiety came from resonance Raman spectroscopy. A bent Fe-O-Fe unit has three normal modes of vibration: a symmetric stretch [ν_s(Fe-O-Fe)], an asymmetric stretch [ν_{as}(Fe-O-Fe)], and a bending mode [(Fe-O-Fe)]. All three are Raman active with the ν_s(Fe-O-Fe) mode expected to be much more intense than the other two. Klotz and co-workers[24] first discovered the ν_s(Fe-O-Fe) vibration as a sharp peak at 507 cm^{-1} in the resonance Raman spectrum of azidomethemerythrin (Fig. 2). It was later found[25-27] that all methemerythrins display a peak near 510 cm-1 (Table 1).

The initial suggestion[27] that this peak is due to ν_s(Fe-O-Fe) was based on the similar frequency of analogous vibrations in various

M-O-M model compounds. However, in contrast with the facile oxo bridge exchange exhibited by most Fe-O-Fe complexes,[15] incubation of the protein in ^{18}O water had no effect on the frequency of the ~510-cm^{-1} peak.[26] This discrepancy was resolved when Kurtz et al.[27] found that addition of sodium azide to oxyhemerythrin in $H_2{}^{18}O$ resulted in azidomethemerythrin with ν_s(Fe-O-Fe) at 493 cm^{-1} (Fig. 2). Similar shifts could also be induced by adding salts of cyanide or cyanate to oxyhemerythrin in ^{18}O water, but all other anions were found to have no effect on bridge exchange.[25] A more general method of bridge exchange was recently reported by Shiemke et al.[18] These authors found that the ~510-cm^{-1} peak shifts 14 cm^{-1} to lower frequency in all methemerythrins when these are prepared from deoxyhemerythrin which had been incubated in $H_2{}^{18}O$ (Table 1).

The bridge substitution experiments also revealed the asymmetric and bending modes of the Fe-O-Fe moiety (Table 1). The asymmetric stretching mode is a common feature in all of the methemerythrin spectra. It occurs between 750 and 785 cm^{-1} and shifts ~35 cm^{-1} to lower energy with ^{18}O exchange of the bridge. In contrast to the general observation of ν_s(Fe-O-Fe) and ν_{as}(Fe-O-Fe), the bending mode has been observed for only a limited number of adducts of methemerythrin (Table 1). The closely related azide (Fig. 2) and cyanamide derivatives have well resolved δ(Fe-O-Fe) peaks of moderate intensity near 290 cm^{-1}; both shift ~5 cm^{-1} to lower energy upon ^{18}O bridge substitution. The bending mode of thiocyanatomethemerythrin also occurs at 290 cm^{-1}, although it is not resolved from the several components of the intense feature centered at 293 cm^{-1}.[28]

The Fe-O-Fe vibrational frequencies of the ferric hemerythrins (Table 1) are essentially independent of the exogenous ligand, and the slight variations in frequency that are observed do not correlate with any property of the exogenous ligand (e.g., size, ligand field strength, or π-donor/acceptor ability). However, the frequencies of the symmetric and asymmetric stretching vibrations in binuclear complexes having a single atom bridge are strongly affected by the bridge angle.[29,30] Thus, the slight variations in Fe-O-Fe frequencies of the methemerythrins probably stem from small differences in the bridge angle brought about by exogenous ligand substitution. Given the ν_s(Fe-O-Fe) and/or ν_{as}(Fe-O-Fe) frequencies and their respective shifts with ^{18}O-bridge substitution, this angle may be calculated.[29a] For example, a value of 130° has been determined for azidomethemerythrin,[27] which compares well with the bridge angle of 129-135° determined by x-ray crystallography.[10,31] The inverse relationship between bridge angle and ν_s(Fe-O-Fe)[29a] is demonstrated by the oxo-bridged binuclear iron models listed in Table 1 (the triply-bridged structures have angles smaller than hemerythrin; the singly-bridged structures have larger angles). The relatively invariant Fe-O-Fe vibrational frequencies of the ferric hemerythrins indicate that these structures have similar bridge angles, reflecting the constraints placed on the binuclear iron site by the protein tertiary structure. Furthermore, recent x-ray crystallographic studies of deoxyhemerythrin indicate that reduction to the ferrous state also has little effect on the overall structure of the binuclear iron center.[9]

Role of Fe-O-Fe in Optical Spectra: Non-chromophoric methemerythrins. The optical spectra of the various derivatives of ferric hemerythrin share many similar characteristics (Table 2, Fig. 3).

Generally, they have two peaks in the near UV region of the spectrum with the stronger of the two located between 320-335 nm ($\varepsilon \simeq 5600\text{-}7200\ M^{-1}\ cm^{-1}$ per Fe_2). On the basis of their visible spectra, the methemerythrins may be divided into two classes: chromophoric and non-chromophoric (Table 2). The former exhibit intense ligand to metal charge transfer (LMCT) transitions ($\varepsilon > 3000\ M^{-1}\ cm^{-1}$ per Fe_2) between 400 and 600 nm, whereas the latter have only a weak feature at ~480 nm ($\varepsilon < 800$ M-1 cm^{-1}) in addition to ligand field transitions at lower energies.[16]

The nearly identical optical spectra among the non-chromophoric methemerythrins is an indication that the observed transitions originate from a common ligand. In the resonance Raman spectra of this class of derivatives, only Fe-O-Fe vibrations exhibit strong intensity enhancement. The ν_s(Fe-O-Fe) mode is moderately enhanced with 457.9 nm excitation (50- to 100-fold enhancement vs. $\nu_1(SO_4^{2-})$ at 981 cm^{-1}),[25,28] and strongly enhanced with near UV excitation (3- to 5-fold greater enhancement at 363.8 nm versus 457.9 nm).[28] The high energy excitation also enhances the ν_{as}(Fe-O-Fe) mode which cannot be observed at all with visible excitation of the non-chromophoric derivatives.[18,28] These enhancement characteristics strongly suggest that charge transfer from the oxo bridge to the iron contributes strongly to all of the electronic transitions in the optical spectra of the non-chromophoric methemerythrins.[28]

Model compounds. Although most oxo-bridged binuclear iron complexes reproduce the magnetic and Mossbauer parameters of the methemerythrins, they are generally inadequate spectral models for the ferric forms of the protein.[15] A particular example of this is the study

by Shriver and coworkers,[32] who examined several oxo-bridged compounds but found no resonance enhancement of Fe-O-Fe vibrations with visible excitation. In fact, for most of these dimers the Fe-O-Fe vibrations were not observed even in normal Raman scattering. We have examined many of the same complexes with near-UV excitation with the same result: Fe-O-Fe vibrations (if observed) are not strongly enhanced.[33] Complexes in this category include those with saturated aliphatic nitrogen ligands (e.g., the singly-bridged Fe(HEDTA) dimer and the triply-bridged TACN dimer) and those with phenolate ligands (e.g., the singly-bridged Fe(Salen) dimer). The ferric phenolate ligation in the purple acid phosphatase proteins[34] may therefore be responsible for the fact that these proteins do not exhibit strongly enhanced Fe-O-Fe vibrations,[33] despite the mounting evidence that an oxo-bridged iron dimer is present.

Exceptions to the above behavior are shown by the singly-bridged $Fe(phen)_2$ and the triply-bridged $Fe(HBpz_3)$ dimers,[19,30] the ligands of which bind via unsaturated, heterocyclic nitrogens, as do the imidazoles in hemerythrin. The $Fe_2O(OAc)_2(HBpz_3)_2$ complex is a particularly good spectroscopic model for the binuclear ferric center of hemerythrin. The model compound has two near-UV transitions (slightly more intense than in hemerythrin, Table 2) and, as in the protein, the higher energy band is the stronger of the two.[19,22] Excitation coincident with these near-UV transitions in the $HBpz_3$ capped complex affords strong enhancement of the ν_s(Fe-O-Fe) Raman vibration[19] at a frequency similar to that of hemerythrin. In addition, resonance-enhanced δ(Fe-O-Fe) and infrared-active ν_{as}(Fe-O-Fe) vibrations are observed at frequencies similar to those in the protein (Table 1). A nearly identical set of near-UV electronic transitions and Fe-O-Fe vibrations (Tables 1,2) is

observed for the enzyme ribonucleotide reductase from E. coli.[35] Thus, it is likely that this protein also contains a (μ-oxo)bis(μ-carboxylato)Fe_2 core. Further more, since its symmetric Fe-O-Fe vibration exhibits a similar resonance enhancement profile to that of non-chromophoric methemerythrins, the reductase very likely also possesses imidazole ligands from the protein.

The visible spectra of the two triply-bridged model complexes are reminiscent of the non-chromophoric methemerythrins in the location of their absorption maxima and in the size of their extinction coefficents (Table 2). The assignment of the visible transitions of the non-chromophoric methemerythrins as O^{2-} (bridge)→ Fe(III) charge transfer is fairly certain, but the same cannot be said for the triply-bridged models. Moderate to strong enhancement (50- to 100-fold vs. sulfate) of ν_s(Fe-O-Fe) is observed with visible excitation of these protein derivatives,[28] whereas much weaker visible enhancement (10-fold vs. sulfate) is observed for the $HBpz_3$ and TACN capped models.[33] In addition, vibrations of the carboxylate and/or capping ligands are resonance enhanced in the model spectra,[19,22] but only Fe-O-Fe vibrations are observed in the resonance Raman spectra of the non-chromophoric methemerythrins (Tables 1 and 3). In fact, among all the hemerythrin derivatives examined there is only one example (methemerythrin, Table 3) of endogenous ligand vibrations being Raman active.[28] In that one case the carboxylate bending mode gains intensity only through coupling to ν_s(Fe-O-Fe), indicating that the carboxylate and imidazole ligands do not contribute to the optical spectra of the protein.[28]

These differences with respect to Raman enhancements in the visible region may indicate that the electronic transitions responsible

for vibronic coupling are localized on the Fe-O-Fe moiety in the protein but extend over additional ligand groups in the model compounds. This type of enhancement mechanism is assumed to occur via orbital mixing among the different ligand types or between ligand and metal and has the effect of distributing the excited state distortion throughout the molecule. Such an effect might also explain the greater number of electronic transitions in the visible region for the triply-bridged models and the dramatic change in these transitions upon substitution of the carboxylates with bridging phosphate[36] or H_2Bpz_2 groups.[22] In view of the similar atomic structure of their binuclear iron centers the above dissimilarities between the models and hemerythrins are puzzling. The cause of these differences in electronic structure remains a subject for further investigation.

Chromophoric Methemerythrins. The near-UV enhancement of the chromophoric methemerythrins is analogous to that of the non-chromophoric derivatives: ν_s(Fe-O-Fe) and ν_{as}(Fe-O-Fe) are strongly enhanced and other modes, if observed, are weak.[18,28] Thus the near-UV transitions of the chromophoric methemerythrins can also be assigned as oxo bridge to Fe(III) charge transfer.[18] This is not surprising given the similar energy and intensity of these transitions among all the ferric hemerythrins (Table 2). The chromophoric methemerythrins also exhibit strong enhancement of Fe-O-Fe vibrations with visible excitation, often greater than with near-UV excitation. Though a detailed enhancement profile has been constructed only for azidomethemerythrin,[18] this behavior appears to be a general property of the chromophoric methemerythrins: excitation into the 452 nm $SCN^- \rightarrow$ Fe(III) or the 425 nm $NCNH^- \rightarrow$ Fe(III) charge transfer bands of thiocyanato- and

cyanamidomethemerythrin, respectively, enhance all three Fe-O-Fe vibrations as well as exogenous ligand vibrations.[18,28]

The visible spectrum of azidomethemerythrin appears to consist of multiple electronic transitions. This is borne out by its enhancement profile (Fig. 3). The maxima at 430 and 520 nm provide enhancement only for ν_s(Fe-O-Fe) and ν_{as}(Fe-O-Fe) and, thus, are assigned as O^{2-} (bridge) → Fe(III) charge transfer. These transitions may be analogous to the O^{2-} (bridge) → Fe(III) charge transfer at ~480 nm in the non-chromophoric methemerythrins, with perhaps additional contribution from exogenous ligand based charge transfer. There is an additional transition at ~495 nm which obviously corresponds to a N^{3-} → iron charge transfer transition since it provides maximal enhancement of both Fe-N and N≡N stretching vibrations of the bound azide (Fig. 3).

A somewhat unusual feature of the excitation profiles for azidomethemerythrin is that the Fe-O-Fe bending mode is in resonance with the 495 nm N_3^- → (Fe(III) charge transfer transition (Fig. 3), rather than any of the electronic transitions assigned as O^{2-} → Fe(III). A possible explanation relates to the fact that the Fe-N stretch of the bound azide requires movement of the ligand-binding iron atom (Fe_b of Figure 1) toward the center of the binuclear iron cluster. This requires analogous movement of the second iron in order to maintain the molecular center of mass, yielding an overall motion that approximates the Fe-O-Fe bending vibration. Since the excited state distortion[37] of an L^- (exogenous ligand) → Fe(III) charge transfer transition encompasses this Fe-O-Fe motion, any such electronic transition will enhance the Fe-L (exogenous ligand) stretch as well as δ(Fe-O-Fe). This latter generalization appears to hold true for all the chromophoric

methemerythrins. The δ(Fe-O-Fe) mode is a general feature of these derivatives (Table 1) and is in resonance with exogenous ligand Fe charge transfer transitions.[18,28]

Ligand Vibrations. The visible spectra of the chromophoric methemerythrins (including oxyhemerythrin, Section 4) are quite strongly influenced by the nature of the exogenous ligand. This is demonstrated by the variation in the energy of the visible charge transfer band upon changing the exogenous ligand (Table 2) and by the resonance enhancement of exogenous ligand Raman vibrations with visible excitation.[25-27] Of the four chromophoric methemerythrins for which intense exogenous ligand vibrations are observed (Table 3), the N_3^- and SCN^- derivatives have been thoroughly studied via isotopic substitution and their Raman spectra have been completely assigned. Excitation of azidomethemerythrin with visible light yields a Raman spectrum with strong peaks at 375 and 2050 cm^{-1} (Fig. 4), in addition to Fe-O-Fe vibrations discussed above.[24,27] These features shift to 368 and 1983 cm^{-1}, respectively, upon substitution of $^{15}N_3^-$ for $^{14}N_3^-$ (Fig. 4), and identify these peaks as the Fe-N stretch [ν(Fe-N)] and N≡N stretch [ν(N≡N)], respectively, of the bound azide ligand (Table 3). Similarly, various isotopes of SCN^- have been used to identify peaks at 2043 and 840 cm^{-1} as the C≡N [ν(C≡N)] and C-S [ν(C-S)] stretching vibrations of thiocyanatomethemerythrin.[26,27] Although heavy isotopes of SCN^- induced no shift in the 298 cm^{-1} peak, this feature was suggested to contain the iron-thiocyanate vibration owing to its large intensity.[27] Our studies have shown that the 298 cm^{-1} peak contains at least three components, a major one being the Fe-O-Fe bending mode (Table 1).[28] The other components have reasonable frequencies for the Fe-N stretch and Fe-N-C bend of the bound thiocyanate

and show the expected shift to lower energy (~275 cm^{-1}) when the sulfur is replaced by selenium in selenocyanatomethemerythrin (Table 3).

Study of these ligand vibrations has provided much information on the manner of ligand binding to methemerythrin. For example, thiocyanate has the ability to bind to iron via either the nitrogen or the sulfur atom. The frequencies of $\nu(C\equiv N)$ and particularly $\nu(C-S)$ can be used to distinguish these linkage isomers, and in the case of thiocyanatomethemerythrin, led to the proposal that the SCN^- binds to the iron via its nitrogen atom to give the complex, $Fe-N\equiv C-S$.[27] This was subsequently verified by x-ray diffraction studies of thiocyanatomethemerythrin.[39] In view of their similar Raman spectra (Tables 1, 3), it is likely that $SeCN^-$ binds in a manner analogous to that of SCN^-.

Given the presence of a binuclear iron center in hemerythrin, it was recognized that the azide ion could bind either to a single iron, or bridge the two metals via one or both of the terminal nitrogen atoms (Fig. 5). Kurtz et al.[27] used unsymmetrically-labeled azide, $^{15}N^{14}N^{14}N^-$, to discriminate among these three possible structures before the endogenous bridging ligands were identified crystallographically. Structure a (Fig. 5), in which the terminal nitrogen atoms are equivalent, should yield a single $(N\equiv N)$ peak, whereas structures b and c, with inequivalent terminal nitrogens, should show a splitting of $\nu(N\equiv N)$ with $^{15}N^{14}N^{14}N^-$. In the observed spectrum just such a splitting occurs with peaks at 2044 and 2032 cm^{-1},[27] thereby ruling out structure a. Subsequent x-ray crystallographic studies[10] revealed that structure c is indeed correct for azidomethemerythrin (Fig. 1).

The optical[28] and resonance Raman[25,28] spectral properties of the cyanamide adduct of methemerythrin are very similar to those of azidomethemerythrin (Tables 1-3). Thus, even in the absence of isotope substitution data, the ligand vibrations of cyanamidomethemerythrin can be assigned by analogy to those of the N_3^- adduct (Table 3). The deuterium isotope shift of ν(Fe-N) from 384 to 379 cm^{-1} shows that cyanamide exists as $NCNH^-$ rather than NCN^{2-}.[28] This observation indicates that cyanamide binds to the iron via its protonated nitrogen. This complex, Fe-NH-C≡N, is analogous to that observed for azidomethemerythrin (Figs. 1, 5c).

The only exogenous ligand vibrations observed for the non-chromophoric methemerythrins are the Fe-OH stretch of hydroxomethemerythrin and the Fe-N stretch of the bound OCN^- in cyanatomethemerythrin (Table 3). The former is assigned on the basis of shifts in $H_2{}^{18}O$ and D_2O.[40] The iron-cyanate stretch is identified primarily by the similarity of its frequency to the Fe-N vibrations of azide and cyanamide. The cyanate vibration is enhanced only with near-UV excitation,[28] whereas the Fe-OH stretch is observed with both visible and near-UV excitation. However, in contrast with the chromophoric derivatives, the Fe-L stretch of the OH^- and OCN^- adducts are minor features in their resonance Raman spectra, indicating that these exogenous ligands make little or no contribution to the optical spectra.

The resonance Raman spectrum of (ligand-free) methemerythrin has a shoulder at 530 cm^{-1} [41] which gains intensity by its close proximity to the 512-cm^{-1} ν_s(Fe-O-Fe) mode.[28] This peak is most likely due to the O-C-O bending vibration [δ(O-C-O)] of bridging carboxylate(s). Such vibrations typically occur near 600 cm^{-1}. The low frequency of this

vibration and its consequent resonance enhancement may be due to the distortion of the binuclear iron structure in ligand-free methemerythrin relative to that of the ligated methemerythrins.[10] The 530-cm^{-1} peak of methemerythrin is the only example of the endogenous iron ligands (i.e., carboxylate and histidine groups) contributing to the resonance Raman spectra of hemerythrin.[18,25-28] This contrasts with the behavior of the triply-bridged models, for which several vibrations of carboxylate and capping ligands are observed.[19,22]

OXYHEMERYTHRIN

Vibrations of the Bound Peroxide. The physiologically important form of the protein, oxyhemerythrin, has been extensively studied by many physical techniques (including Mossbauer, EXAFS, magnetic susceptibility, and x-ray diffraction), the results of which have been reviewed elsewhere.[3,5,27] Although recent EXAFS and x-ray diffraction studies have been very informative, much of what is known about the structure of oxyhemerythrin has been determined by resonance Raman spectrosocopy. Over 30 years ago, Klotz and Klotz (on the basis of the formation of Fe(II)-phenanthroline complexes from denatured protein) proposed that the iron of deoxyhemerythrin is in the ferrous state and that oxyhemerythrin contains Fe(III)-bound peroxide.[42] Subsequent investigations were consistent with this ferric-peroxide formulation, although in these studies the oxidation state of the O_2 group was inferred by measuring properties of the iron atoms, e.g., by Mössbauer and electronic spectroscopy and magnetic susceptibility.[5] The resonance Raman spectrum of oxyhemerythrin was first observed by Dunn et al. in 1973.[43]

Excitation into its 500-nm charge transfer transition yielded well-defined peaks at 503 and 844 cm^{-1}. These peaks were identified as the Fe-O_2 stretch [ν(Fe-O_2)] and the O-O stretch [ν(O-O)] of the bound dioxygen on the basis of their shifts to 480 and 798 cm^{-1}, respectively, when oxyhemerythrin was prepared with $^{18}O_2$.[43] Excitation profiles maximize at 525 nm,[18,44] indicating that $O_2^{2-} \rightarrow$ Fe(III) CT is an important component of the visible absorption band (Fig. 6).

Observation of the ν(O-O) frequency in the resonance Raman spectrum of oxyhemerythrin provided the first direct evidence of the oxidation state of the bound O_2 group and its steric disposition relative to the iron center. A strong correlation exists between the O-O stretching frequency and the oxidation state of O_2: 1550 cm^{-1} for dioxygen (O_2), 1150 cm^{-1} for superoxide (O_2^-) and 850 cm^{-1} for peroxide (O_2^{2-}).[45] Thus, an O-O stretching frequency of 844 cm^{-1} clearly demonstrates that the dioxygen moiety in oxyhemerythrin has been reduced to the peroxide level.[43]

Klotz and coworkers[46] recognized that such a peroxide could adopt any of several steric dispositions with respect to the binuclear iron center (Fig. 7). Structures a-c are analogous to those illustrated earlier for azidomet hemerythrin (Fig. 5), but peroxide has the additional capacity to bind through both oxygen atoms simultaneously in a "side-on" structure (Fig. 7d). The resonance Raman spectrum of oxyhemerythrin prepared from unsymmetrically-labeled oxygen gas (^{16}O-^{18}O) was used to discriminate among these possible structures.[27,46] Two O-O stretching frequencies at 825 and 818 cm^{-1} and two Fe-O_2 stretching frequencies at 501 and 485 cm^{-1} were observed (Fig. 8), thereby demonstrating that the two oxygen atoms of the peroxide are

inequivalent. Structures b and c (Fig. 7) are the only ones consistent with these results. X-ray crystallography of oxyhemerythrin[9] rules out structure b. Furthermore, the deuterium isotope effect on $\nu(Fe-O_2)$ and $\nu(O-O)$ (Table 3) indicates that the peroxide moiety is protonated (HOO^-),[18,26] providing additional evidence that the peroxide binds to the iron via a single oxygen atom.

The octameric protein from P. gouldii has been used in most of the resonance Raman studies of hemerythrin. An analogous monomeric O_2 storage protein, myohemerythrin, has been isolated from the retractor muscle of T. zostericola. The resonance Raman spectrum of oxymyohemerythrin is essentially identical to that of the octameric coelomic protein,[47] indicating conservation of the binding site structure in these proteins despite only 45% amino acid homology between their protomers.[48] Maintenance of the active site structure also extends to other species as shown by a spectroscopic comparison (resonance Raman, optical, and circular dichroism) of oxyhemerythrin and azidomethemerythrin from P. gouldii, P. agassizii, T. dyscrita, and T. zostericola.[44] Recently, Richardson et al.[6] showed that oxyhemerythrin from Lingula reevii has optical and resonance Raman spectra nearly identical to those from the other species, which leads to the conclusion that the structure of the O_2 adduct is conserved. The cooperative oxygen binding that is unique, among hemerythrins, to the Lingula protein must therefore be controlled by factors removed from the ligand binding site.[6]

Fe-O-Fe Vibrations. The $\nu_s(Fe-O-Fe)$ and $\nu_{as}(Fe-O-Fe)$ vibrations of oxyhemerythrin can be observed at 486 and 753 cm^{-1}, respectively, with ultraviolet excitation.[18] These peaks shift to 472 and 717 cm^{-1}, respectively, upon ^{18}O substitution of the bridging oxygen (Fig. 9). It

can, therefore, be concluded that the structure of oxyhemerythrin is analogous to that shown in Figure 1 for azidomet hemerythrin, having an oxo-bridged binuclear iron center with the hydroperoxide bound end-on to the ligand binding iron.[18] Recent x-ray diffraction[9] and EXAFS[23] studies of oxyhemerythrin support this conclusion.

The Fe-O-Fe vibrations of oxyhemerythrin were not detected in earlier investigations using visible excitation[25,27] because, unlike the methemerythrins, they are enhanced only with near-UV excitation (Fig. 6). Whereas this strong selective enhancement of Fe-O-Fe vibrations with near-UV excitation is analogous to the methemerythrins (Fig. 3), the complete lack of resonance Raman enhancement with visible excitation is puzzling. Both oxyhemerythrin and the chromophoric methemerythrins have visible spectra dominated by exogenous ligand-to-metal charge transfer transitions, but only the latter exhibit strong enhancement of Fe-O-Fe vibrations with visible excitation. Therefore, the electronic transitions that are responsible for the enhancement of Fe-O-Fe vibrations in both chromophoric and non-chromophoric methemerythrin using visible light must become altered by hydroperoxide ligation in oxyhemerythrin. The determining factor in this effect of hydroperoxide may be its ability to form a strong intramolecular hydrogen bond to the oxo bridge (next section).

Hydrogen Bonding. An unusual feature of the oxyhemerythrin resonance Raman spectrum is the low frequencies of its ν_s(Fe-O-Fe) and ν_{as}(Fe-O-Fe) vibrations. Whereas the methemerythrins have ν_s(Fe-O-Fe) frequencies between 506 and 516 cm^{-1}, that of oxyhemerythrin occurs some 20-30 cm^{-1} lower, at 486 cm^{-1} (Table 1). Similarly, the asymmetric Fe-O-Fe stretch of oxyhemerythrin, at 753 cm^{-1}, is ~30 cm^{-1} lower than

that of most methemerythrins (Table 1).[18] This reduction in vibrational frequencies has been attributed to hydrogen bonding between the oxo bridge and the hydroperoxide of oxyhemerythrin (Fig. 10). The redistribution of bond energies accompanying the formation of such a hydrogen bond are likely to weaken the oxo bridge bonds and thereby lower the Fe-O-Fe vibrational frequencies.[18,40] Further evidence of this hydrogen bond is the shift of ν_s(Fe-O-Fe) from 486 cm^{-1} in H_2O to 490 cm^{-1} in D_2O.[40] This type of deuterium isotope effect is unique to oxyhemerythrin, indicating that it is due to factors at the ligand binding site rather than general deuterium exchange of protein residues[18,40] The frequency increase of ν_s(Fe-O-Fe) in D_2O indicates that the deuterium bond is weaker than the analogous hydrogen bond, a phenomenon which has been observed in other systems with intramolecular hydrogen bonds.[40]

A recent crystallographic study revealed that the peroxide group in oxyhemerythrin is located nearer to the oxo bridge than is the azide ligand of azidomethemerythrin.[9] This finding was also attributed to the hydrogen bond interaction between the hydroperoxide ligand and oxo bridge. On that basis, a scheme (Fig. 10) was proposed which accounts for the rapid, pH-independent oxygenation of deoxyhemerythrin.[9] The smaller antiferromagnetic coupling constant of oxyhemerythrin ($-J$ = 77 cm^{-1}) relative to methemerythrin (134 cm^{-1})[13] has also been attributed to hydrogen bonding of the oxo bridge in the former.[40]

The high thermodynamic stability of oxyhemerythrin relative to other ferric-peroxide complexes, as well as its preference for end-on peroxide binding rather than the more common side-on structure have been attributed to the hydrogen bond interaction between the hydroperoxide

ligand and the oxo bridge.[40] Recently, similar types of hydrogen bonds have been proposed in other proteins, often having pronounced effects on their resonance Raman spectra. For instance, deuterium isotope and pH effects on the Fe(IV)=O stretch in the resonance Raman spectrum of horseradish peroxidase compound II have been interpreted in terms of hydrogen bonding between the ferryl-oxo group and a distal residue (perhaps histidine).[49] In a protein more relevant to oxyhemerythrin, the superoxide moieties of oxymyoglobin and oxyhemoglobin appear to be hydrogen bonded to distal histidines.[50,51] Such hydrogen bond interactions have been shown to affect the resonance Raman spectra of these proteins as well: the O-O stretch of cobalt-substituted O_2Hb and O_2Mb shifts 3-5 cm^{-1} to higher frequency in D_2O.[52] Hydrogen bonding between the O_2 group and porphyrin substituents has also been implicated in the oxygen complexes of several metalloporphyrins.[53] In all of the above examples it is likely that hydrogen bonding confers added stability to these structures.

Hydrogen bonding to the oxo bridge has also been proposed as the source of the unusual features in the resonance Raman spectra of hydroxomethemerythrin.[40] Whereas all other methemerythrins show a single peak at ~510 cm^{-1}, the resonance Raman spectrum of hydroxomethemerythrin (Fig. 11a) has two peaks at 492 and 506 cm^{-1}.[25,40,41] The shifts of both peaks to lower frequency upon ^{18}O bridge substitution (Fig. 11c, Table 1) show that both frequencies are ν_s(Fe-O-Fe) vibrations, and lead to the conclusion that the hydroxide adduct exists in two distinct conformations (Fig. 12). The cis conformer has a hydrogen bond between the bound hydroxide ligand and the oxo bridge and gives rise to the 492-cm^{-1} ν_s(Fe-O-Fe) peak, whereas the trans conformer lacks this

hydrogen bond and, therefore, has ν_s(Fe-O-Fe) at 506 cm^{-1} similar to other (non-hydrogen bonded) methemerythrins (Table 1). As with the Fe-O-Fe vibrations of oxyhemerythrin, the relatively low ν_s(Fe-O-Fe) frequency of cis-hydroxomethemerythrin results from electron withdrawal out of the oxo bridge bonds by the hydrogen bond interaction.[40]

Additional evidence for the hydrogen bond in hydroxomethemerythrin has been obtained from the temperature-dependent equilibrium between the cis and trans conformations.[40] A change in the sample temperature induces a redistribution of intensity between the two ν_s(Fe-O-Fe) modes and hence, reflects the different relative concentrations of the two conformers. As expected, the 492-cm^{-1} peak of the cis conformer becomes the dominant feature at low temperature, owing to the stabilizing influence of the intramolecular hydrogen bond. The temperature dependence of the change in relative concentration, measured by the relative intensities of the two ν_s(Fe-O-Fe) peaks, yields a hydrogen bond enthalpy of -0.4 kcal/mole, a value similar to many other highly strained intramolecular hydrogen bonds.[40]

As with oxyhemerythrin, deuterium substitution affects the ν_s(Fe-O-Fe) modes of hydroxomethemerythrin; however, in this case, hydrogen bonding is not the determining factor. In D_2O solution of hydroxomethemerythrin, peaks are observed at 518, 495, and 463 cm^{-1} (Fig. 11d), compared to 492 and 506 cm^{-1} in H_2O. The frequencies of the peaks in D_2O depend on the mass of the oxo bridge as well as that of the hydroxide oxygen. The interpretation of these results is that Fermi resonance occurs between the ν_s(Fe-O-Fe) modes and the Fe-O-D bend of the hydroxide ligand.[40]

REDUCED HEMERYTHRINS

The structural and spectroscopic properties of the ferric hemerythrins, including oxy- and methemerythrin derivatives, are now fairly well understood. Lately, the focus of hemerythrin research has shifted to the reduced hemerythrins: the deoxy (Fe(II)-Fe(II)) and semi-met (Fe(II)-Fe(III)) forms. In particular, the chemical nature of the bridges between the iron atoms is being investigated for both these forms of the protein. In the case of the semi-methemerythrins, there is the added question whether a specific iron atom is reduced (and if so, which iron atom) or whether the semi-met state is delocalized over both metal ions.

Harrington et al.[56] first proposed the existence of the semi-met oxidation level on the basis of kinetic results for the reduction of methemerythrin to the deoxy state by dithionite. Such a mixed oxidation state has been confirmed by its distinctive EPR spectrum: an S=1/2 system resulting from antiferromagnetic coupling of high spin Fe(III) and Fe(II).[57] In fact, two spectroscopically distinct semi-methemerythrins have been characterized: $(\text{semi-met})_R$ and $(\text{semi-met})_O$ prepared by one electron reduction of methemerythrin or one electron oxidation of deoxyhemerythrin, respectively.

Sulfide-Bridged Hemerythrins. The first semi-met derivative to be characterized by resonance Raman spectroscopy was semi-metsulfide hemerythrin.[58] Although at the time this derivative was not recognized to be at the semi-met oxidation level, the structural conclusions based on its resonance Raman spectrum (namely replacement of the oxo bridge by sulfide) have been borne out by subsequent study. This derivative of

hemerythrin is prepared by adding S^{2-} to anaerobic solutions of methemerythrin.[58] Kurtz et al.[59] showed that this particular derivative was actually at the semi-met oxidation level as a result of one electron reduction by sulfide. It was later demonstrated that the semi-met derivative could be oxidized to the met level by subsequent addition of oxidizing agents such as $K_3Fe(CN)_6$.[60] Both of these sulfide derivatives have been characterized by resonance Raman spectroscopy.

The optical spectrum of semi-metsulfide hemerythrin has a broad peak at 500 nm and a prominent shoulder at 340 nm (Table 2).[58,60] Resonance Raman spectra obtained by excitation into either of these bands have only a single peak at 444 cm^{-1}, the enhancement of which is 5-fold greater with 363.8-nm than with 514.5-nm excitation.[60] Isotopic substitution with ^{34}S causes the 444-cm^{-1} peak to shift to 438 cm^{-1}. The magnitude of this shift, together with the absence of an effect of D_2O, led Freier et al.[58] to assign the 444-cm^{-1} peak to the symmetric Fe-S-Fe stretching vibration. The absence of a ~510-cm^{-1} peak with near UV excitation is strong evidence that sulfide has replaced the oxo bridge in this derivative.[60] This is not surprising, given the well-documented ability of sulfide to bridge iron atoms (as in the iron-sulfur proteins)[61] and the propensity of the hemerythrin bridge to exchange under reducing conditions.[18]

The optical spectrum of methemerythrin-sulfide is more complex than that of the semi-met derivative (Table 2).[60] In contrast to the oxo-bridged methemerythrins, this sulfide-bridged derivative has no well-resolved features in the near-UV region of the spectrum. The resonance Raman spectrum of methemerythrin-sulfide is also more complex than that of the semi-met adduct, being somewhat reminiscent of the

resonance Raman spectra of the iron-sulfur proteins.[62] Strong fundamentals are observed at 431 and 327 cm^{-1} (Table 1) with weaker combination and overtone bands at 653, 757, 858, and 1282 cm^{-1}.[60] The two fundamentals are assigned as ν_s(Fe-S-Fe) and ν_{as}(Fe-S-Fe), respectively. Since isotope substitution data are not available for this derivative, these assignments are based on the large intensity of the 431-cm^{-1} peak (totally symmetric modes usually show the greatest Raman intensity) and comparison to the resonance Raman spectra of the Fe_2S_2 unit in iron-sulfur proteins and model compounds.[60]

The low frequency of the asymmetric stretch relative to the symmetric stretch of methemerythrin-sulfide contrasts sharply with the results for the oxo-bridged methemerythrins (Table 1). This difference is interpreted as arising from a much smaller bridge angle in the sulfide derivative.[60] A decrease in the bridge angle upon substitution of S^{2-} for O^{2-} is expected since the Fe-Fe distance is fixed by the protein (see above discussion of Fe-O-Fe bridge angle), and the iron-sulfur bridge bonds are longer than the oxo bridge bonds. Assuming a 0.35 Å increase in the bridge bond lengths, one calculates a bridge angle of 98°.[60] The decreased bridge angle in the sulfide derivative is further supported by calculation[60] of a value of 80° from ν_s(Fe-O-Fe) and ν_{as}(Fe-O-Fe) using the secular equations of Wing and Callahan,[29a] and force constants similar to those of Fe_2S_2 systems. Recently the EXAFS of methemerythrin-sulfide was interpreted as indicating an Fe-Fe distance of 3.4 Å, and an iron-sulfur bridge bond distance of 2.2 Å which together yield a bridge angle of 100°.[63]

The sulfide-bridged hemerythrins, at both met and semi-met oxidation levels, will not bind exogenous ligands.[60] This has been

attributed to steric constraints caused by the increased bulk of the sulfide bridge. This contrasts sharply with the behavior of $(semi\text{-}met)_R$ and $(semi\text{-}met)_O$ derivatives. These latter species bind many of the same exogenous ligands as methemerythrin, although with considerably lower affinity.[5b] The resulting anion adducts have identical properties regardless of whether they are prepared from $(semi\text{-}met)_R$ or $(semi\text{-}met)_O$.[5b]

Semi-met Azide Hemerythrin. The visible spectra of the azide adduct of semi-methemerythrin and methemerythrin bear greater similarity to each other than do those of met and semi-met sulfide. Azidosemi-methemerythrin has maximal absorbance at 470 nm (ε = 2400 M^{-1} cm^{-1}), whereas azidomethemerythrin has a maximum at 446 nm (ε = 3700 M^{-1} cm^{-1}).[5b,14a] Retention of the azide to iron charge transfer transition provides evidence that the ligand-binding iron remains ferric in semi-methemerythrin and, hence, that the coordinatively-saturated iron has been reduced. Comparison of the NMR spectra of the met and semi-met azide derivatives is also consistent with the ligand-binding iron remaining in the ferric state.[64] Further support for this conclusion comes from comparison of the resonance Raman spectra of the azide adducts of semi-met and methemerythrin.[65] The shift of $\nu(Fe\text{-}N_3^-)$ from 374 cm^{-1} to 359 cm^{-1} (Table 3) reflects a change in the oxidation state of the binuclear iron center, but is probably too small to be due to reduction of the ligand binding iron. The $\nu(N\equiv N)$ mode is not affected at all by reduction to the semi-met level and shows the identical splitting with $^{15}N^{14}N^{14}N^-$ as azidomethemerythrin. Thus, azide must be bound in the same end-on manner in the met and semi-met derivatives.

The most striking difference between the resonance Raman spectra of the met and semi-met azide derivatives is the lack of the 507 cm^{-1} ν_s(Fe-O-Fe) and 292 cm^{-1} δ(Fe-O-Fe) modes in the reduced form.[65] In addition, the intense near-UV charge transfer bands of the met derivatives have been replaced in most semi-met derivatives by unresolved shoulders at ~360 nm with extinction of ~3000 M^{-1} cm^{-1}.[5b] These differences may result from replacement of the oxo bridge by a hydroxide bridge in the one electron reduced form of hemerythrin, as has also been proposed for the structure of fully reduced deoxyhemerythrin (Fig. 10). This likelihood is supported by the order of magnitude decrease in the antiferromagnetic coupling constant of the semi-met hemerythrins.[64] Furthermore, hydroxide-bridged analogues of the triply-bridged models in the Fe(II)-Fe(II)[21] and Fe(III)-Fe(III)[66] states have reduced magnetic coupling constants, altered UV-visible spectra and lack any resonance Raman bridge vibrations,[67] analogous to the semi-methemerythrins. However, the properties of an Fe(III)-O-Fe(II) center are not known since there are as yet no examples of mixed oxidation state binuclear iron complexes with either an oxo or hydroxo bridge. Thus the possibility remains that the altered properties of the semi-methemerythrins relative to the fully oxidized forms may simply result from the one electron reduction with no change in the nature of the bridge.

Deoxy-NO Hemerythrin. More direct evidence for the presence of a hydroxo bridge in the semi-met derivatives comes from the resonance Raman spectrum of deoxy-NO hemerythrin. This derivative is formed upon addition of gaseous NO to anaerobic solutions of deoxyhemerythrin.[68] Although the use of formal oxidation states are ambiguous when dealing with metal nitrosyls,[69] the deoxy-NO adduct of hemerythrin has been

formulated as (Fe(II),Fe(III)NO^-),[68] and thus should be structurally analogous to the semi-met derivatives. However, unlike other semi-met hemerythrins, formation of the deoxy-NO adduct is reversible: addition of N_3^-, OCN^- or F^- causes bleaching of the deoxy-NO color and loss of its characteristic EPR spectrum.[68] The resonance Raman spectrum of deoxy-NO hemerythrin with visible excitation contains a strong peak at 432 cm^{-1} with a shoulder at 420 cm^{-1}.[70] Assignment of these peaks as ν(Fe-N) and δ(Fe-N-O) of the bound nitrosyl is substantiated by their shifts to 424 and 416 cm^{-1} with substitution of ^{15}NO, and shifts to 426 and 413 cm^{-1} upon substitution of $N^{18}O$ (Table 3). Preparation of the deoxy-NO derivative in D_2O also causes a shift of the bending mode to 414 cm^{-1} whereas the stretching mode is unaffected. Since metal-bound nitrosyls are not known to be protonated, we have interpreted the D_2O effect to indicate the presence of a hydroxide bridge which is hydrogen bonded to the NO group, resulting in a structure similar to the intermediate in Figure 10. Since the formation of deoxy-NO is reversible, we may speculate that little or no structural rearrangement of the binuclear iron center accompanies its formation. This would imply that deoxyhemerythrin also contains a hydroxide bridge, a possibility which is supported by other spectroscopic results (near-IR,[16] CD and EPR,[71] NMR,[64] and EXAFS[72]) as well as crystallographic studies.[9] The presence of a hydroxide bridge in deoxyhemerythrin also allows explanation of the rapid, pH-independent oxygenation reaction according to the scheme of Figure 10.

REFERENCES

1. R. E. Dickerson and I. Geis, Hemoglobin, Benjamin/Cummings, Menlo Park, CA, 1983.
2. G. Preaux and C. Gielens, in R. Lontie, Ed., Copper Proteins, Vol. II, CRC Press, Boca Raton, FL, 1984, pp. 159-205.
3. I. M. Klotz and D. M. Kurtz, Jr., Acc. Chem. Res., **17**, 16 (1984).
4. S. Asher, Vol. 3, Chapter 4 of this series.
5. (a) J. Sanders-Loehr and T. M. Loehr, Adv. Inorg. Biochem., **1**, 235 (1979). (b) R. G. Wilkins and P. C. Harrington, Adv. Inorg. Biochem., **5**, 52 (1983). (c) J. Sanders-Loehr, "Binuclear Iron Proteins," in T. M. Loehr, A. B. P. Lever, and H. B. Gray, Eds., Iron Proteins, in press.
6. D. E. Richardson, R. C. Reem, and E. I. Solomon, J. Am. Chem. Soc., **105**, 7781 (1983).
7. W. A. Hendrickson and J. L. Smith, in J. Lamy and J. Lamy, Eds., Invertebrate Oxygen Binding Proteins: Structure, Active Site and Function, Marcel Dekker, New York, 1981, pp. 343-352.
8. L. C. Sieker, R. E. Stenkamp, and L. H. Jensen, in H. B. Dunford, D. Dolphin, K. N. Raymond, and L. C. Sieker, Eds., The Biological Chemistry of Iron, D. Reidel Publishing Co., Boston, 1982, p. 161.
9. R. E. Stenkamp, L. C. Sieker, L. H. Jensen, J. D. McCallum, and J. Sanders-Loehr, Proc. Natl. Acad. Sci. USA, **82**, 713 (1985).
10. R. E. Stenkamp, L. C. Sieker, and L. H. Jensen, J. Am. Chem. Soc., **106**, 618 (1984).
11. R. E. Stenkamp, L. C. Sieker, and L. H. Jensen, J. Inorg. Biochem., **19**, 247 (1983).

12. S. Sheriff, W. A. Hendrickson, and J. L. Smith, Life Chem. Rep. Suppl. Series, **1**, 305 (1983).

13. J. W. Dawson, H. B. Gray, H. E. Hoenig, G. R. Rossman, J. M. Schredder, and R. H. Wang, Biochemistry, **11**, 461 (1972).

14. (a) K. Garbett, D. W. Darnall, I. M. Klotz, and R. J. P. Williams, Arch. Biochem. Biophys., **135**, 419 (1969). (b) Y. L. York and A. J. Bearden, Biochemistry, **9**, 4549 (1970). (c) P. E. Clark and J. Webb, Biochemistry, **20**, 4628 (1981).

15. K. S. Murray, Coord. Chem. Rev., **12**, 1 (1974).

16. J. Sanders-Loehr, T. M. Loehr, A. G. Mauk, and H. B. Gray, J. Am. Chem. Soc., **102**, 6992 (1980).

17. E. I. Solomon, N. C. Eickman, R. R. Gay, K. W. Penfield, R. S. Himmelwright, and L. D. Loomis, in J. Lamy and J. Lamy, Eds., Invertebrate Oxygen Binding Proteins: Structure, Active Site and Function, Marcel Dekker, New York, 1981, pp. 487-502.

18. A. K. Shiemke, T. M. Loehr, and J. Sanders-Loehr, J. Am. Chem. Soc., **106**, 4951 (1984). (Chapter 3 of this dissertation.)

19. W. H. Armstrong, A. Spool, G. C. Papaefthymiou, R. B. Frankel, and S. J. Lippard, J. Am. Chem. Soc., **106**, 365 (1984.

20. (a) K. Wieghardt, K. Pohl, and W. Gebert, Angew. Chem. Int. Ed. Engl., **22**, 727 (1983). (b) K. Wieghardt, K. Pohl, and D. Ventur, Angew. Chem. Int. Ed. Engl., **24**, 392 (1985).

21. P. Chaudhuri, K. Wieghardt, B. Nuber, and J. Weiss, Angew. Chem. Int. Ed. Engl., **24**, 778 (1985).

22. A. Spool, I. D. Williams, and S. J. Lippard, Inorg. Chem., **24**, 2156 (1985).

23. (a) W. T. Elam, E. A. Stern, J. D. McCallum, J. Sanders-Loehr, J. Am. Chem. Soc., **104**, 6369 (1982). (b) Hendrickson, W. A., M. S. Co., J. L. Smith, and K. O. Hodgson, Proc. Natl. Acad. Sci. USA, **79**, 6255 (1982).

24. J. B. R. Dunn, D. F. Shriver, and I. M. Klotz, Biochemistry, **14**, 2689 (1975).

25. S. M. Freier, L. L. Duff, D. F. Shriver, and I. M. Klotz, Arch. Biochem. Biophys., **205**, 449 (1980).

26. D. M. Kurtz, Jr., Ph.D. Dissertation, Northwestern University, 1977.

27. D. M. Kurtz, Jr., D. F. Shriver, and I. M. Klotz, Coord. Chem. Rev., **24**, 145 (1977).

28. A. K. Shiemke, Ph.D. Dissertation, Oregon Graduate Center, 1985.

29. (a) R. M. Wing and K. P. Callahan, Inorg. Chem., **8**, 871 (1969). (b) J. A. Thich, B. H. Toby, D. A. Powers, J. A. Potenza, and H. J. Schugar, Inorg. Chem., **20**, 3314 (1981).

30. S. Sheriff, J. L. Smith, and W. A. Hendrickson, personal communication

31. R. M. Solbrig, L. L. Duff, D. F. Shriver, and I. M. Klotz, J. Inorg. Biochem., **17**, 69 (1982).

32. D. W. Wheeler, A. K. Shiemke, B. A. Averill, T. M. Loehr, and J. Sanders-Loehr, manuscript in preparation.

33. B. C. Antanaitis, T. Strekas, and P. Aisen, J. Biol. Chem., **257**, 3766 (1982).

34. J. E. Plowman, T. M. Loehr, C. K. Schauer, and O. P. Anderson, Inorg. Chem., **23**, 3553 (1984).

35. (a) B.-M. Sjoberg, T. M. Loehr, and J. Sanders-Loehr, Biochemistry,

21, 96 (1982). (b) B.-M. Sjoberg, T. M. Loehr, and J. Sanders-Loehr, unpublished results.

36. W. A. Armstrong and S. J. Lippard, J. Am. Chem. Soc., **107**, 3730 (1985).
37. T. G. Spiro, Acc. Chem. Res., **7**, 339 (1974).
38. K. Nakamoto, Infrared Spectra of Inorganic and Coordination Compounds, 3rd ed., Wiley-Interscience, New York, 1978.
39. R. E. Stenkamp, L. C. Sieker, and L. H. Jensen, J. Mol. Biol., **126**, 457 (1978).
40. A. K. Shiemke, T. M. Loehr, and J. Sanders-Loehr, J. Am. Chem. Soc., in press (1985). (Chapter 4 of this disertation.)
41. J. D. McCallum, A. K. Shiemke, and J. Sanders-Loehr, Biochemistry, **23**, 2819 (1984).
42. I. M. Klotz and T. A. Klotz, Science, **121**, 477 (1955).
43. J. B. R. Dunn, D. F. Shriver, and I. M. Klotz, Proc. Natl. Acad. Sci. USA, **70**, 2582 (1973).
44. J. B. R. Dunn, A. W. Addison, R. E. Bruce, J. S. Loehr, and T. M. Loehr, Biochemistry, **16**, 1743 (1977).
45. L. Vaska, Acc. Chem. Res., **9**, 175 (1976).
46. D. M. Kurtz, Jr., D. F. Shriver, and I. M. Klotz, J. Am. Chem. Soc., **98**, 5033 (1976).
47. L. L. Duff, G. L. Klippenstein, D. F. Shriver, and I. M. Klotz, Proc. Natl. Acad. Sci. USA, **78**, 4138 (1981).
48. G. L. Klippenstein, J. L. Cote, and S. E. Ludham, Biochemistry, **15**, 1128 (1976).
49. A. J. Sitter, C. M. Reczek, and J. Terner, J. Biol. Chem., **260**, 7515 (1985).

50. B. Shaanan, Nature (London), **296**, 683 (1982).

51. S. E. V. Phillips and B. P. Schoenborn, Nature (London), **292**, 81 (1982).

52. T. Kitagawa, M. R. Ondrias, D. L. Rousseau, M. Ikeda-Saito, and Y. Yonetani, Nature (London), **298**, 869 (1982).

53. (a) D. Lavelette, C. Tetreau, J. Mispelter, M. Momenteau, and J.-M. Lhoste, Eur. J. Biochem., **145**, 555 (1984). (b) F. A. Walker and J. Bowen, manuscript submitted (1985).

54. L. Petersson, A. Graslund, A. Ehrenberg, B.-M. Sjoberg, and P. Reichard, J. Biol. Chem., **255**, 6706 (1980).

55. B.-M. Sjoberg, T. M. Loehr, and J. Sanders-Loehr, manuscript in preparation.

56. P. C. Harrington, D. J. A. De Waal, and R. G. Wilkins, Arch. Biochem. Biophys., **191**, 444 (1978).

57. (a) L. M. Babcock, Z. Bradic, P. C. Harrington, R. G. Wilkins, and G. S. Yoneda, J. Am. Chem. Soc., **102**, 2849 (1980). (b) B. B. Muhoberac, D. C. Wharton, L. M. Babcock, P. C. Harrington, and R. G. Wilkins, Biochim. Biophys. Acta, **626**, 337 (1980).

58. S. M. Freier, L. L. Duff, R. P. Van Duyne, and I. M. Klotz, Biochemistry, **18**, 5372 (1979).

59. D. M. Kurtz, Jr., J. T. Sage, M. Hendrich, P. Debrunner, and G. S. Lukat, J. Biol. Chem., **258**, 2115 (1983).

60. G. S. Lukat, D. M. Kurtz, Jr., A. K. Shiemke, T. M. Loehr, and J. Sanders-Loehr, Biochemistry, **23**, 6416 (1984).

61. J. M. Berg and R. H. Holm, in T. G. Spiro, Ed., Iron-Sulfur Proteins, Wiley, New York, 1982, pp. 1-66.

62. T. G. Spiro, "Iron-Sulfur Proteins," Chapter 5 of this volume.

63. M. J. Maroney, A. L. Roe, L. Que, Jr., J. C. Nocek, G. S. Lukat, and D. M. Kurtz, Jr., Rev. Port. Quim., **27**, 158 (1985)

64. M. J. Maroney, R. B. Lauffer, L. Que, Jr., and D. M. Kurtz, Jr., J. Am. Chem. Soc., **106**, 6445 (1984).

65. M. J. Irwin, L. L. Duff, D. F. Shriver, and I. M. Klotz, Arch. Biochem. Biophys., **224**, 473 (1983).

66. W. H. Armstrong and S. J. Lippard, J. Am. Chem. Soc., **106**, 4632 (1984).

67. D. W. Wheeler, T. M. Loehr, and J. Sanders-Loehr, unpublished results.

68. J. C. Nocek, D. M. Kurtz, Jr., J. T. Sage, P. Debrunner, M. J. Maroney, and L. Que, Jr., J. Am. Chem. Soc., **107**, 3382 (1985).

69. J. H. Enemark and R. D. Feltham, Coord. Chem. Rev., **13**, 339 (1974).

70. J. C. Nocek, D. M. Kurtz, Jr., A. K. Shiemke, T. M. Loehr, and J. Sanders-Loehr, manuscript in preparation.

71. R. C. Reem and E. I. Solomon, J. Am. Chem. Soc., **106**, 8323 (1984).

72. E. A. Stern, J. Ke, F. Ellis, A. K. Shiemke, and J. Sanders-Loehr, manuscript in preparation.

73. Z. Bradic, R. Conrad, and R. G. Wilkins, J. Biol. Chem., **252**, 6069 (1977).

74. A. W. Addison and R. E. Bruce, Arch. Biochem. Biophys., **183**, 328 (1977).

TABLE 1. Frequencies of Fe-O-Fe Vibrations of Hemerythrin and Some Related Proteins and Model Compounds[a]

Sample	ν_s(Fe-O-Fe) ^{16}O (^{18}O)	ν_{as}(Fe-O-Fe) ^{16}O (^{18}O)	δ(Fe-O-Fe) ^{16}O (^{18}O)	Ref.
Non-Chromophoric Methemerythrins				
Cyanomet	512 (498)	782 (754)	---	18,28
Cyanatomet	509 (497)	782 (756)	---	18,28
Chloromet	510 (496)	783 (746)	---	28,40
Formatomet	513 (498)	784 (n.d.)[b]	---	28,40
Met-perchlorate	512 (496)	752 (715)	---	28,40
Met (no ligand)	512 (496)	752 (715)	---	18,28
Hydroxomet (trans)	506 (491)	---	---	40
Fluoromet	509 (n.d.)	n.d.	n.d.	25
Bromomet	512 (n.d.)	n.d.	n.d.	25
Iodomet	508 (n.d.)	n.d.	n.d.	25
Nitritomet	516 (n.d.)	n.d.	n.d.	25
Chromophoric Methemerythrins				
Azidomet	507 (493)	768 (733)	292 (286)	18
Cyanamidomet	508 (495)	778 (739)	294 (289)	28,40
Thiocyanatomet	514 (498)	780 (742)	~290 (~284)[b]	18,40
Selenocyanatomet	516 (n.d.)	n.d.	~275[c] (n.d.)	25
Hydrogen Bonded Hemerythrins				
Oxy	486 (472)	753 (716)	---	18
Hydroxomet (cis)	492 (477)	780 (740)	---	40
Sulfide Bridged Hemerythrins[d]				
Semi-met Sulfide	444 (438)	---	---	58,60
Metsulfide	431 (n.d.)	327 (n.d.)	---	60
Ribonucleotide Reductase				
Subunit B2	496 (481)	758 (733)	---	35

(continued)

(Table 1, continued)

Triply-Bridged Model Complexes				
$[Fe_2O(CH_3COO)_2(TACN)_2]^{2+}$	540 (523)[f]	749 (716)[e]	---	22
$Fe_2O(CH_3COO)_2(HBpz_3)_2$	528 (511)	751 (721)[e]	278 (269)	19
Singly-Bridged Model Complexes				
$[Fe_2O(phen)_4(H_2O)_2]^{4+}$	395 (390)	827 (788)f	---	34
$[Fe_2OCl_6]^{2-}$	458 (440)	870 (826)	203 (198)	31

[a]Frequencies in cm^{-1} determined from Raman spectra; ν = stretch, δ = bend; n.d. = not determined, --- = not observed. [b]One of several components is observed to shift with ^{18}O bridge substitution. [c]Bending mode is probably a component of this peak but no isotope data are available. [d]Vibrations are ν_s(Fe-S-Fe) or ν_{as}(Fe-S-Fe), value in parentheses is for ^{34}S substitution. [e]Determined from IR spectrum. [f]Reported frequency from Raman, similar IR frequency also observed.

TABLE 2. Optical Spectral Parameters for Hemerythrin and Related Compounds[a]

Sample	Visible Charge Transfer Bands[b] λ_{max} (ε)	Near UV Charge Transfer Bands[c] λ_{max} (ε)	λ_{max} (ε)	Ref.
Oxyhemerythrin	500 (2300)	360(5400)	330(6900)	14a,44
Non-Chromophoric Methemerythrins				
Cyanomet	493 (770) sh	374 (5300)	330 (6400)	14a
Cyanatomet	480 (700) sh	377 (6500)	334 (6550)	14a
Chloromet	490 (750) sh	380 (6000)	329 (6600)	14a
Formatomet	480 (600) sh	362 (6000)	331 (6200)	40,73
Met	480 (600) sh	355 (6400)[d]		14a
Hydroxomet	480 (550) sh	362 (5900)	320 (6800)	14a
Fluoromet	480 (400) sh	362 (5000)	317 (5600)	14a
Bromomet	505 (950) sh	387 (5400)	331 (6500)	14a
Iodomet	480 (1200) sh	340 (6300)		14a
Nitritomet	480 (770) sh	377 (5400)	330 (5900)	73
Dicyanamidomet	480 (880) sh	380 (6040)	328 (6220)	74
Chromophoric Methemerythrins				
Azidomet	446 (3800)	370 (4800) sh	327 (7200)	14a,44
Cyanamidomet	435 (3400) sh	365 (5500) sh	325 (7200)	28
Thiocyanatomet	452 (5200)	370 (4900) sh	327 (7200)	14a
Selenocyanatomet	508 (3850)	363 (5650) sh	331 (6440)	74
Sulfidomet[e]	464 (4500) 540 (3300)	360 (6000) sh		60
Semi-Met Hemerythrins				
Semi-met Sulfide[e]	510 (1100)	340 (4000) sh		60
Semi-met Azide	470 (2400)	315 (4400)		5b
Deoxy-NO	408 (1000) 600 (400)	n.o.		68
Ribonucleotide Reductase				
Subunit B2	500 (800)sh	370 (7200)	325 (9400) sh	54

(continued)

(Table 2, continued)

Model Complexes

$[Fe_2O(CH_3COO)_2(TACN)_2]^{2+}$ [f]	464 (1074) 506 (796)	373 (4000) sh	335 (7360)	22
$Fe_2O(CH_3COO)_2(HBpz_3)_2$ [g]	457 (1010) 492 (932)	358 (8200) sh	339 (9270)	19
$[Fe_2O(phen)_4(H_2O)_2]^{4+}$	unresolved	350 (8000) sh		34

[a] λ_{max} reported in nm and ε in M^{-1} cm^{-1} per binuclear iron center; sh = shoulder, n.d. = not determined, n.o. = not observed. [b] Predominantly O^{2-}(bridge) → Fe(III) for the non-chromophoric methemerythrins and exogenous ligand → Fe(III) for the chromophoric methemerythrins. [c] Oxo bridge to iron charge transfer. [d] Broad band, probably contains two components. [e] All transitions are predominantly sulfide to iron charge transfer. [f] In methanol. [g] In $CHCl_3$ solvent.

TABLE 3. Ligand Vibrations of Hemerythrin Derivatives[a]

	Metal-Ligand Stretch[b]		Internal Ligand Vibrations[c]			Ref.
Sample	Frequency	Shift (Isotope)	Assignment	Frequency	Shift (Isotope)	
Oxyhemerythrin	503	-23 ($^{18}O_2$)	ν(O-O)	844	-48 ($^{18}O_2$)	43,18
		-3 (D_2O)			+4 (D_2O)	
Chromophoric Methemerythrins						
Azidomet	375	-7 ($^{15}N_3^-$)	ν(N≡N)	2050	-67 ($^{15}N_3^-$)	24
Cyanamidomet	384	-5 (D_2O)	ν(C≡N)	2169	n.d.	28
Selenocyanatomet	~275	n.d.	ν(C≡N)	2043	-26 ($^{15}NCSe^-$)	25
Thiocyanatomet	~298	n.o.	ν(C-S)	840	-6 ($NC^{34}S^-$)	27
		($^{15}NCS^-$, $NC^{34}S^-$)	ν(N≡C)	2043	-26 (^{15}NCS-)	27
Non-Chromophoric Methemerythrins						
Cyanatomet	382	n.d.	n.o.			28
Met	n.o.		δ(O-C-O)[d]	530	n.d.	28
Perchloromet	n.o.		δ(O-C-O)[d]	530	n.d.	28
Hydroxomet	565	-27 ($H_2{}^{18}O$)	n.o.			40
		-5 (D_2O)				

(continued)

(Table 3, continued)

Semi-Met Hemerythrins						
Semi-met Azide	359	-5 ($^{15}N_3^-$)	ν(N≡N)	2050	-66 ($^{15}N_3^-$)	65
Deoxy-NO	432	-8 (^{15}NO)	δ(Fe-N-O)	420	-4 (^{15}NO)	70
		-6 ($N^{18}O$)			-7 ($N^{18}O$)	70

[a]Values for frequencies reported in cm^{-1} from resonance Raman spectra; n.d. = not determined, n.o. = not observed. [b]Fe-L stretch of exogenous ligand and shifts due to heavy isotopes when available. [c]Internal vibration (ν = stretch, δ = bend) of the exogenous ligand, except where noted. [d]Vibration of endogenous carboxylate bridge.

FIGURE CAPTIONS

Figure 1. Structure of the binuclear iron center of azidomethemerythrin (from Ref. 10).

Figure 2. Resonance Raman spectra of azidomethemerythrin in D_2O (lower), in H_2O (middle), and with ^{18}O-substituted bridge (upper). Excitation wavelength is 530.9 nm (from Ref. 18).

Figure 3. Resonance Raman enhancement profiles for azidomethemerythrin. The electronic absorption spectrum is shown in the upper panel. Middle and lower panels show enhancement profiles for the symmetric Fe-O-Fe vibration (507 cm^{-1}), the Fe-N(azide) stretch (375 cm^{-1}), the N≡N(azide) stretch (2048 cm^{-1}) and the Fe-O-Fe deformation at 292 cm^{-1}. From Ref. 18.

Figure 4. Resonance Raman spectra of azidomethemerythrin with $^{14}N_3^-$ (upper) and $^{15}N_3^-$ (lower). Shifts of the 375-cm^{-1} Fe-N(azide) and 2048-cm^{-1} N≡N(azide) vibrations are indicated. Adapted from Ref. 24.

Figure 5. Possible geometries for azide binding to a binuclear iron center.

Figure 6. Resonance Raman enhancement profiles for oxyhemerythrin. The electronic absorption spectrum is shown in the upper panel. The middle and lower panels show enhancement profiles for the

symmetric Fe-O-Fe vibration (486 cm^{-1}), the $Fe-O_2$ stretch (503 cm^{-1}), and the O-O stretch (844 cm^{-1}) of the bound peroxide. From Ref. 18.

Figure 7. Posible geometries for peroxide binding to a binuclear iron center.

Figure 8. Resonance Raman spectra of oxyhemerythrin prepared with 58 atom % ^{18}O gas in the O-O stretching region (upper) and the $Fe-O_2$ stretching region (lower). The vertical lines a, b, c, and d in the spectra refer to calculated peak positions for structures illustrated by Figures 7b and 7c. The vertical lines e, f, and g in the lower spectrum refer to calculated peak positions for the structure shown in Figure 7d. From Ref. 49.

Figure 9. Resonance Raman spectra of oxyhemerythrin with ^{16}O bridge (upper) and ^{18}O bridge (lower) obtained with 363.8-nm excitation. From Ref. 18.

Figure 10. Proposed interconversion mechanism for deoxy and oxyhemerythrin. From Ref. 9.

Figure 11. Resonance Raman spectra of hydroxomethemerythrin in solution (278 K) obtained with 363.8 nm excitation. The isotopic compositions of the bridge and solvent are listed to the right of each spectrum. From Ref. 40.

Figure 12. Proposed structures for the ligand binding site of hydroxomethemerythrin in the (a) cis conformation and (b) trans conformation. Endogenous ligands are shown in Figure 1. From Ref. 40.

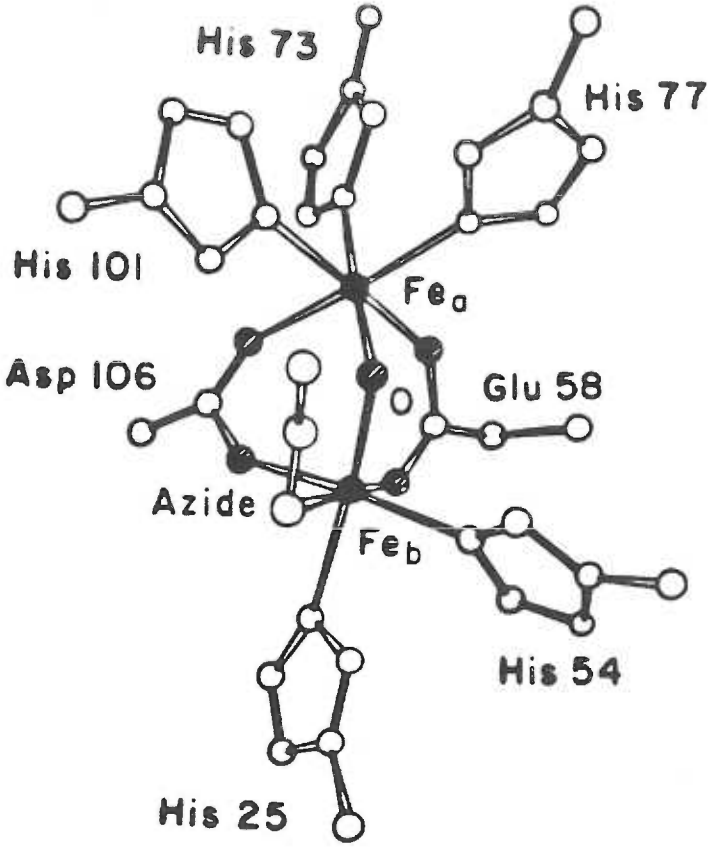

Figure 1

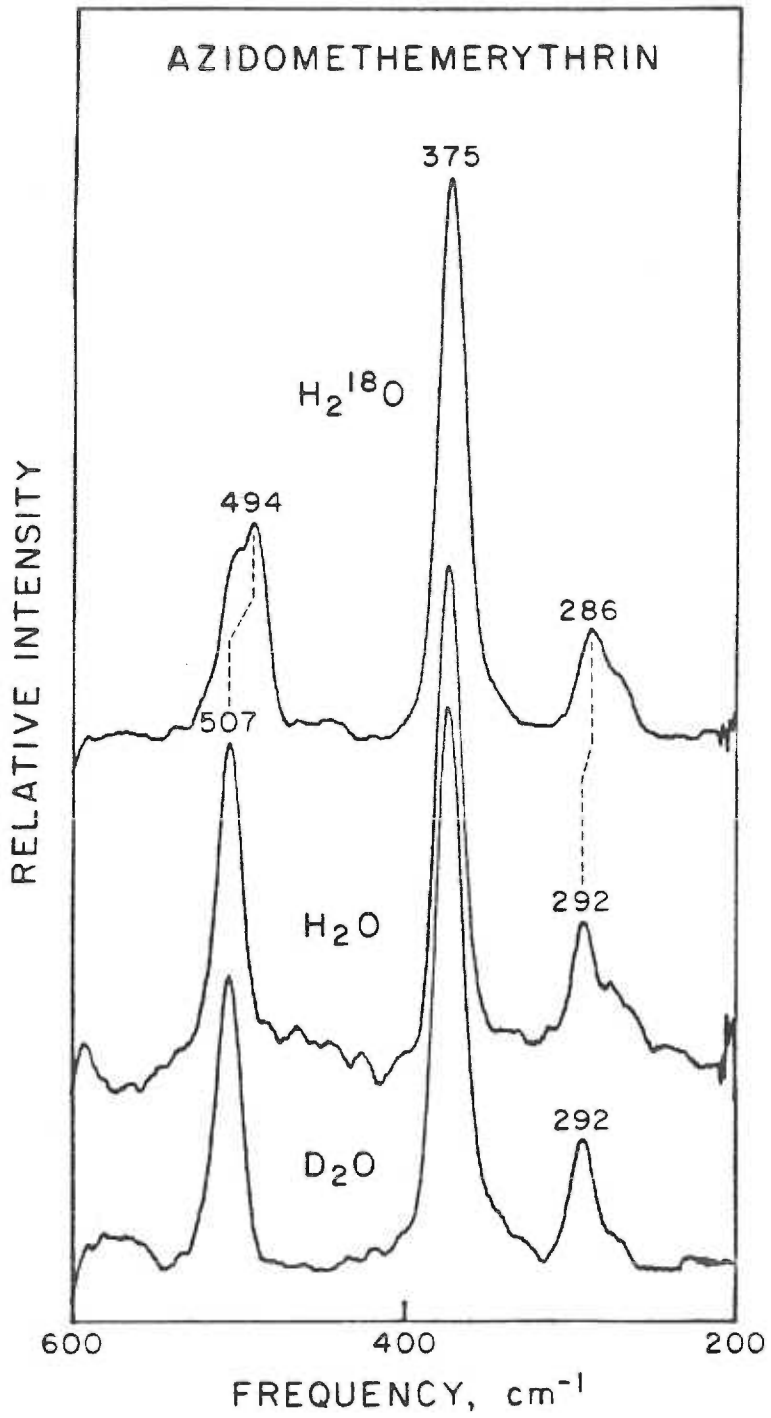
AZIDOMETHEMERYTHRIN
375
$H_2{}^{18}O$
494
286
507
H_2O
292
D_2O
292
RELATIVE INTENSITY
600
400
200
FREQUENCY, cm^{-1}

Figure 2

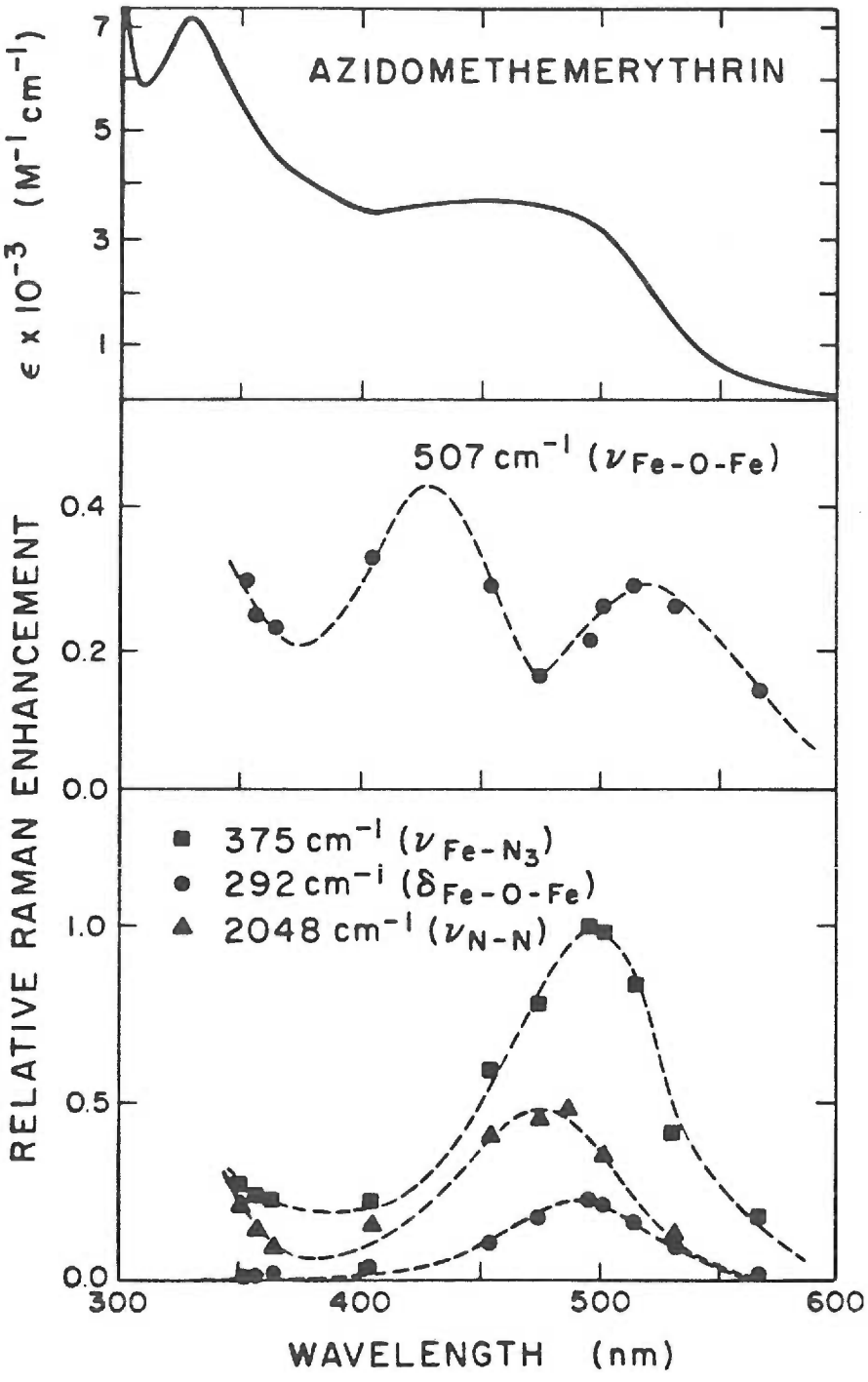
AZIDOMETHEMERYTHRIN
ε x 10⁻³ (M⁻¹ cm⁻¹)
7
5
3
1
507 cm⁻¹ (ν Fe-O-Fe)
RELATIVE RAMAN ENHANCEMENT
0.4
0.2
0.0
375 cm⁻¹ (ν Fe-N3)
292 cm⁻¹ (δ Fe-O-Fe)
2048 cm⁻¹ (ν N-N)
1.0
0.5
0.0
300
400
500
600
WAVELENGTH (nm)

Figure 3

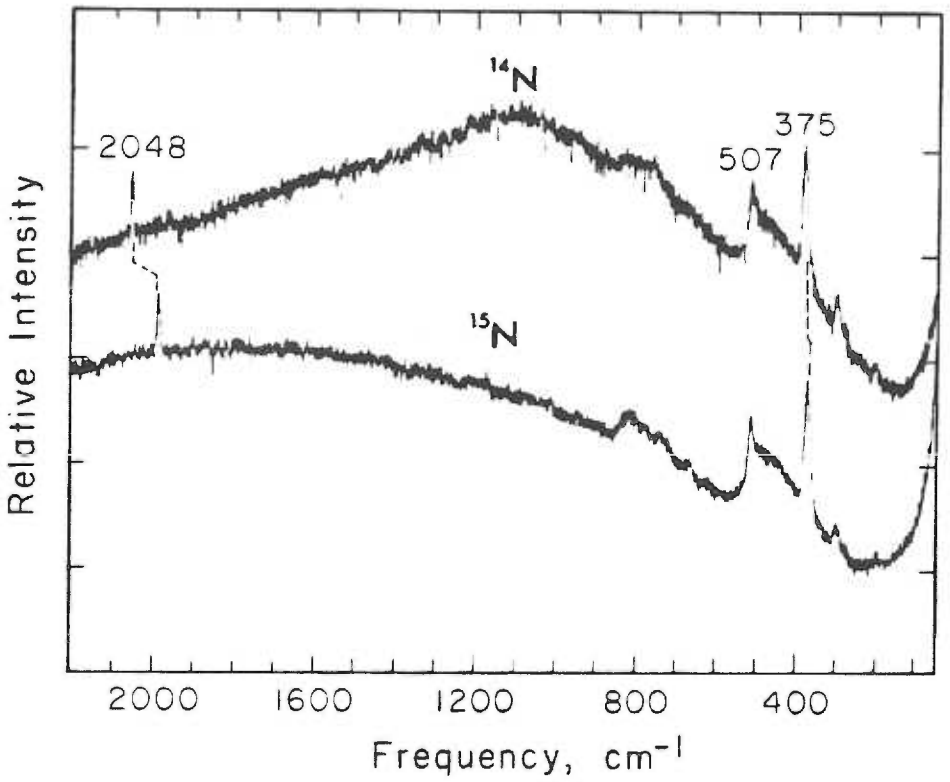
^{14}N
2048
375
507
^{15}N
Relative Intensity
2000
1600
1200
800
400
Frequency, cm^{-1}

Figure 4

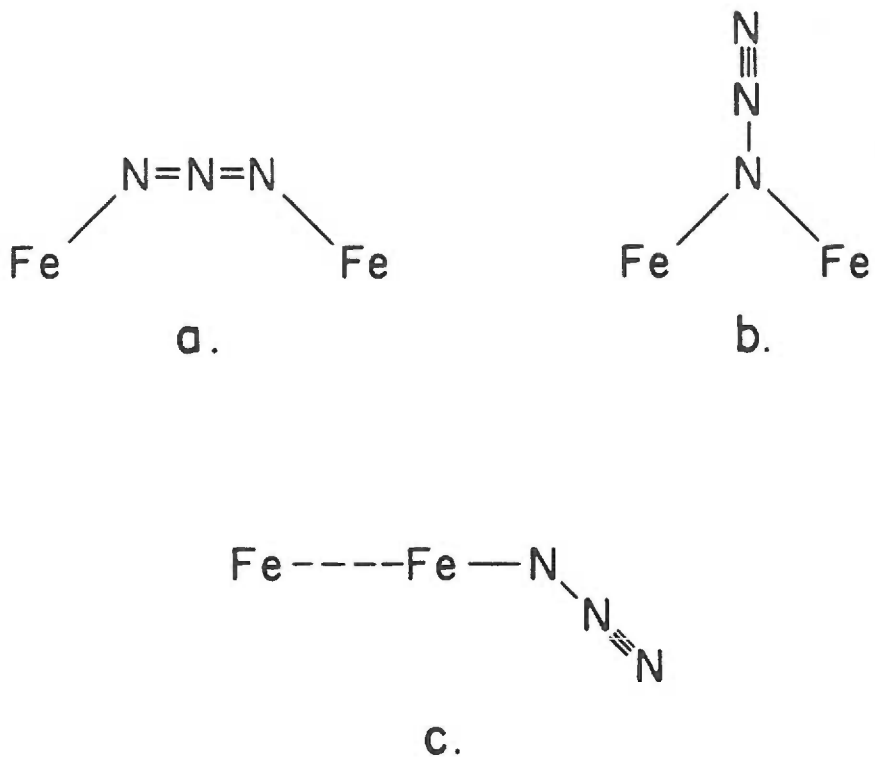

Figure 5

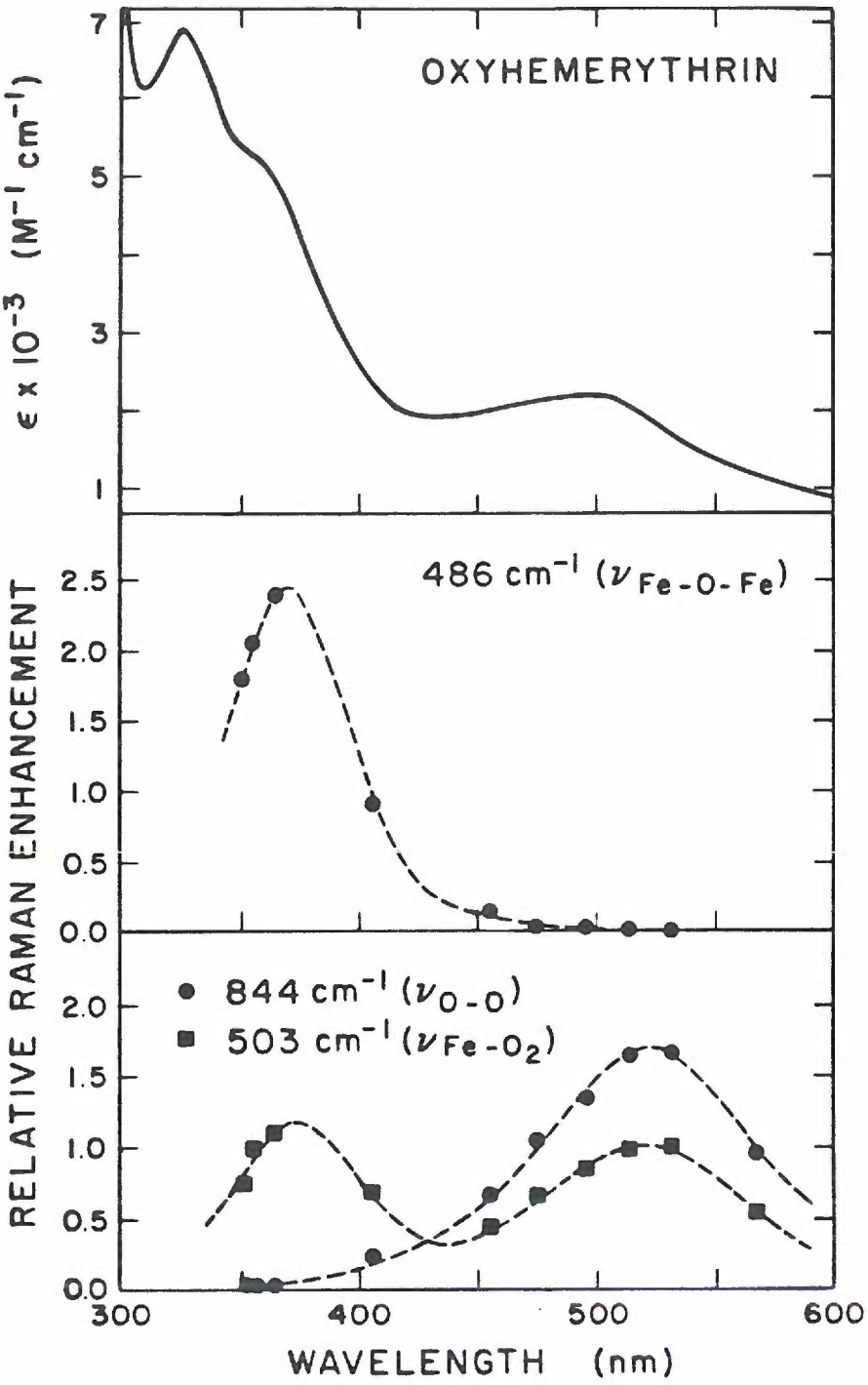
OXYHEMERYTHRIN
ε x 10⁻³ (M⁻¹ cm⁻¹)
7
5
3
1
486 cm⁻¹ (ν Fe-O-Fe)
RELATIVE RAMAN ENHANCEMENT
2.5
2.0
1.5
1.0
0.5
0.0
844 cm⁻¹ (ν O-O)
503 cm⁻¹ (ν Fe-O₂)
300
400
500
600
WAVELENGTH (nm)

Figure 6

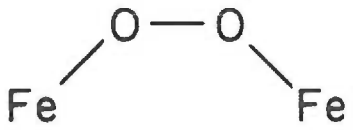

a.

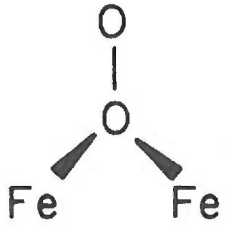

b.

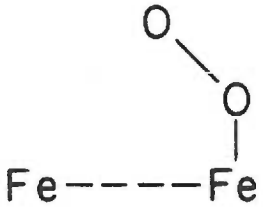

c.

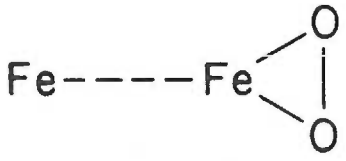

d.

Figure 7

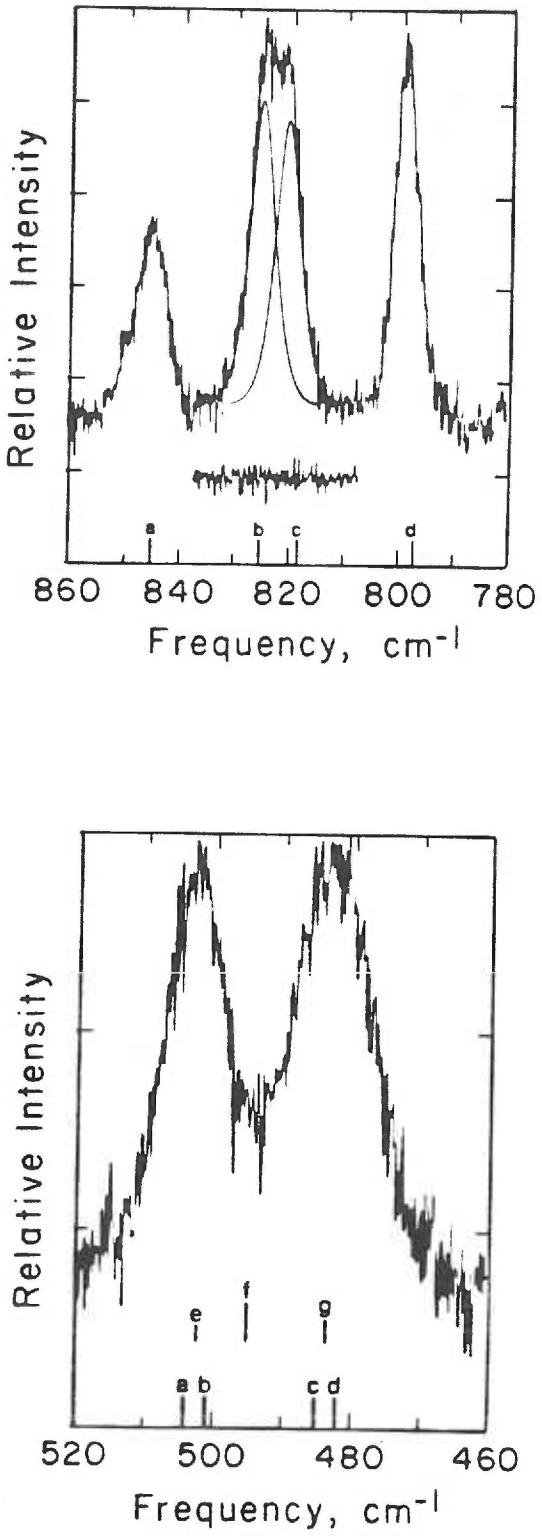
Relative Intensity
a
b
c
d
860
840
820
800
780
Frequency, cm⁻¹
Relative Intensity
e
f
g
a b
c d
520
500
480
460
Frequency, cm⁻¹

Figure 8

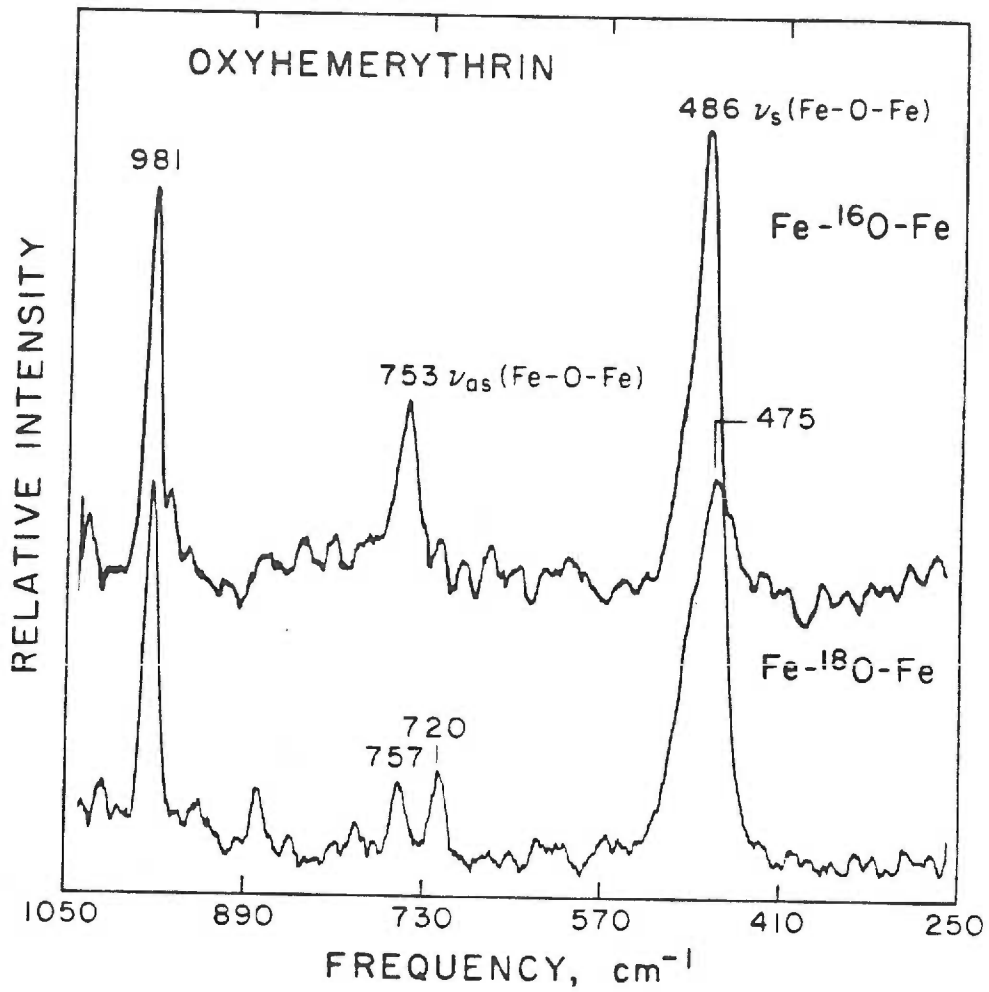
OXYHEMERYTHRIN
486 ν_s(Fe-O-Fe)
981
Fe-^{16}O-Fe
753 ν_{as}(Fe-O-Fe)
475
Fe-^{18}O-Fe
720
757
RELATIVE INTENSITY
1050
890
730
570
410
250
FREQUENCY, cm^{-1}

Figure 9

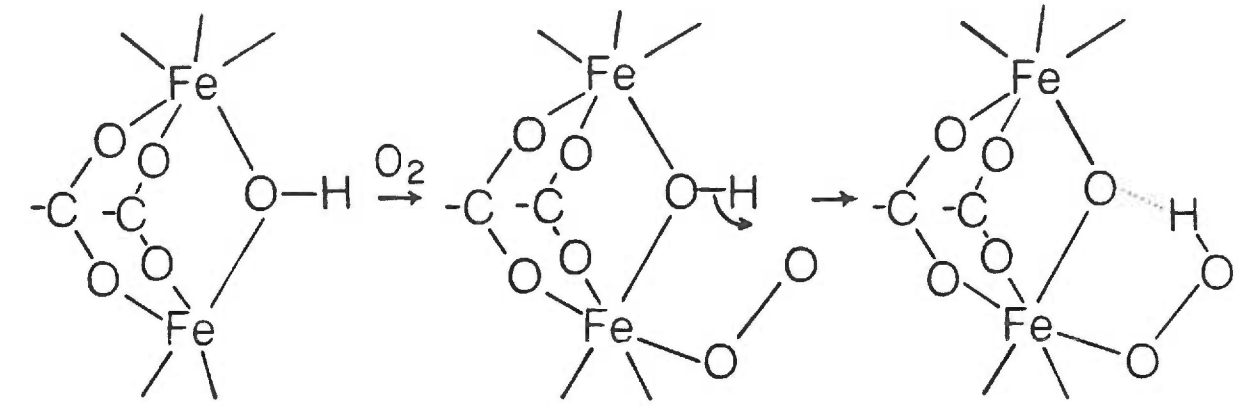

Figure 10

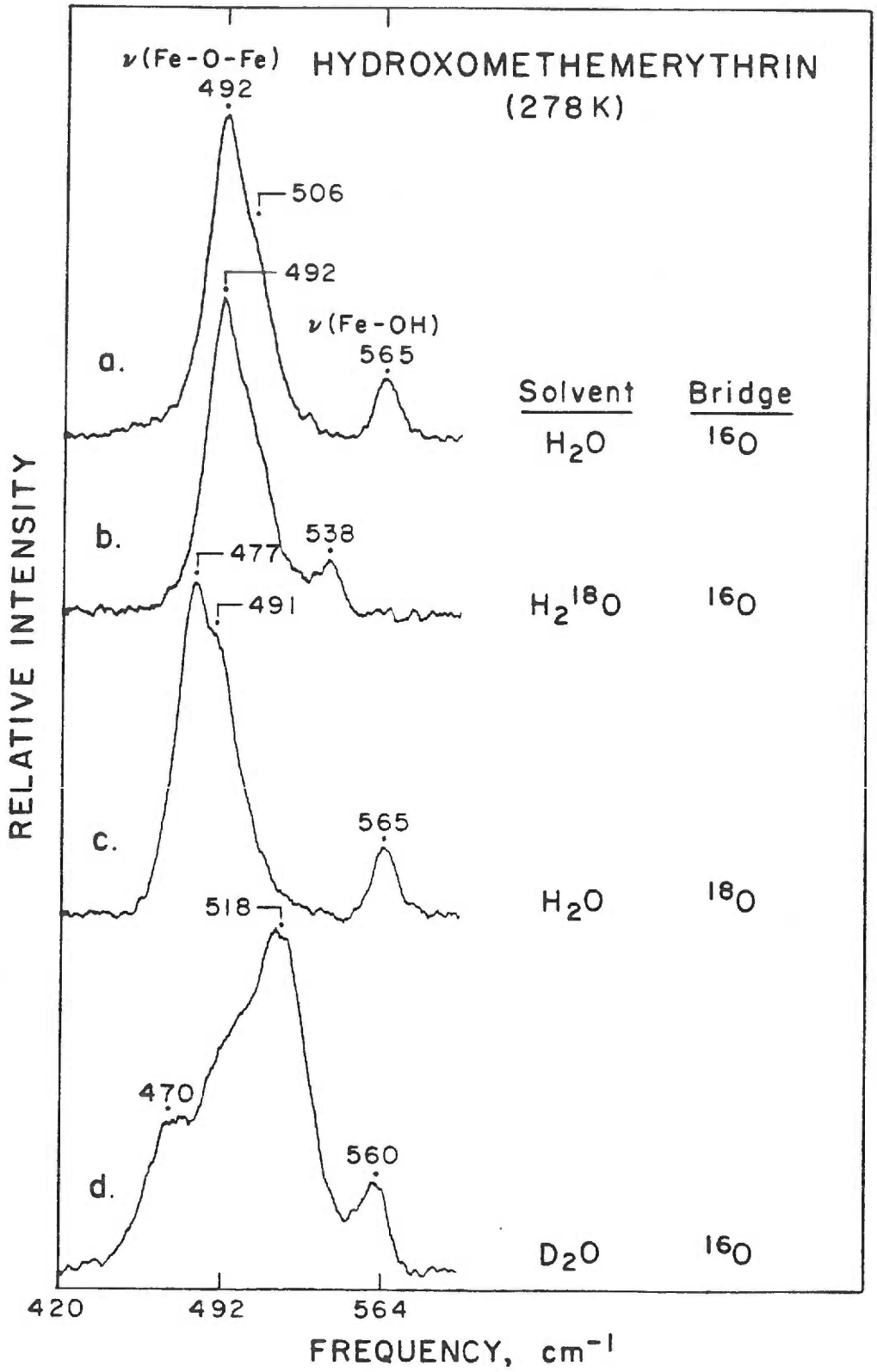
ν(Fe-O-Fe)
492
HYDROXOMETHEMERYTHRIN
(278 K)
506
492
ν(Fe-OH)
565
a.
Solvent
Bridge
H2O
16O
b.
477
538
491
H2 18O
16O
c.
565
518
H2O
18O
d.
470
560
D2O
16O
RELATIVE INTENSITY
420
492
564
FREQUENCY, cm-1

Figure 11

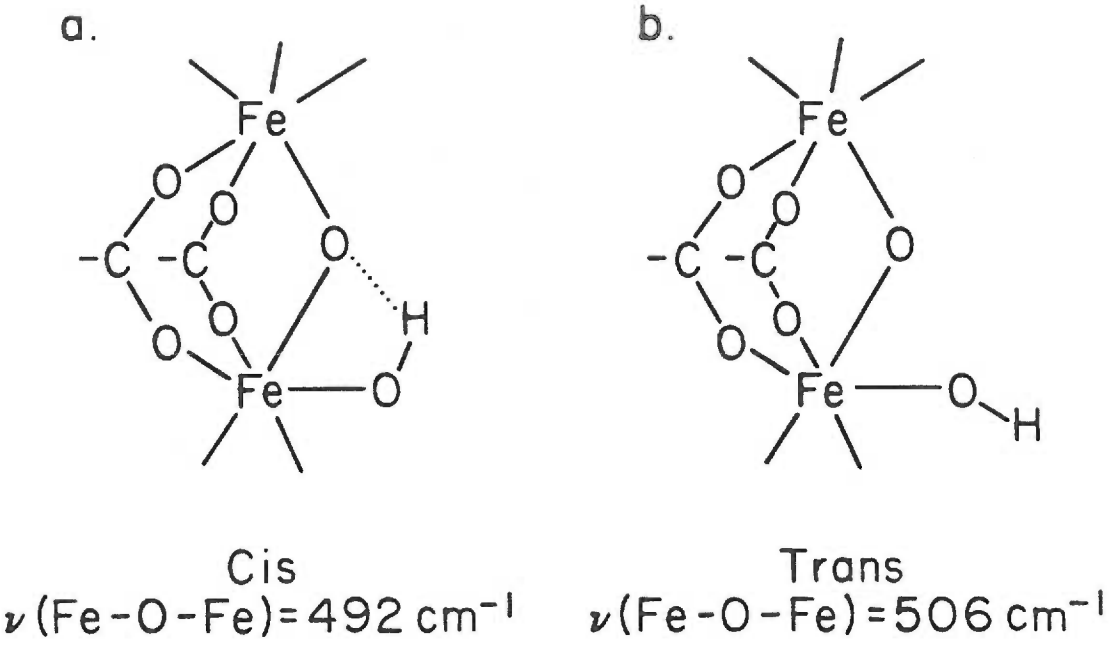
a.
Fe
O
O
C
C
O
O
O
H
O
Fe
O
b.
Fe
O
O
C
C
O
O
O
Fe
O
H
Cis
ν(Fe-O-Fe)=492 cm⁻¹
Trans
ν(Fe-O-Fe)=506 cm⁻¹

Figure 12

Chapter II.

Experimental Methods.

INTRODUCTION.

This chapter summarizes the materials and methods used to perform the work on which this thesis is based. Although several of the chapters in this thesis (those intended as separate publications) contain experimental sections, they are by necessity short and lacking in detail. This methods section contains considerably more detail. It is divided into two sections: Hemerythrin and Spectroscopy. The former presents the methods involved in handling the protein including isolation, purification, derivatization and isotopic labeling. The section on spectroscopy illustrates the various methods used to obtain resonance Raman (RR) spectra of hemerythrin.

HEMERYTHRIN

Isolation and Purification. Phascolopsis gouldii marine worms are the source of hemerythrin for the majority of the experiments in this work as well as most of the physical studies published elsewhere. The most significant exceptions are the x-ray diffraction studies which use the protein from Themiste dyscrita due to its more favorable crystal morphology. The P. gouldii worms are obtained from the supply department of the Marine Biological Laboratory, Woods Hole, MA. (catalog number L-48). It typically takes two weeks between the placement of the order and delivery of the worms. A longer lead time is usually required to obtain the T. dyscrita since they are provided as a gift by Dr. Robert Terwilliger of the Oregon Institute of Marine Biology, Charleston, OR. Approximately 0.75-1.0 g of protein can be obtained from 2 dozen P. gouldii worms or 10-15 T. dyscrita worms.

Upon receipt, the worms should be transferred to fresh sea water (or 0.54 M NaCl if sea water is not available). Higher yields are obtained if the protein is isolated from the worms immediately upon their arrival. If necessary, the worms can be stored in the refrigerator for a short time but care should be taken to replace the sea water (or NaCl solution) frequently (every other day). The T. dyscrita seem better able to withstand long term storage than the P. gouldii.

The isolation is performed essentially as published.[1] The worm is held large end down inside a large beaker (on ice). A half-inch incision is made in the body of the worm with a scalpel or dissecting scissors and the hemolymph solution is allowed to drain. Flush the body cavity twice using 0.54 M NaCl solution and a Pasteur pipet. Filter the collected hemolymph solution through glass wool into a small Erlenmeyer flask (also on ice). Transfer the hemolymph to 50 ml plastic centrifuge tubes and centrifuge at 1000 x g (3000 rpm in an SS-34 rotor) for ~15 minutes. Pour off the supernatant and wash the cells by resuspending the pellet in NaCl solution with gentle mixing. Combine the erythrocyte suspension into a single tube and centrifuge again at 1000 x g for ~15 minutes. Repeat this washing procedure until the supernatant is clear. After the final wash carefully pour off as much supernatant as possible and draw off the remainder with a pipet without removing any of the erythrocytes. Lyse the cells by osmotic shock by adding an amount of cold distilled water 2-3 times the volume of the pellet (15-25 ml of H_2O for two dozen worms). It is important that the minimum amount of distilled water is used since the subsequent crystallization step is facilitated by high protein concentration. Keep this suspension on ice, stir frequently and allow 30-45 minutes for complete lysis. Centrifuge

at 13,000 x g (10,500 rpm in a SS-34 rotor) for 30 minutes to remove the cell membranes and other undissolved material. Often there is some lipid which comes to the top of the solution during this centrifugation. If so use a pipet to remove the supernatant without drawing off this white lipid layer. If the pellet still has any red color it is sometimes possible to add a little more distilled water (~5 ml) and extract the rest of the hemerythrin. If a second lysis is done centrifuge again and add to the previous supernatant. Transfer the supernatant to small centrifuge tubes (e.g. 6 ml plastic tubes) and centrifuge for 45 minutes at 30,000 x g (16,000 rpm in an SS-34 rotor).

Hemerythrin is purified by crystallization. The protein isolation is performed as above for both P. gouldii and T. dyscrita but the conditions for crystallization are slightly different for the two proteins. In the case of P. gouldii, dialyze the hemerythrin (predominantly in the oxy form) vs. a ~100 fold excess of 15% (V/V) ethanol in water until the protein crystallizes. Dialysis was done using Spectrapor 3 dialysis tubing in 18 mm width, 3500 MW cutoff (from Spectrum Medical Industries, Los Angeles, CA), and plastic closures. The T. dyscrita protein can be crystallized in the oxy form but is more reproducibly crystallized when in the met form. The protein is oxidized by addition of a 4-fold molar excess per protein monomer of solid $K_3Fe(CN)_6$ (allow 1-2 hours for complete reaction). The protein concentration must be determined prior to oxidation by using the absorbance and extinction coefficients at 500 nm for oxyhemerythrin. The fully oxidized protein has a greenish-yellow color. The excess ferricyanide should be removed prior to crystallization by dialysis vs. 0.1 M Tris/SO_4^{2-} (pH 8.5). The extent of crystallization depends on the protein concentration: the

higher the concentration the more readily it crystallizes. If the protein concentration is less than 2 mM in monomer it should be concentrated prior to crystallization (model 8050 stirred ultrafiltration cell and Diaflo XM-50 membrane, Amicon Corp., Lexington MA). Crystallize the T. dyscrita protein by dialyis against a 100-fold excess of dilute Tris buffer. Start with 0.04 M Tris/SO_4^{2-} (pH 7.5). If crystals do not appear within 24 hours lower the buffer concentration by diluting with water (i.e. to 0.02 M, 0.01 M, etc.).

Rinse the crystals out of the dialysis bag, into a beaker, with fresh, cold dialysis solution. Collect the crystals by slow centrifugation (~500 x g in a table top centrifuge) for 3-5 minutes. Pour off the supernatant. Wash the crystalline protein by suspending it in a fresh aliquot of the solution used for crystallization (15% ethanol for P. gouldii or dilute Tris buffer for T. dyscrita). Wash 2-3 times to remove other proteins (unusually high absorbance at 280 nm indicates that this washing was incomplete). After the final wash dissolve the protein in the minimum amount (~20 ml for 1 gram of protein) of storage buffer (usually 0.2 M Tris-sulfate, pH 8.0). The P. gouldii protein requires ~30 minutes to completely dissolve whereas the T. dyscrita protein must usually be left overnight. Centrifuge the resultant solution at 30,000 x g in narrow plastic centrifuge tubes for at least 45 minutes to remove any undissolved material.

Once the protein is dissolved in the appropriate buffer it is best stored as a sterile solution at 5°C. It is usually necessary to first pass the solution through a coarse prefilter to remove undissolved material or lipid which may clog the sterile filter. Filter sterilize with a 0.45 μm sterile filter into a sterile serum bottle. It is best to

filter only 5-10 ml at a time in case the filter becomes clogged. Close the serum bottle with a sterile septum stopper and store in the refrigerator.

Derivatization of Hemerythrin. The various forms of hemerythrin and the methods required for their interconversion are summarized in Figure 1. What follows is a detailed description of the interconversion procedures for the P. gouldii protein. Identical methods can be used for the T. dyscrita protein unless otherwise stated.

Methemerythrin. The met form of hemerythrin is prepared by oxidation. The oxidizing agent most often used is $K_3Fe(CN)_6$. In most cases the protein is oxidized from the oxy form but this reagent will also oxidize deoxyhemerythrin to methemerythrin (Fig. 1).[2] Oxidation is accomplished by addition of solid $K_3Fe(CN)_6$ to the protein solution in a four-fold molar excess per hemerythrin monomer. Once the oxidant is dissolved the solution should be allowed to sit (at 5°C) for about 30 minutes to permit complete reaction (1-2 hours for T. dyscrita). The solution should have a bright yellow-green color if the oxidation is complete. The excess ferricyanide is best removed by extensive dialysis (2 changes of ~100-fold excess of buffer). Hydroxomethemerythrin can be prepared at this step by dialyzing in buffer of pH 9.5-10 (I typically used 0.05 M Tris-sulfate in this pH range). The protein is not stable for long periods if the solution pH is above 10 but the pH must be at least 9.5 for complete conversion to the hydroxide form of P. gouldii hemerythrin (pK_a = 7.5-7.9 depending on ionic strength). If (ligand-free) methemerythrin is desired, dialyze the freshly oxidized protein against buffer of pH 6-6.5 (0.05 M MES is typically used). The

protein is not stable below pH of 6.0 and contamination with the hydroxide form is significant above pH 6.5.

The ligated methemerythrins may be prepared in either of two ways: methemerythrin can be dialyzed against a buffer solution containing the appropriate ligand; or a solid salt of the ligand (usually a sodium or potassium salt) can be added directly to the protein solution. The latter method is much faster but the former method has the advantage that high local concentrations of the anion are prevented. Such high local concentrations occur upon addition of solid reagents and may cause some protein denaturation.

Azide, thiocyanate, and cyanate bind very strongly to hemerythrin so only a 50-fold excess of these anions is required to get complete conversion to the ligated derivative. Since these anions will displace hydroxide from hydroxomethemerythrin they can be prepared from methemerythrin at any pH from 6 to 10. They will also displace peroxide from oxyhemerythrin and can thus be prepared from the latter. Chloride and formate bind much more weakly and should be prepared from (ligand-free) methemerythrin at pH of ~6.2. A ~500-fold molar excess of chloride will allow complete formation of chloromethemerythrin whereas a ~2000-fold molar excess of formate is required. Cyanamide is purchased from Sigma Chemicals as H_2NCN and it should be used quickly since it appears to have a short shelf life. Since the pK_a for the formation of $NCNH^-$ (the actual ligand) is 11,[3] cyanamidomethemerythrin should be prepared from methemerythrin at high pH. However the cyanamide anion is unstable in solutions of pH 8.5 or higher (it may undergo hydrolysis, hydration and dimerization to yield urea, dicyanamide or dicyandiamide),[3] so in practice a large excess (~500-fold) of H_2NCN is added to methemerythrin at inter-

mediate pH values (8.0-8.5). Similarly, the pK_a of cyanide is 9.2 so cyanomethemerythrin is prepared at high pH (9.8). At this pH the cyanide must displace hydroxide, thus a large excess of CN^- (~500-fold) is necessary to get complete conversion to cyanomethemerythrin. The weakly bound ligands such as Cl^-, $HCOO^-$, and CN^- can, if desired, be removed from the protein as can ClO_4^-. This is best accomplished by dialysis against a large excess of buffer at pH 9.8 such that hydroxide will compete with other exogenous ligands.

Hydroxomet and (ligand-free) methemerythrin can be easily interconverted by changing the pH of the buffer. However, this is true only in the absence of perchlorate. Although perchlorate binds to the surface of the protein rather than at the binuclear iron center,[4] its binding interferes with the conversion of methemerythrin to hydroxomethemerythrin (the pK_a for this reaction increases from 7.6 to >9.0 when perchlorate is bound).[5] A 500-fold excess of ClO_4^- will afford complete conversion to perchloromethemerythrin. The optical spectra of these various derivatives are shown in Figures 2-4 and the extinction coefficients are collected in Table 2 of chapter 1.

Deoxyhemerythrin. Deoxyhemerythrin can be prepared from oxy, hydroxomet, thiocyanatomet, or (ligand-free) methemerythrin. The same procedure is used in each case. The protein solution is loaded into a dialysis bag and placed in 900 ml of buffer in a one liter Erlenmeyer flask. This flask is placed in an ice bath on a stirrer, stoppered and bubbled with N_2 or Ar gas, with stirring, for 30 minutes (Fig. 3). Remove the stopper and quickly add solid KSCN and $Na_2S_2O_4$ (sodium dithionite, BDH purity, from Gallard-Schlesinger Chemical Mfg. Corp., Carle Place, NY; see page 10 for storage and handling of dithionite).

The final concentration of SCN^- should be equal to the protein (monomer) concentration and the dithionite concentration should be four times that of the protein. The thiocyanate is added because reduction of thiocyanatomethemerythrin by dithionite is faster than the reduction of the other derivatives.[6] Once the thiocyanate and dithionite are added replace the stopper and bubble the solution for another 20 minutes. Close off both valves and dialyze for ~24 hours. If after this time the protein solution is not clear add more dithionite, again bubbling the solution before and after adding the reagent.

Once the hemerythrin is fully reduced it should be dialyzed against fresh anaerobic buffer to remove excess dithionite and thiocyanate. (If dithionite is present when oxygen is admitted they will react to form radicals which can denature the protein. Also, excess SCN^- may react with oxyhemerythrin to form thiocyanatomethemerythrin.) The anaerobic buffer can be prepared by bubbling and stirring as above (Fig. 5). The dialysis bag with the protein should be transferred to the fresh buffer in a glove bag filled with a N_2 atmosphere and the solution then flushed again with gas. After this second dialysis (~100-fold excess of buffer) the protein may be oxygenated by exposure to air (while in a test tube) or by dialysis against O_2 saturated buffer. The former procedure takes ~3 hours for complete oxygenation, the latter takes about a day. Although the freshly isolated protein is predominantly in the oxy form it also contains a considerable amount of methemerythrin (up to 20%). The amount of methemerythrin in any oxyhemerythrin sample will slowly increase with time due to autooxidation. Thus, pure oxyhemerythrin is obtained only by oxygenation of deoxyhemerythrin.

Storage and Use of Dithionite. Sodium dithionite will react with molecular oxygen even in the solid form and the reaction products are deleterious to proteins, thus care should be taken in its storage. The laboratory supply is stored in a dessicator with a N_2 atmosphere. A small amount of dithionite (5-10 g) should be removed from the stock and placed in a serum bottle with a septum stopper. This latter portion is available for regular use thereby minimizing the exposure of the general supply to O_2. The serum bottle containing the dithionite should be purged with N_2 after each use. If the dithionite is no longer free-flowing or smells of H_2S it probably has oxidized. Sodium dithionite can be tested by adding a small amount (10 grains) to a solution of cupric sulfate. If the dithionite is still active a black precipitate will develop in the blue solution, if not the solution will turn yellow.

Isotope Exchange: Oxo Bridge. It has long been known that the oxo bridge of the oxidized forms of hemerythrin does not readily exchange with solvent. In fact, incubation of these forms of the protein in $H_2{}^{18}O$ for several months will not afford exchange of the oxo bridge.[7] Kurtz et al.[8] found that addition of azide to oxyhemerythrin in $H_2{}^{18}O$ buffer caused rapid exchange, yielding azidomethemerythrin with an ^{18}O labeled bridge. This work was extended by Freier et al.[9] who found that similar behavior occurred upon addition of cyanide or cyanate to oxyhemerythrin. However this method of bridge exchange also results in the irreversible formation of these particular ligated methemerythrins, precluding conversion (with retention of the label) to other forms of the protein, particularly oxyhemerythrin. Since kinetics imply that deoxyhemerythrin is an intermediate of the reaction between oxyhemerythrin and azide, cyanide or cyanate,[10] we investigated whether the bridge exchange

actually occurs in the reduced form of the protein. We found that bridge exchange does occur in deoxyhemerythrin but at a much slower rate than with the addition of N_3^-, CN^-, or OCN^- to oxyhemerythrin.[11]

For exchange of the oxo bridge, deoxyhemerythrin is prepared as outlined above. After removing excess reagents (by dialysis against anaerobic buffer) the deoxyhemerythrin is dialyzed against anaerobic 15% ethanol (v/v) in water to crystallize the protein. In a glove bag with a N_2 or Ar atmosphere, transfer the crystalline suspension to a small centrifuge tube (e.g. a 6 ml plastic tube), seal the tube with a septum stopper and centrifuge at ~1000 g for ~5 minutes to separate the solid protein. A table top centrifuge is satisfactory for this purpose. Return the tube to the glove bag and remove the supernatant. At this point the deoxy crystals could be dissolved in the anaerobic, labeled buffer. However, the protein crystals contain a significant amount of water (~50%) which will dilute the label upon dissolution. To alleviate this problem and to achieve more complete labeling, the crystals may be suspended in unbuffered, labeled water for 1-2 days to replace the water in the crystals. Little of the protein dissolves under these conditions because it is very insoluble in low ionic strength solutions. The protein crystals are again centrifuged and dissolved in the labeled buffer. The container should be tightly stoppered and stored (at 5°C) for several days because the bridge exchange is very slow. Since the bridge will exchange only when hemerythrin is in its reduced form, exclusion of oxygen during this entire process is crucial.

For ^{18}O bridge exchanges, 4-5 μmoles of protein monomer was dissolved in 1 ml of $H_2{}^{18}O$ buffer (final concentration of 4-5 mM in monomer). The buffer was approximately 0.05 M Tris/SO_4^{2-} (pH 8) with 0.2 M

SO_4^{2-}. It was prepared by adding 3 µl of 6M H_2SO_4 to one ml of $H_2{}^{18}O$ and then titrating to pH 8 with solid Tris (approximately 6 mg is required). Sodium sulfate is added (28.4 mg, 0.2 M) to increase the ionic strength of the buffer.

After incubation of deoxyhemerythrin in labeled buffer for several days it may finally be oxygenated by exposing the solution to the atmosphere for several hours. The labeled buffer can be recovered by concentrating the oxyhemerythrin and saving the filtrate. At this point the protein may be manipulated and derivatized as above without loss of the labeled bridge.

Buffer Exchange. The following procedure has been used primarily to exchange normal buffers for an isotopically labeled buffer (e.g. D_2O, $H_2{}^{18}O$ or $D_2{}^{18}O$) but the same procedure may be used for any new buffer. This procedure requires the protein to be as concentrated as possible. For small samples (which permit use of small volumes of expensive labeled buffer) concentration is best accomplished with a Centricon (Amicon) concentrator. Using this device hemerythrin may readily be concentrated to 50 µl of solution or 15 mM in monomer (whichever comes first). At concentrations greater than ~15 mM the protein begins to precipitate and clog the filter. Once concentrated, the protein solution is then diluted with the new buffer. Therefore, exchange is most complete if the protein solution is concentrated to less than 0.1 ml. For instance, 50 µl of protein solution diluted to 2 ml with new buffer (maximum volume of the Centricon is 2 ml) results in 97% new buffer with 3% old buffer. Repeating this concentration-dilution procedure (50 µl diluted to 2 ml) yields esentially complete replacement with new buffer. If only small amounts of the new buffer are available (as with $H_2{}^{18}O$ or $D_2{}^{18}O$) best

exchange is accomplished by several cycles of concentration and dilution with small volumes rather than diluting once with a larger volume of labeled buffer. For example, if 2 ml of $H_2{}^{18}O$ buffer are available then concentrating the protein to 50 µl followed by dilution to 2 ml will yield 97% exchange. However, four successive cycles of concentration to 50 µl and dilution to 0.5 ml yields > 99% exchange with labeled buffer. After exchange with a labeled buffer the protein was always allowed to stand overnight (tightly stoppered at 5°C) in the new buffer to permit equilibration.

Isotopically Labeled Ligands. Methemerythrin adducts with isotopically labeled ligands can be prepared as above; i.e. sodium or potassium salts of the labeled anion may be added to met or hydroxomethemerythrin. Formatomethemerythrin with deuterated formate was prepared from the sodium salt of $DCOO^-$. Kurtz reports use of labeled salts of azide or thiocyanate to study isotope shifts in azidomet and thiocyanatomethemerythrin.[7] Deuteration of the cyanamide ligand was accomplished by adding normal cyanamide (H_2NCN) to methemerythrin in D_2O. The ligand protons are readily exchangeable, especially in the pH region where they begin to ionize (pH 8-9).

Raman Spectroscopy

Instrumentation. The Raman spectra shown in this thesis were obtained on a computer controlled Jarrell-Ash spectrophotometer which has largely been described in a previous publication from this laboratory.[12] Spectra-Physics 164-05 (Ar) or 164-01 (Kr) ion lasers were the source of incident radiation. The detector was an RCA C31034A photomultiplier tube (at -25°C) with an ORTEC Model 9302 amplifier/discriminator.

Solution Spectra of Hemerythrin. All my spectra of hemerythrin derivatives in solution were obtained using a recirculating flow cell. For use of this device at least 0.75 ml of sample solution is required and best results are obtained with 1.5 ml or more. The hemerythrin solutions were typically 1-2 mM in hemerythrin monomer. Higher concentrations may be used if the incident laser frequency is not strongly absorbed (e.g. visible excitation of non-chromophoric methemerythrins).

The flow cell is made from a capillary tube (both ends open and fire-polished) and two pieces of Tygon tubing (19 mm and 47 mm long, 1/32" i.d. and 3/32" o.d.). Soaking one end of each piece of tubing in acetone for 2-3 minutes causes the tubing to swell. The capillary tube may then be spliced between the two sections of Tygon tubing (excess acetone should be immediately rinsed off with water). The long section of Tygon tubing is placed in a peristaltic pump and the capillary tube into the sample holder as shown in Figure 6. Typical flow rates are 1.5-2 ml per minute, which correspond to a setting of 4-5 on a Buchler Polystaltic pump (model 61173).

Prior to starting an experiment with the flow cell the sample should be filtered or centrifuged in the Micro-Centrifuge (Fisher model 235) for 5-10 minutes to remove particles from the solution. (Particles scatter light as they flow through the beam thereby increasing the noise level of the spectrum.) During the experiment, the sample reservoir is held in a Lauda constant temperature bath containing methanol and set for -2°C. The methanol in the bath is cooled by circulation through a heat exchanger containing crushed dry ice. Temperature is maintained by adjusting the flow rate through the heat exchanger and then heating the

bath. This method will maintain temperature for 3-4 hours before the dry ice needs to be replenished.

Although flowing the sample past the laser beam decreases the rate of deterioration compared with a stationary arrangement, sample decomposition will still occur, especially if the sample absorbs strongly at the excitation wavelength being used. As decomposition takes place, particles of denatured protein may form in the solution. If so it will be necessary to remove the particles by filtering or centrifuging the sample. In addition to forming particles, some of the denatured protein will adhere to the glass of the capillary tube at the focal point of the laser. As this process becomes extensive the noise and background level of the spectrum will increase. It is possible to mitigate this problem by periodically moving the sample tube transverse to the laser beam, thereby changing the position at which the beam strikes the sample. For the same reason it is necessary to thoroughly rinse the flow cell after each use.

If a reasonably fresh sample is being used the decomposition of the protein is normally not a problem. Under these circumstances fairly high laser power can be used without destroying the sample (20-30 mW of near UV or 60-70 mW of visible excitation). If the sample begins to decompose the power should be kept under 15 mW of near UV or 30 mW of visible excitation. Alternatively the protein concentration may be decreased.

Spectra of Frozen Hemerythrin. Since the spectra of frozen samples are acquired in a back-scattering geometry, high protein concentrations provide the best results. In this work, concentrations of 5-12 mM in hemerythrin monomer were typically used. Once concentrated to this level, 10-15 μl of protein solution were loaded into a melting point

capillary. For spectra at 90 K the sample was frozen rapidly in the copper cold finger of a Dewar containing liquid N_2.[13] Under these conditions the methemerythrins were stable to laser irradiation with excitation wavelengths above 400 nm, but not with near UV excitation. Oxyhemerythrin decomposed under these conditions with near UV as well as 406.7 nm excitation.

Variable temperature experiments were done using the Varian E-4540 variable temperature controller as shown in Figure 7. In these experiments the sample is again contained in a capillary tube. This is held in a partially silvered and jacketed glass tube through which flows cold N_2 gas. The gas is cooled to ~100 K by passing through liquid N_2, and then heated to the desired temperature just prior to reaching the sample. This device can therefore be maintained at temperatures above 100 K. In my experiments with this device (see chapt. 4 and 5), 406.7 nm excitation was used and the hemerythrin began to decompose to a significant extent at temperatures above ~220 K (depending somewhat on the form and age of the protein).

At temperatures below 120 K very high gas flow (~40 SCFH) is required to maintain the sample temperature. At higher temperatures N_2 flow rates of 20 SCFH are sufficient. The dial setting of the Varian temperature controller is woefully inaccurate. For this reason temperatures were measured with a thermocouple and potentiometer before and after experiments. The sample temperature at a particular dial setting is also not very reproducible, thus the temperature should be measured for each experiment.

Recent results indicate that the proteins instability toward near UV excitation at liquid N_2 temperatures is due to thermal decomposition.

The high absorbtivity causes localized heating and decomposition of the protein. With the laboratory's newly acquired Air Products Displex closed cycle helium refrigerator, sample temperatures of ~10 K can be reached. Under these circumstances it may be possible to obtain spectra on frozen hemerythrin samples with excitation wavelengths below 400 nm.

Curve Fitting Procedure. For much of the work discussed in this thesis it was necessary to determine the relative intensities of overlapping peaks (see chapters 3 and 4). In such cases intensities were quantitated using a computer generated curve fitting program. This program will sum spectral components chosen by the operator and allow comparison to data. The operator decides upon the number of components and enters the peak position, band width (full-width at half maximum), and relative intensities for each. The peak shape of all components is entered as Gaussian or Lorentzian or any combination thereof. The computer displays the sum of the components which may be compared to the data by calling up the desired file and simultaneously plotting the data and computer generated fit. The procedure becomes iterative at this point: the number of peaks and their positions, widths, intensities and shape are varied until an adequate fit is achieved. A example of such a computer generated fit is shown in Figure 8.

REFERENCES

1) Klotz, I.M.; Klotz, T.A.; Fiess, H.A. Arch. Biochem. Biophys. **1957**, 68, 284-299.

2) Wilkins, R.G.; Harrington, P.C. Adv. Inorg. Biochem. **1983**, 5, 52-85.

3) "Cyanamide"; American Cyanamid Corp., Process Chemicals Dept., 1963, Wayne, New Jersey.

4) Stenkamp, R.E.; Sieker, L.C.; Jensen, L.H. J. Mol. Biol. 1978, **126**, 457-466.

5) Garbett, K.; Darnall, D.W.; Klotz, I.M. Arch. Biochem. Biophys. 1971, **142**, 471-480.

6) Olivas, E.; deWall, D.J.A.; Wilkins, R.G. J. Inorg. Biochem. 1979, **11**, 205-212.

7) Kurtz, D.M., Jr., Ph.D. Dissertation, Northwestern University, Evanston, IL, 1977.

8) Kurtz, D.M.; Shriver, D.F.; Klotz, I.M. Coord. Chem. Rev. **1977**, 24, 145-178.

9) Freier, S.M.; Duff, L.L.; Shriver, D.F.; Klotz, I.M. Arch. Biochem. Biophys. **1980**, 205, 449-463.

10) Meloon, D.R.; Wilkins, R.G. Biochemistry **1976**, 15, 1284-1290.

11) Shiemke, A.K.; Loehr, T.M.; Sanders-Loehr, J. J. Am. Chem. Soc. **1984**, 106, 4951-4956. Chapter 4 of this thesis.

12) Loehr, T.M.; Keyes, W.A.; Pincus, P.A. Anal. Biochem. **1979**, 96, 456-463.

13) Sjoberg, B.-M.; Loehr,T.M.; Sanders-Loehr, J. Biochemistry **1982**, 21, 96-102.

FIGURE CAPTIONS

Figure 1. Scheme showing the reagents required for interconversion of various hemerythrin derivatives.

Figure 2. Optical spectra of chromophoric hemerythrins. Oxyhemerythrin (a), cyanamidomethemerythrin (b), azidomethemerythrin (c), thiocyanatomethemerythrin (d). Upper spectra have each been offset by two ordinate units for greater clarity.

Figure 3. Optical spectra of non-chromophoric methemerythrins. Cyanomethemerythrin (a), chloromethemerythrin (b), formatomethemerythrin (c), cyanatomethemerythrin (d). Upper spectra have each been offset by two ordinate units for greater clarity.

Figure 4. Optical spectra of non-chromophoric methemerythrins. Methemerythrin (a), methemerythrin-perchlorate (b), hydroxomethemerythrin (c). Upper spectra have each been offset by two ordinate units for greater clarity.

Figure 5. Apparatus used for anaerobic reduction of hemerythrin.

Figure 6. Flow cell arrangement used to obtain solution spectra of hemerythrin. The support for the capillary tube has been omitted from the top view for clarity.

Figure 7. Apparatus used for variable temperature spectra of hemerythrin.

Figure 8. Computer generated fit of the resonance Raman spectrum of hydroxomethemerythrin. a) The three components used for the fit, b) the sum of the three components, c) the resonance Raman spectrum of hydroxomethemerythrin and the computer generated fit. The spectrum was obtained at 278 K, 363.8 nm excitation, scan rate of 0.5 cm^{-1}/sec, and is the sum of twelve scans. The table in the upper right summarizes the parameters of the three components used for the fitting.

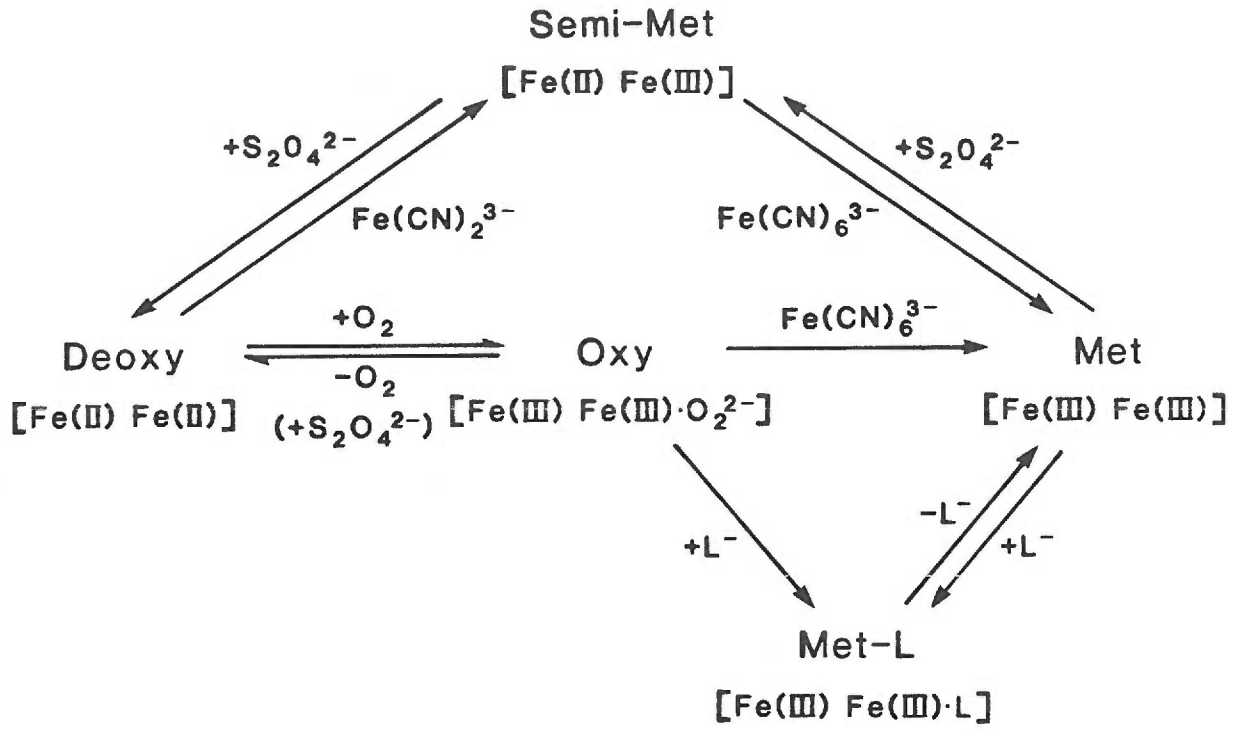
Semi-Met
[Fe(II) Fe(III)]
+S2O4 2-
Fe(CN)2 3-
+S2O4 2-
Fe(CN)6 3-
Deoxy
[Fe(II) Fe(II)]
+O2
-O2
(+S2O4 2-)
Oxy
[Fe(III) Fe(III)·O2 2-]
Fe(CN)6 3-
Met
[Fe(III) Fe(III)]
+L-
-L-
+L-
Met-L
[Fe(III) Fe(III)·L]

Figure 1

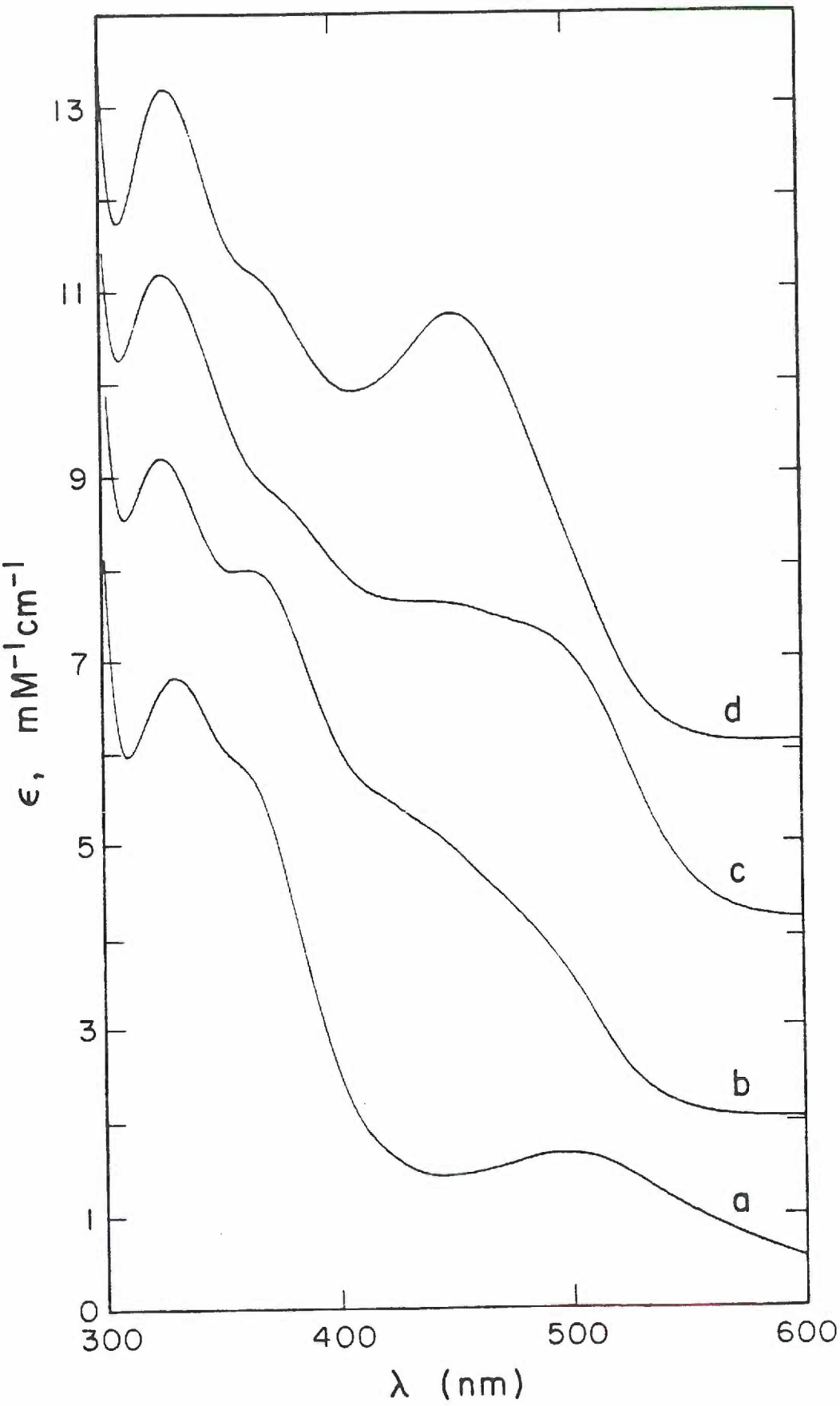

Figure 2

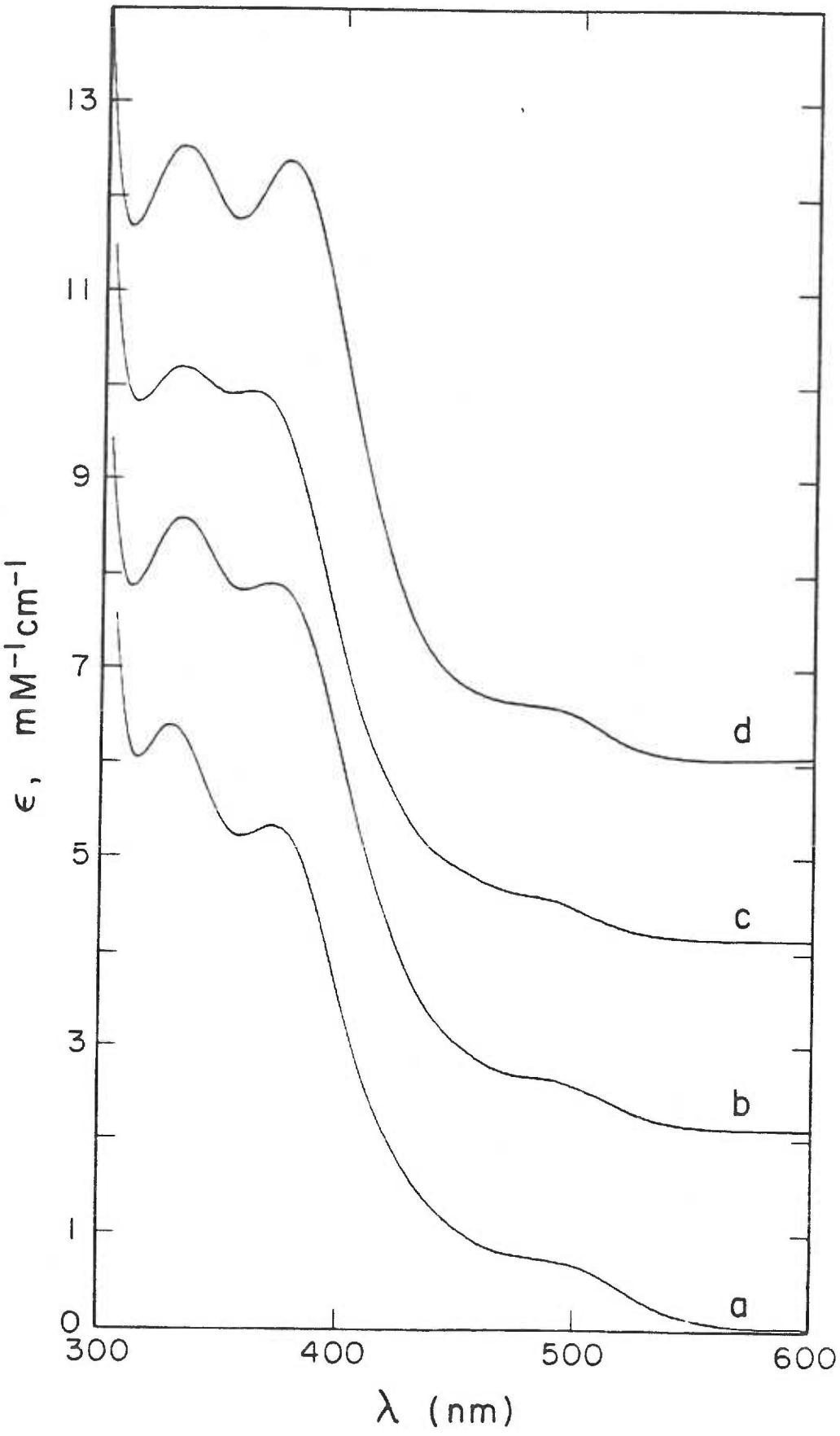

Figure 3

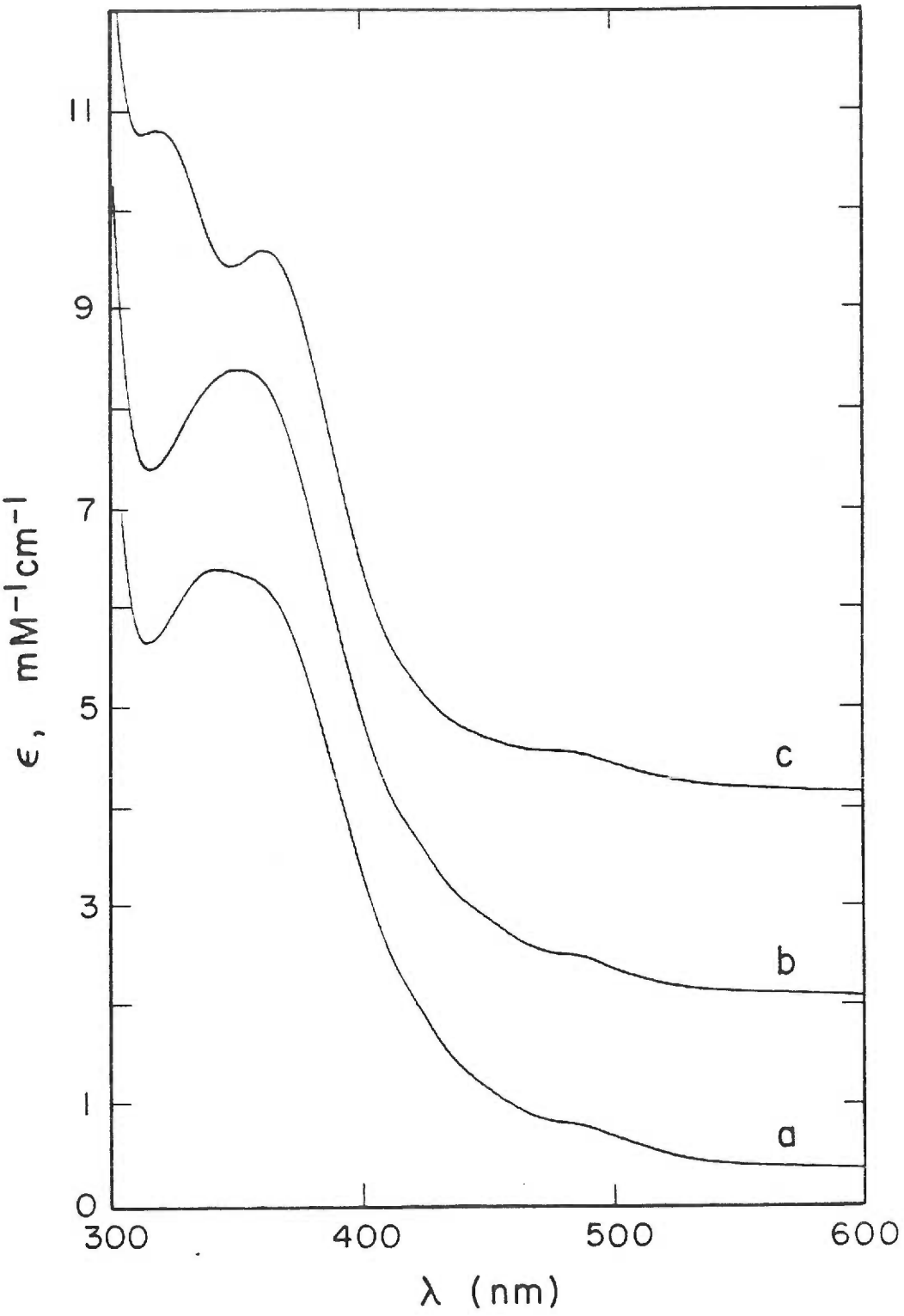

Figure 4

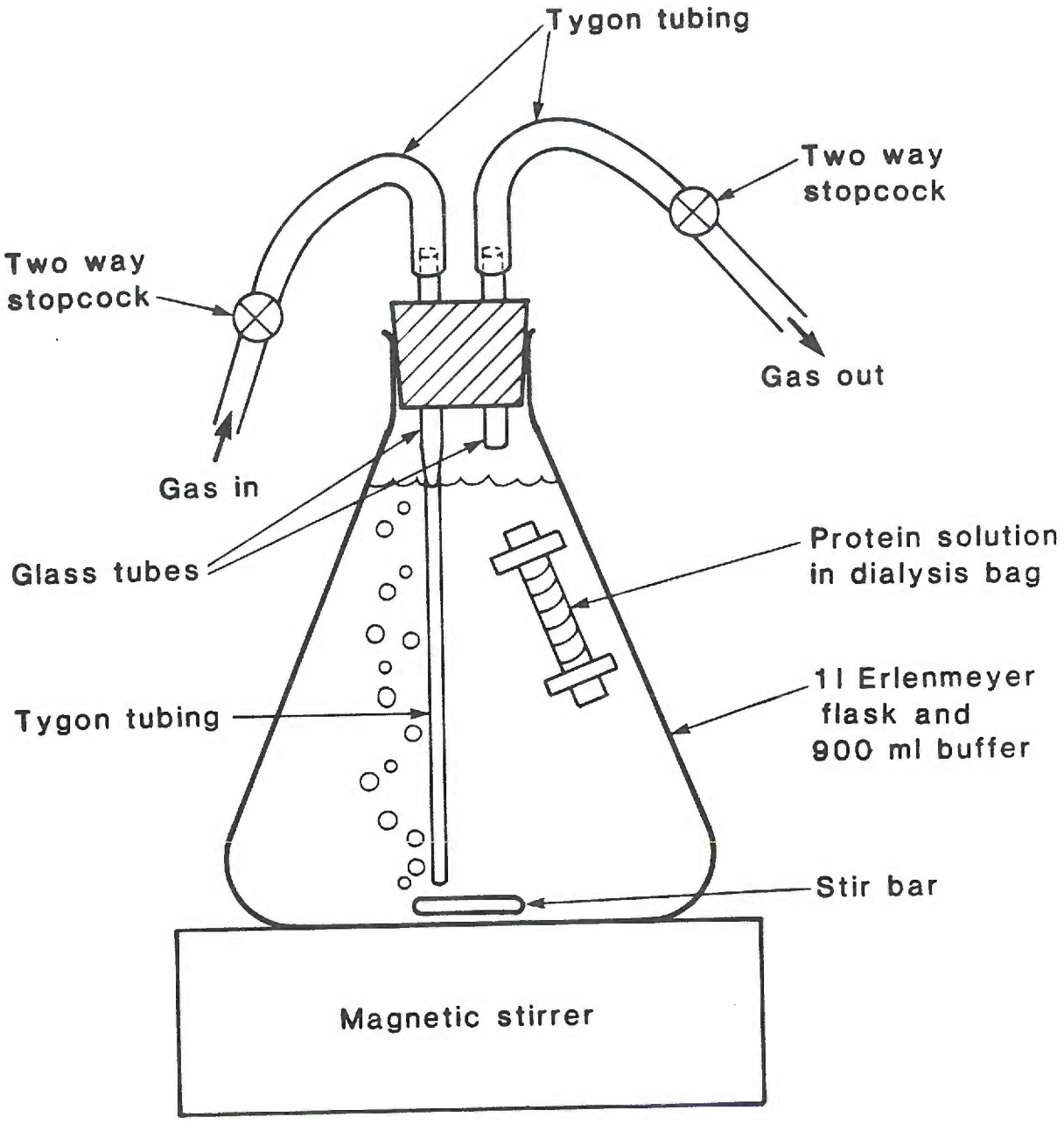
Tygon tubing
Two way stopcock
Two way stopcock
Gas out
Gas in
Glass tubes
Protein solution in dialysis bag
Tygon tubing
1 l Erlenmeyer flask and 900 ml buffer
Stir bar
Magnetic stirrer

Figure 5

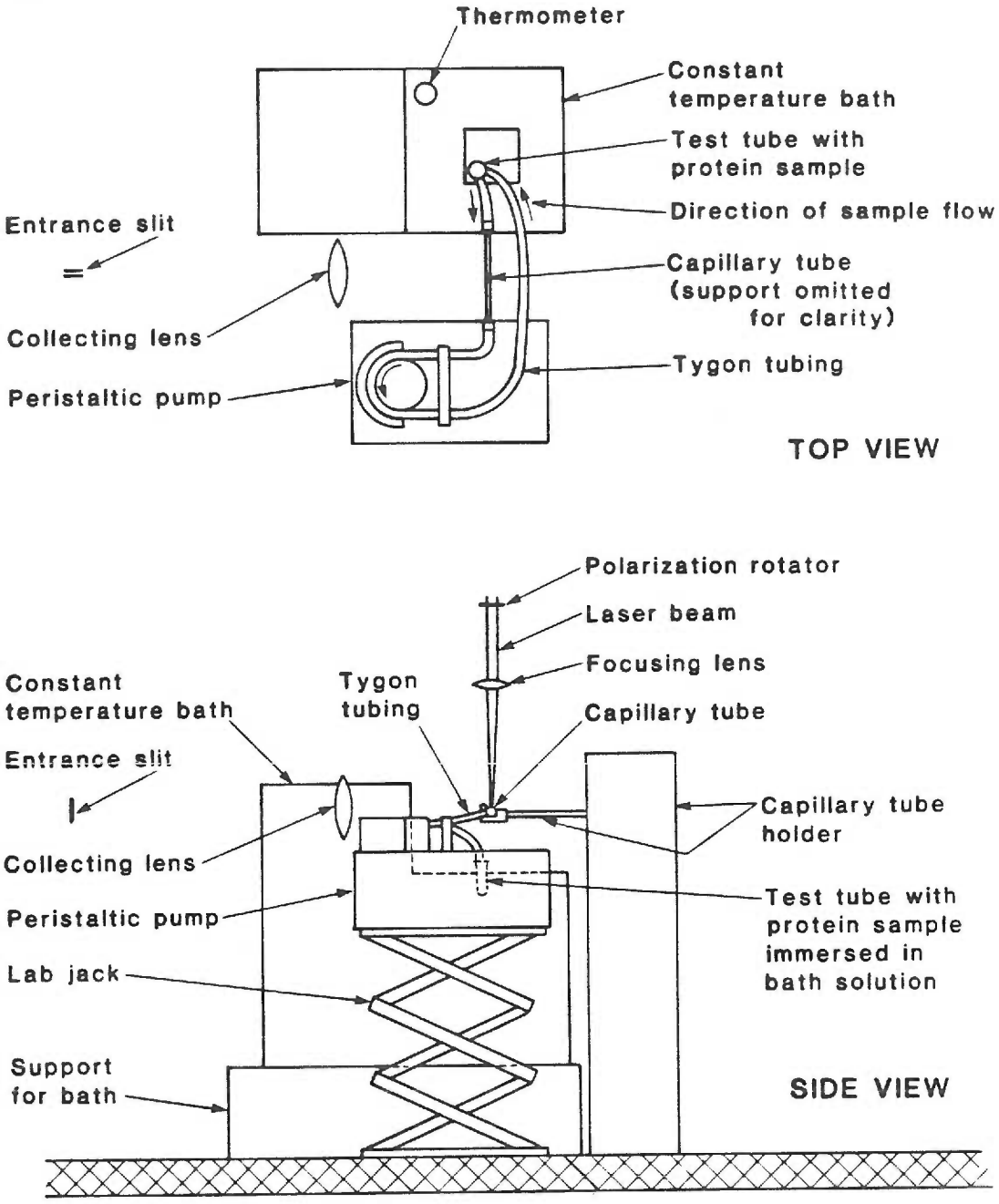
Thermometer
Constant temperature bath
Test tube with protein sample
Direction of sample flow
Entrance slit
Capillary tube (support omitted for clarity)
Collecting lens
Tygon tubing
Peristaltic pump
TOP VIEW
Polarization rotator
Laser beam
Focusing lens
Constant temperature bath
Tygon tubing
Capillary tube
Entrance slit
Capillary tube holder
Collecting lens
Test tube with protein sample immersed in bath solution
Peristaltic pump
Lab jack
Support for bath
SIDE VIEW

Figure 6

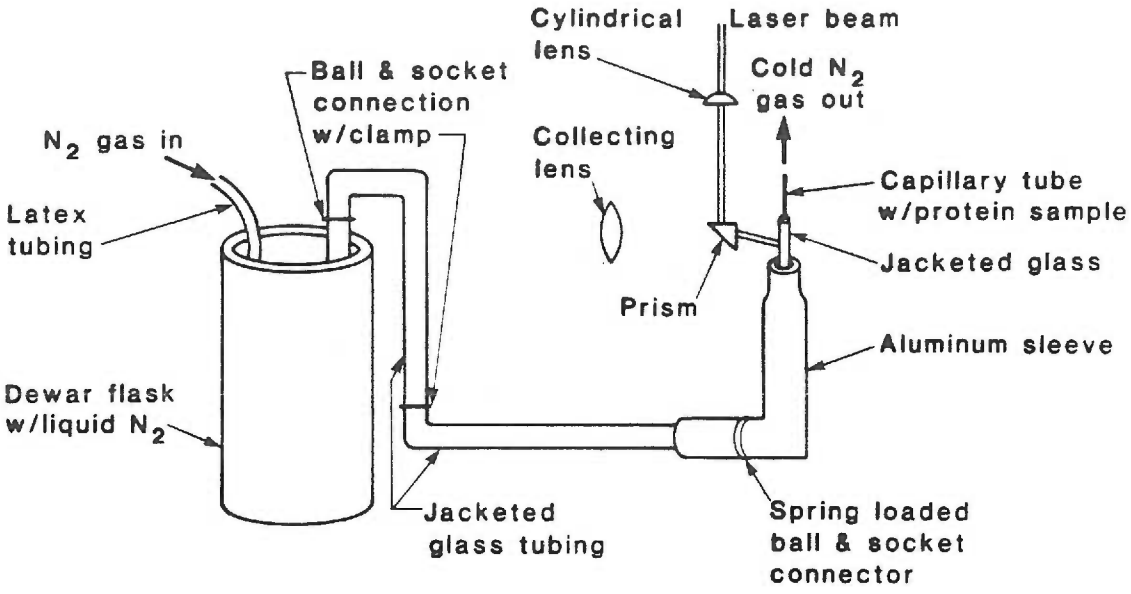
Cylindrical lens
Laser beam
Ball & socket connection w/clamp
Cold N_2 gas out
N_2 gas in
Collecting lens
Capillary tube w/protein sample
Latex tubing
Jacketed glass
Prism
Aluminum sleeve
Dewar flask w/liquid N_2
Jacketed glass tubing
Spring loaded ball & socket connector

Figure 7

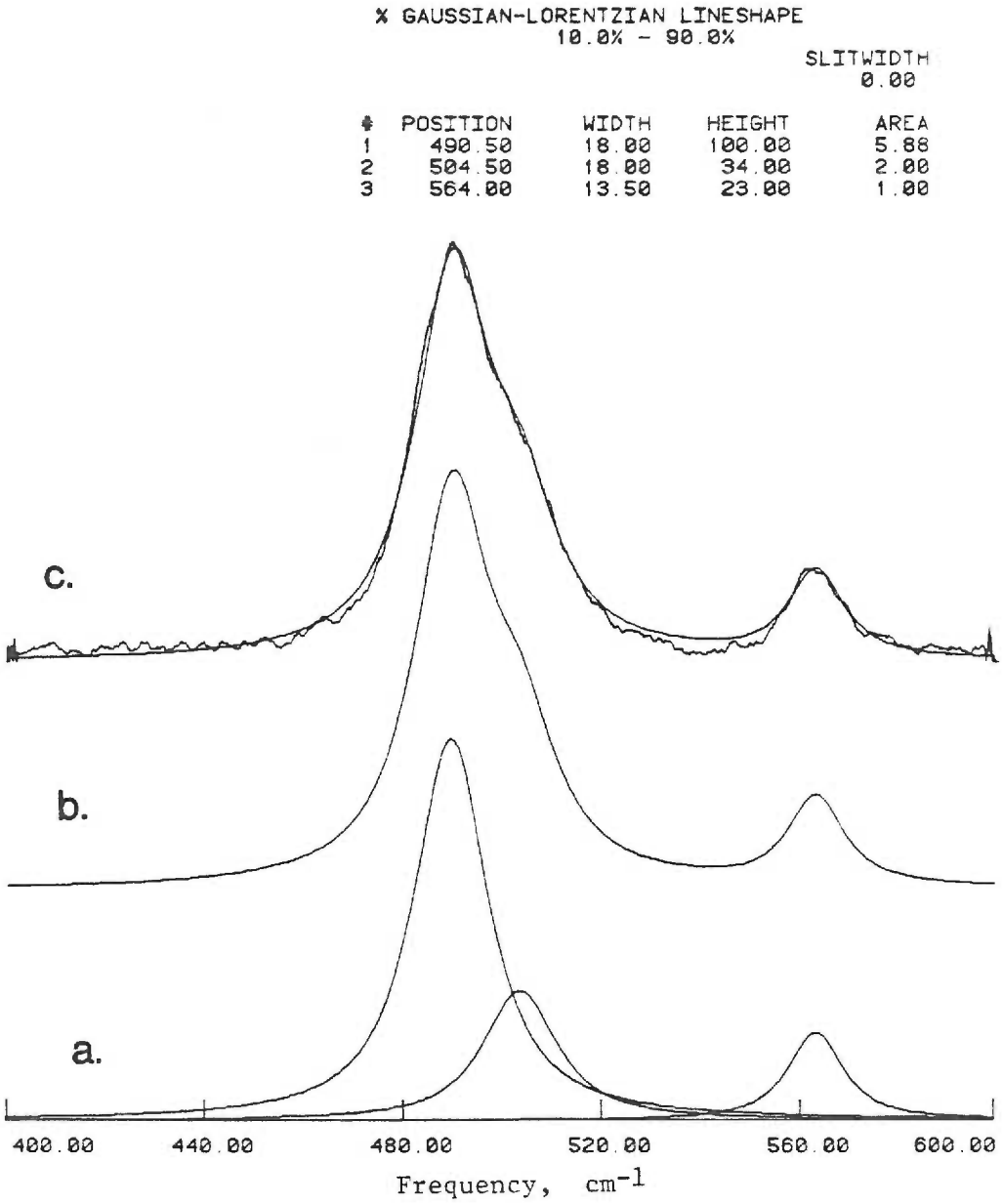
% GAUSSIAN-LORENTZIAN LINESHAPE
10.0% - 90.0%
SLITWIDTH
0.00
POSITION WIDTH HEIGHT AREA
1 490.50 18.00 100.00 5.88
2 504.50 18.00 34.00 2.00
3 564.00 13.50 23.00 1.00
c.
b.
a.
400.00
440.00
480.00
520.00
560.00
600.00
Frequency, cm-1

Figure 8

CHAPTER III

Resonance Raman Study of the Oxo-Bridged Binuclear Iron Center in Oxyhemerythrin.

Andrew K. Shiemke, Thomas M. Loehr, and Joann Sanders-Loehr

As published in the Journal of the American Chemical Society, 1985, **106**, 4951-4956.

ABSTRACT

Oxyhemerythrin, the respiratory protein of the marine sipunculid, Phascolopsis gouldii, was investigated by resonance Raman spectroscopy. The presence of a μ-oxo-bridged binuclear iron center in oxyhemerythrin was established by finding ν_s(Fe-O-Fe) at 486 cm^{-1} with ultraviolet excitation. In $H_2{}^{18}O$ solvent, the 486-cm^{-1} vibrational mode shifts to ≈475 cm^{-1}, a shift similar in magnitude to that observed for other μ-oxo bridged Fe(III) proteins, such as several methemerythrins and ribonucleotide reductase. A study of the enhancement profile of the ν_s(Fe-O-Fe) mode in oxyhemerythrin indicates that resonance occurs by coupling to the ≈360-nm transition, and serves to assign this band to an O^{2-} → Fe(III) charge transfer process. By contrast, although the ν_s(Fe-O-Fe) mode in azido-methemerythrin at 507 cm^{-1} is also strongly enhanced in the UV, this mode is observable with visible light excitation. Its enhancement profile is complex, showing apparent maxima at ≈525, 430, and <350 nm. These data indicate that significant differences exist in the electronic structures of the two chromophores. Further new findings in the present study are the observation of spectral lines at ≈753 cm^{-1} in oxyhemerythrin and 768 cm^{-1} in azidomethemerythrin that are assigned to the asymmetric vibration of the Fe-O-Fe bridge atoms. These frequencies also undergo isotope shifts in $H_2{}^{18}O$ by ≈35 cm^{-1} to lower energy, as expected from model complexes where the infrared active ν_{as}(Fe-O-Fe) have been well documented. In addition, the Fe-O-Fe deformation has been identified in azidomethemerythrin where it occurs at 292 cm^{-1} in $H_2{}^{16}O$ and 286 cm^{-1} in $H_2{}^{18}O$. The new data

provide a firm ground for the resonance Raman spectroscopic characterization of this structural unit in metalloproteins. D_2O solvent effects were also investigated; whereas azidomethemerythrin shows no deuterium-sensitive vibrational modes, both ν(O-O) at 844 cm^{-1} and ν(Fe-O_2) at 503 cm^{-1} in oxyhemerythrin were seen to shift in D_2O by +4 and -3 cm^{-1}, respectively. Since the deuterium isotope effect appears to be specific for oxyhemerythrin, it is likely that the bound-peroxide is protonated. The ability of the hydroperoxide moiety to undergo internal hydrogen bonding with the μ-oxo bridge oxygen may be the key to electronic structural differences in oxyhemerythrin relative to methemerythrin and ligated methemerythrins.

End of Abstract

Introduction

Hemerythrin is the respiratory protein of several marine invertebrates. The oxygen binding site of hemerythrin contains two non-heme irons which reversibly bind one molecule of dioxygen.[2,3] The deoxy form of the protein contains high-spin Fe(II) with octahedral coordination.[4] Upon binding dioxygen, charge is transferred from both irons to the dioxygen to give a peroxide complex, $[Fe(III)]_2\text{-}O_2^{2-}$. This representation of the active site of oxyhemerythrin is supported by spectroscopic studies which have shown both irons to be high-spin Fe(III) with effectively octahedral symmetry[4,5] and by resonance Raman studies which have located the dioxygen stretching vibration at 844 cm^{-1}, a frequency characteristic of peroxide.[6,7] Whereas deoxyhemerythrin is magnetically dilute, the oxy form contains antiferromagnetically-coupled irons with an exchange coupling constant (-J) of 77 cm^{-1}.[8] The structural feature responsible for this coupling has been proposed to be a μ-oxo bridge by analogy to the behavior of model complexes and methemerythrins.[5,8] Model compounds which closely reproduce the bridging geometry as well as the optical and magnetic properties of methemerythrins have recently been synthesized.[9]

In methemerythrin, both iron atoms are irreversibly oxidized to Fe(III) and the binuclear iron center exhibits a high affinity for small anions (e.g., N_3^-, CN^-, SCN^-, OCN^-).[5] The crystal structures of methemerythrins from Themiste dyscritum and Phascolopsis gouldii show that the two iron atoms are bound to amino acid side chains within four nearly parallel α-helical segments of a single polypeptide chain.[10,11] In the 2.2 Å resolution structure of azidomethemerythrin the active site contains two face-sharing octahedral iron atoms bridged by the carboxyl groups of aspartate and glutamate as well as by a μ-oxo group.[12] The presence of the μ-oxo bridge in methemerythrins is in agreement with the optical

properties,[4] the strong antiferromagnetic coupling ($-J = 134\ cm^{-1}$),[8] and, in particular, the Fe-O-Fe vibrational mode at $\approx 510\ cm^{-1}$ which undergoes a spectral shift upon isotopic exchange with the aqueous solvent.[13]

Preliminary x-ray crystallographic data for oxyhemerythrin[14] indicate that its active site structure is very similar to that of azidomethemerythrin, in which the peroxide and azide ions bind at the same site and the three bridging ligands remain intact. Further evidence that the structure of the binuclear iron center of methemerythrins is maintained in oxyhemerythrin comes from the similarity of their electronic[4,5,15] and x-ray absorption spectra,[16] as well as the magnitude of their antiferromagnetic coupling. EXAFS data[16] indicate that two short Fe-O bonds are present in both azidomethemerythrin (Fe-O = 1.80 Å) and oxyhemerythrin (Fe-O = 1.83 Å), as expected for a μ-oxo bridge. Resonance Raman experiments using mixed isotopes suggest that both peroxide and azide are bound in an end-on fashion at the active site.[17]

The most notable exceptions to the spectral similarities between met- and oxyhemerythrin come from Mössbauer and resonance Raman spectroscopy. Mössbauer spectra of oxyhemerythrins show a well-resolved pair of quadrupole-split doublets indicating the presence of two inequivalent iron atoms. In azidomethemerythrins, on the other hand, the two irons are more nearly chemically equivalent as judged by their Mössbauer parameters.[5,18,19] Although the differences in the Mössbauer spectra are not well understood, the similarities of the electronic spectra, EXAFS, and preliminary crystal structure would lead one to expect only a minor structural difference between azidomet- and oxyhemerythrin. In resonance Raman spectra obtained with visible light excitation, all methemerythrins exhibit a resonance-enhanced peak between 507-516 cm^{-1} assigned to the symmetric stretch of a bent Fe-O-Fe moiety.[13,17] No such vibrational mode was observed for oxyhemerythrin. We have now resolved this ambiguity and obtained direct evidence for the μ-oxo bridge in

oxyhemerythrin by finding that both the symmetric and asymmetric Fe-O-Fe vibrational modes are detectable using ultraviolet excitation. However, differences in the Fe-O-Fe frequencies and enhancement profiles between oxy- and met-hemerythrins again indicate a structural variation in their active sites. Deuterium isotope exchange experiments point to protonation of the bound peroxide, as had been postulated earlier to explain anomalous Mössbauer results.[5]

Experimental Section

Hemerythrin. Phascolopsis gouldii marine worms were obtained from the Marine Biological Laboratory, Woods Hole, MA. Oxyhemerythrin was prepared from the coelomic fluid of the worms using a procedure similar to that published by Klotz et al.[20] The protein was purified by crystallization via dialysis against 15% ethanol in water, then dissolved in sample buffer: 0.05 M Tris, 0.12 M sulfate (pH 8.0). The protein was stored as a sterile solution at 5°C. For resonance Raman spectral measurements, samples were dialyzed extensively against Raman buffer: 0.05 M Tris-sulfate (pH 8.0) containing 0.3 M SO_4^{2-} as an internal intensity standard. Azidomethemerythrin was prepared by dialyzing oxyhemerythrin versus Raman buffer containing 0.01 M N_3^-.

Oxygen Exchange. Raman buffer was prepared by adding 6.0 mg of solid Tris base and 42.6 mg of Na_2SO_4 to 1.0 mL of $H_2{}^{18}O$ (95.4 atom %, Monsanto Company) to give 0.05 M Tris and 0.3 M sulfate. This was titrated with concentrated H_2SO_4 to a pH of 8.0. Oxygen exchange into oxyhemerythrin was accomplished as follows. Thiocyanatomethemerythrin (≈2 mM in hemerythrin monomer, 0.1 M in thiocyanate) was reduced to deoxyhemerythrin by dialysis against an anaerobic solution of dithionite (≈8 mM) in sample buffer. Excess dithionite and thiocyanate were removed by extensive anaerobic dialysis against sample buffer. The deoxyhemerythrin was then crystallized by anaerobic dialysis against 20% ethanol in water. The deoxy crystals were collected under N_2 and dissolved in 1.0 mL of $H_2{}^{18}O$ Raman buffer which had been

degassed with dry N_2. The solution was placed in a sealed vial and stored at 4°C for 2 days. The protein was then converted to oxyhemerythrin by exposure to air for 6 h and used immediately for Raman experiments. Optical spectra indicated that the samples contained >90% oxyhemerythrin.

For the preparation of azidomethemerythrin,[13] oxyhemerythrin was first crystallized by dialysis against 15% ethanol in water. The crystals were then dissolved in 1.0 mL of $H_2{}^{18}O$ Raman buffer. Solid NaN_3 was added to give a final concentration of 0.01 M and, thereby, convert the oxyhemerythrin to azidomethemerythrin with concomitant bridge exchange. Hydroxomet- and met-(anion-free) hemerythrins were prepared from ^{18}O-bridged oxyhemerythrin which was prepared as described above. The oxyhemerythrin was oxidized by addition of a 5-fold excess of $K_3Fe(CN)_6$ and then dialyzed versus 0.05 M 2-(N-morpholino)-ethanesulfonate, 0.3 M sulfate (pH 6.0) in H_2O to give ^{18}O-bridged methemerythrin or versus 0.05 M Tris, 0.3 M sulfate (pH 9.0) in H_2O to give ^{18}O-bridged hydroxomethemerythrin. Thiocyanatomethemerythrin was prepared from ^{18}O-bridged methemerythrin by the addition of 50X KSCN. When the optical spectrum showed that conversion was complete, the sample was dialyzed versus 0.05 M Tris, 0.3 M sulfate, 0.025 M SCN^- (pH 8.0) in H_2O.

Deuterium Exchange. D_2O buffer was prepared 6-fold concentrated (1.8 M $SO_4{}^{2-}$) by adding 0.75 mL of conc. H_2SO_4 to 7.5 mL of D_2O. Solid Tris base was added to give a pD of 8.55. The solvent was removed using a rotary evaporator and the remaining solid was redissolved in 45 mL of D_2O to give 0.3 M $SO_4{}^{2-}$-Tris (pD 8.55). The D_2O buffer exchange was accomplished in either of two different ways: (1) protein was dialyzed against the D_2O buffer for ≈2 days; (2) concentrated protein (≈6 mM) was applied to a Sephadex G-25 column (≈2.5 mL column volume) which had been saturated with D_2O buffer and was then eluted with D_2O buffer. The second method was much faster, being complete in ≈30 min, though both methods gave identical results.

Azidomethemerythrin in D_2O buffer was prepared by adding solid NaN_3 to oxyhemerythrin in D_2O buffer, to give a final azide concentration of 0.01 M.

Spectroscopy. Resonance Raman spectra were collected on a computer-interfaced Jarrell-Ash spectrophotometer[21] equipped with Spectra-Physics 164-05 (Ar) and 164-01 (Kr) ion lasers, an RCA C31034 photomultiplier tube, and an ORTEC Model 9302 amplifier/discriminator. Both lasers are equipped with ultra high-field magnets to enhance ultraviolet output. Typical sample concentrations were 1-1.5 mM in hemerythrin monomer. Sample decomposition was minimized through use of a flow cell. A reservoir of 2-3 mL protein solution was placed in a constant temperature bath maintained at 3-5°C. The sample was pumped through 0.8 mm i.d. tygon tubing and a 1.6 mm o.d. quartz capillary tube (situated transverse to the incident laser beam) in a recirculating system with a flow rate of ≈1.5 mL/min. In all cases a 90°-scattering geometry was used and multiple scans were collected to enhance the signal-to-noise ratio. Sample integrity was monitored by obtaining optical spectra (Cary 16) both before and after exposure to the laser beam. Only upon prolonged exposure of oxyhemerythrin to UV laser light was there any appreciable sample degradation; however, even these samples typically retained >80% activity as measured by the A_{500}/A_{326} ratio, using extinction coefficients reported by Dunn et al.[7] For the resonance Raman enhancement profiles, 0.3 M SO_4^{2-} (ν_1 = 981 cm^{-1}) was used as the internal intensity standard. Corrections for self-absorption were made[22] but found to be insignificant compared to the uncertainty inherent in the measurement.

Results and Discussion

Fe-O-Fe Vibrations. The resonance Raman spectrum of oxyhemerythrin obtained with 363.8 nm excitation is shown in Figure 1. In $H_2{}^{16}O$, the protein shows a

strongly enhanced feature at 486 cm^{-1} and a weaker feature at ≈753 cm^{-1}. When the protein is prepared in $H_2{}^{18}O$, these two peaks shift to lower energy by 11 and 33 cm^{-1}, respectively (Fig. 1 and Table I). The isotope dependence identifies these vibrations as Fe-O modes and the exchangeability with solvent oxygen implies that they are associated with an Fe-O-Fe moiety in oxyhemerythrin. The 486 cm^{-1} peak can be assigned to the symmetric stretching vibration on the basis of its intensity, frequency, depolarization ratio, and on the magnitude of its O-isotope shift (see below). The symmetric Fe-O-Fe mode has been observed previously in a number of methemerythrin species using visible light excitation, but never in oxyhemerythrin.[13,17] The failure to detect this vibrational mode of oxyhemerythrin was due to the fact that, in contrast to the methemerythrins, it is only enhanced with near-UV excitation (Fig. 2). Thus, the present findings provide the first direct evidence for the existence of μ-oxo-bridge in the binuclear iron site of oxyhemerythrin.

Our ability to exchange the μ-oxo-bridge oxygen of oxyhemerythrin is also a new result. In earlier experiments Kurtz et al.[17] and Freier et al.[13] were unable to observe ^{18}O-exchange during the conversion of deoxy to oxyhemerythrin. In their work, crystals of oxyhemerythrin were dissolved in $H_2{}^{18}O$ buffer, reduced with dithionite and then immediately reoxygenated.[13,17] The only obvious procedural differences are that our deoxyhemerythrin was prepared by dithionite reduction of thiocyanatomethemerythrin and that the deoxyhemerythrin (with or without crystallization) was equilibrated in $H_2{}^{18}O$ buffer for 2 days prior to oxygenation. The longer period of exposure of deoxyhemerythrin to $H_2{}^{18}O$ is the most likely explanation for the exchange observed in our experiments. Alternatively, it is possible that we achieved a conformation of deoxyhemerythrin that is more susceptible to bridge exchange by having performed the reduction on the thiocyanato (as opposed

to the oxy) form of the protein. Kinetic studies have shown that thiocyanatomethemerythrin undergoes more facile reduction with dithionite than other forms of methemerythrin.[23] Moreover, the mixed valence Fe(II),Fe(III) semi-methemerythrins are believed to exist in several different conformations.[24]

The ν_s(Fe-O-Fe) assignment in oxyhemerythrin is compatible with analogous vibrations which have been observed in the Raman spectra of other oxo-bridged compounds.[25-29] Systems which have been shown to contain a nonlinear Fe-O-Fe structural unit and give rise to a resonance-enhanced symmetric Fe-O-Fe vibration near 500 cm^{-1} are ribonucleotide reductase,[28] $Fe_2O(CH_3COO)_2(HBpz_3)_2$,[27] $[Fe_2O(o\text{-phenanthroline})_4]^{4+}$,[29] and all forms of methemerythrin[13] (other than sulfidomethemerythrin). The corresponding isotope shifts for ν_s(Fe-O-Fe) with ^{18}O are -15 cm^{-1} for ribonucleotide reductase,[28] -5 to -18 for the model compounds (Table I), and -10 to -16 cm^{-1} for the methemerythrins (Table I). The -11 cm^{-1} shift for oxyhemerythrin is well within this range. Furthermore, all of these systems appear to show maximal resonance enhancement with UV excitation. Although the ν_s(Fe-O-Fe) mode in methemerythrins was originally observed in resonance with visible electronic transitions,[7,13] we have now found additional enhancement with UV excitation for the N_3^- (Fig. 3, middle), CN^-, CNO^-, SCN^-, OH^-, Cl^-, ClO_4^-, and met (anion-free) forms of the protein. Thus, the 486 cm^{-1} peak in the Raman spectrum of oxyhemerythrin shows the characteristics expected for the symmetric stretching vibration of a bent Fe-O-Fe moiety.

The additional oxygen-isotope sensitive vibrational mode at ≈753 cm^{-1} in oxyhemerythrin can be assigned to the asymmetric Fe-O-Fe vibration on the basis of its frequency, its low intensity relative to ν_s(Fe-O-Fe), and its isotope shift. An analogous oxygen isotope-sensitive peak was observed in every form of methemerythrin we investigated (Table I). In all cases, the ν_{as}(Fe-O-Fe) was

maximally enhanced with UV excitation. For oxyhemerythrin and azidomethemerythrin, the UV enhancement profiles of ν_{as}(Fe-O-Fe) appeared to parallel those of ν_s(Fe-O-Fe). The intensity of the asymmetric vibration was difficult to quantitate due to the presence of an additional spectral feature at ≈757 cm^{-1} which becomes apparent in $H_2{}^{18}O$ (Fig. 1). Since this feature was also discernible in all of the methemerythrin samples studied in both $H_2{}^{16}O$ and $H_2{}^{18}O$ and is not attributable to the Raman buffer at this concentration, it is most likely due to a protein moiety such as tryptophan.[30] Although accurate depolarization ratios could not be obtained for the 750-780 cm^{-1} feature, it appears to be depolarized as expected for an asymmetric vibration.

The 750-780 cm^{-1} frequencies and the -33 to -38 cm^{-1} isotope shifts of the asymmetric bridge modes in hemerythrins are comparable to the behavior of μ-oxo-bridged model complexes (Table I). The closest agreement is with the pyrazolylborate complex[9a,27] which has a similar small Fe-O-Fe bridging angle of 123.5° compared to 135° in azidomethemerythrin.[31] The bond angles in the other two model compounds are ≈155° and, thus, are expected to have their asymmetric vibrational modes at higher energy.[32] In model compounds ν_{as}(Fe-O-Fe) is generally observed by ir spectroscopy. The phenanthroline and chloride complexes also give weak Raman bands at corresponding frequencies, but only the protein shows clear-cut resonance enhancement of this vibrational mode. It has been suggested that the protein band is a $\nu_s + \delta$ combination band as in the pyrazolylborate complex.[27] This seems unlikely since the protein peak at ≈750 cm^{-1} exhibits a much greater isotope shift than would be expected for a combination band from a $\Delta\nu_s$ of -11 to -16 and a $\Delta\delta$ of -6 cm^{-1} (see below).

A third $H_2{}^{18}O$-sensitive vibration has been detected in several methemerythrins. In azidomethemerythrin, the peak at 292 cm^{-1} shifts to 286 cm^{-1} in the

^{18}O-substituted protein (Fig. 4). This vibrational mode had previously been assigned to ν(Fe-histidine).[7,13] However, it is more appropriately described as the deformation mode of the Fe-O-Fe moiety. Analogous vibrations have been detected in the Raman spectra of two oxo-bridged model compounds (Δ = -5 to -14 cm^{-1} in $H_2{}^{18}O$) and probably also in thiocyanotomethemerythrin (Table I). However, no δ(Fe-O-Fe) frequencies have yet been observed in either oxyhemerythrin or the hydroxo, cyanato, cyano, and ligand-free forms of methemerythrin.

Enhancement Profiles: Exogenous Ligands. Analysis of Raman spectral intensities as a function of excitation wavelength gives information about the nature of the electronic transitions responsible for the vibronic coupling. The electronic spectra for oxyhemerythrin and azidomethemerythrin are shown in the upper panels of Figures 2 and 3, respectively. The lower panels illustrate enhancement profiles for the vibrations due to the exogenous ligands, $O_2{}^{2-}$ and $N_3{}^-$. The data for the visible region are in good agreement with previously published profiles.[7,13] The intensity of ν(Fe-O_2) of oxyhemerythrin maximizes at 525 nm whereas the intensities of ν(Fe-N_3) and ν(N-N) of azidomethemerythrin maximize at 490 nm and 480 nm, respectively. We have extended these profiles into the near-UV region of the electronic spectrum. The O-O stretching vibration at 844 cm^{-1} in oxyhemerythrin steadily decreases in intensity with increasing frequency of the incident light, vanishing with near-UV excitation. This is not the case for the stretching modes due to Fe-N_3 at 375 cm^{-1} and N-N at 2048 cm^{-1} in the azidomethemerythrin spectrum or Fe-O_2 at 503 cm^{-1} in the oxyhemerythrin spectrum. All three of these vibrations show enhancement into the near UV; the Fe-O_2 stretching mode appears to be coupled to the 360-nm transition in oxyhemerythrin, whereas the Fe-N_3 and N-N stretching frequencies appear to be coupled to the 325-nm transition in azidomethemerythrin.

The enhancement profiles for $\nu(Fe\text{-}O_2)$ and $\nu(Fe\text{-}N_3)$ are in excellent agreement with the single-crystal spectroscopic studies by Solomon et al.[15,33] These authors observed electronic transitions which were polarized perpendicular($\perp$) to the Fe-Fe axis and assigned them to charge transfer resulting from end-on binding of peroxide or azide to a single iron atom. The $\perp$-polarized transitions at ≈500 and ≈360 nm in oxyhemerythrin are presumably responsible for the Raman enhancement maxima of $\nu(Fe\text{-}O_2)$ at 525 and ≈360 nm. Similarly, the $\perp$-polarized transitions at ≈490 and ≈325 nm in azidomethemerythrin are consistent with the observed Raman enhancement maximum of $\nu(Fe\text{-}N_3)$ at 490 nm and an additional maximum <350 nm.

Enhancement Profiles: μ-Oxo Bridge. The symmetric Fe-O-Fe vibrations of azidomethemerythrin and oxyhemerythrin (Figs. 2 and 3, middle) both show the strongest resonance enhancement by coupling with electronic transitions in the 300-400 nm region. These electronic transitions were originally assigned as μ-oxo → Fe(III) charge-transfer bands, based on comparison to the electronic spectra of μ-oxo-bridged iron model complexes.[5] This assignment is consistent with the single-crystal studies in which absorption parallel to the iron-iron axis was found to dominate the UV spectra of oxy- and azidomet-hemerythrin.[15,33] However, Schugar et al.[34] have suggested that these near-UV bands in the model complexes (particularly the $[(Fe\text{-HEDTA})_2O]^{2-}$ complex) are due to simultaneous pair electronic (SPE) transitions, and that the same mechanism may be responsible for the near-UV bands in hemerythrin. It has been pointed out that the nature of the temperature dependence of the intensity of the hemerythrin near-UV bands is inconsistent with an SPE assignment.[33] Our enhancement profiles show that excitation in the near-UV region selectively enhances Fe-O-Fe vibrations. For this reason, we would also assign these electronic bands as charge-transfer bands.

In a theoretical analysis of μ-oxo-bridged binuclear Cr(III) complexes,[35] several electronic bands at ≈350 nm were assigned to transitions from a metal d-orbital to M-O-M bridge orbitals (combinations of d-orbitals from both metals and p-orbitals from the bridging μ-oxo atom[36]). This type of electronic transition would be particularly favorable for the resonance Raman enhancement of Fe-O-Fe vibrational modes by including contributions from all three atoms of the bridge to the terminal molecular orbital for the electronic transition. We suggest that a similar mechanism prevails in the case of the strong enhancement of the symmetric Fe-O-Fe vibrational mode in hemerythrin.

The interpretation of the ν(Fe-O-Fe) excitation profiles in the visible region is less straightforward than for the UV region. Whereas oxyhemerythrin shows no enhancement in the visible region, azidomethemerythrin shows that its ν_s(Fe-O-Fe) is coupled to electronic transitions at both ≈525 and ≈430 nm. This striking difference in the visible enhancement profiles indicates that there must be significant differences in the electronic structures and/or vibronic coupling in the Fe-O-Fe moieties in oxy- and azidomet-hemerythrin. The electronic transitions at ≈525 and ≈430 nm in azidomethemerythrin are probably due to additional charge transfer interactions between various iron d-orbitals and Fe-O-Fe bridge orbitals. In the case of the oxo-bridged chromium complexes, multiple charge transfer transitions have also been ascribed to the M-O-M moiety.[35] Although the 430-530 nm region is not well-resolved in the single-crystal spectra of azidomethemerythrin, a distinct shoulder is observed at ≈500 nm in the spectrum polarized parallel to the Fe-Fe axis[33] indicating the presence of an $O^{2-} \rightarrow$ Fe(III) charge transfer band at ≈500 nm. All of the other methemerythrins are likely to have similar Fe-oxo charge transfer bands in the visible region, as they all exhibit resonance-enhanced Fe-O-Fe vibrations with excitation between 430 and 530 nm.[13]

The excitation profile of δ(Fe-O-Fe) in Figure 3 is surprisingly different from that of ν(Fe-O-Fe). As has been observed previously,[7] the 292 cm^{-1} peak is maximally enhanced with 490 nm excitation, in parallel with the 375-cm^{-1} ν(Fe-N_3) of the exogenous azide ligand. However, δ(Fe-O-Fe) does not appear to be enhanced with uv excitation and is missing entirely in the resonance Raman spectrum of oxyhemerythrin. These results suggest that the δ(Fe-O-Fe) motion is coupled to an N_3^- → Fe(III) electronic transition. The only other δ(Fe-O-Fe) mode which we observed was in the spectrum of thiocyanotomethemerythrin (Table I). These two complexes have markedly more intense electronic absorption bands[5] in the visible region (ε = 3,700 and 5,100 M^{-1} cm^{-1} for N_3^- and SCN^-, respectively) than oxyhemerythrin (ε = 2,200 M^{-1} cm^{-1}) or the other methemerythrins (ε ≦ 1,200 M^{-1} cm^{-1}). Thus, they may be more effective in promoting vibronic coupling of δ(Fe-O-Fe) with a L →Fe(III) charge transfer process.

D_2O Substitution. Additional information about the structure of the binuclear iron center in oxyhemerythrin has been obtained by examining the resonance Raman spectrum of the deuterated protein (Fig. 5). In H_2O solution, ν(O-O) of the bound peroxide is observed at 844 cm^{-1} and ν(Fe-O_2) at 503 cm^{-1}. However, in D_2O solution, ν(O-O) is shifted to 848 cm^{-1} and ν(Fe-O_2) is shifted to 500 cm^{-1}. The computer-generated difference spectra (upper panel) show that these shifts, though small, are readily detectable. The 4-cm^{-1} increase in ν(O-O) and the 3-cm^{-1} decrease in ν(Fe-O_2) agree with the values of +2 cm^{-1} and -3 cm^{-1} reported previously for oxyhemerythrin in D_2O.[37]

The isotopic shifts in deuterated oxyhemerythrin appear to be specific to peroxide binding rather than a general change in protein conformation affecting the structure of the active site. Addition of 0.01 M NaN_3 to the oxyhemerythrin samples used to obtain the data in Figure 5 results in indistinguishable azidomethemerythrins in H_2O and D_2O (Fig. 4). This absence of a deuterium isotope effect in azidomethemerythrin was also reported by Kurtz et al.[17] Since neither the 507-

and 292 cm^{-1} Fe-O-Fe vibrations nor the 375-cm^{-1} Fe-N_3 vibration are affected, there seem to be no deuterium substitution-induced conformational effects on the vibrations in the ligand binding site of the protein. Furthermore, neither the symmetric nor the asymmetric Fe-O-Fe vibration observed in oxyhemerythrin with UV excitation is affected by deuteration. Thus, the ν(Fe-O_2) and ν(O-O) shifts seen upon deuteration appear to be due to effects of the isotope substitution specific to the bound peroxide.

A plausible explanation for the deuterium isotope effect is that the bound dioxygen species in oxyhemerythrin is protonated. The shift of the Fe-O_2 stretching mode from 503 to 500 cm^{-1} is close to that expected for the change in mass when D replaces H in a coordinated hydroperoxide (calculated value, 498 cm^{-1}). The 4 cm^{-1} increase in ν(O-O) is clearly not commensurate simply with a change in mass. However, electronic or structural alterations accompanying deuteration could increase the force constant for ν(O-O) and, thereby, outweigh the mass effect. The ν(O-O) of D_2O_2 similarly shows no mass effect.[38] It is of interest to note that for cobalt-substituted myoglobin and hemoglobin, in which the bound dioxygen is believed to be hydrogen-bonded to the distal histidine, the ν(O-O) shifts from 1124 to 1136 cm^{-1} for oxyCoMb and from 1133 to 1138 cm^{-1} for oxyCoHb upon deuteration.[39]

Other unusual features associated with peroxide binding relative to azide binding are: (1) both ν_{as} and ν_s(Fe-O-Fe) are 20 cm^{-1} lower in oxyhemerythrin than in azidomethemerythrin (Table I); (2) ν_s(Fe-O-Fe) is only enhanced with UV excitation in oxyhemerythrin but with both visible and UV excitation in azidomethemerythrin. Since x-ray absorption spectroscopy and x-ray crystallography have indicated that the active site geometries are very similar in these two forms of the protein,[14,16] the resonance Raman observations described here must be due to more subtle structural and

electronic differences. Metal-ligand bond strengths are unlikely to be an important factor since methemerythrin complexes with a variety of exogenous ligands, including predominantly σ bonders (such as Cl^- and OH^-) and stronger π bonders (such as N_3^- and CN^-), all show resonance enhancement of ν_s(Fe-O-Fe) with visible excitation and these vibrations occur in a remarkably narrow range from 507-516 cm^{-1},[13] some 20-30 cm^{-1} higher in frequency than observed for oxyhemerythrin.

An attractive proposal is that the hydroperoxide ligand in oxyhemerythrin is hydrogen-bonded to the μ-oxo bridge (Fig. 6). This structure would provide an explanation for the distinct lowering of the Fe-O-Fe symmetric stretching frequency in oxyhemerythrin relative to the methemerythrins. Support for the hydrogen-bonded model comes from x-ray crystallography where the electron density contours for the bound dioxygen in oxyhemerythrin appear to be located closer to the Fe-Fe axis than is the case for the bound azide in azidomethemerythrin.[14] An alternative explanation would be that steric restrictions at the exogenous ligand site force the Fe-O-Fe unit to adopt a slightly different conformation in the presence of a protonated peroxide relative to a variety of unprotonated ligands. This seems unlikely in view of the number of bulkier ligands such as linear, N-coordinated NCS^- and bent NO_2^- which still have their Fe-O-Fe vibrations in the high frequency range (Table I and Ref. 13). Moreover, if a change in the Fe-O-Fe angle had occurred in oxyhemerythrin relative to the methemerythrins, then the frequencies for the symmetric and asymmetric vibrations should have shifted in <u>opposite</u> directions[32] rather than both showing an ≈20 cm^{-1} decrease. Yet another possibility is that the lowered frequencies in oxyhemerythrin are due to incomplete oxidation of the iron atoms. However, the amount of residual Fe(II) is probably too small to account for the observed shifts in ν_s and ν_{as} in view of the characteristic high spin Fe(III) isomer shift in the Mössbauer spectrum[5] and the peroxide vibrational frequency in the resonance Raman spectrum[17] of oxyhemerythrin.

Conclusion

The symmetric Fe-O-Fe vibration in oxyhemerythrin has now been located using an ultraviolet source for resonance Raman experiments. This finding provides direct evidence for the presence of a μ-oxo-bridged binuclear iron center in oxyhemerythrin, as had been suggested previously from spectroscopic and structural studies. We have also been able to detect the weaker asymmetric Fe-O-Fe vibration in oxyhemerythrin and in a number of methemerythrin-ligand complexes. Both ν_s and ν_{as} are ≈20 cm^{-1} lower for oxyhemerythrin than for the methemerythrins, indicating a difference in the electronic structure of the Fe-O-Fe moiety. This is corroborated by the fact that the μ-oxo bridge vibrations in oxyhemerythrin are only vibronically coupled with an ultraviolet electronic transition, whereas all the methemerythrins show vibronic coupling of the oxo-bridge vibrations with transitions both in the visible and in the UV region.

Analysis of the effects of deuterium substitution on the vibrations of the bound peroxide in oxyhemerythrin leads to the proposal that this group is protonated. Coordination of a protonated peroxide moiety at the active site is reasonable in view of the fact that no dinegative anions are known to bind to methemerythrins. Protonation serves to reduce the high charge of the end-on peroxy ligand and provides a mechanism for further stabilization of the bound peroxide by hydrogen-bonding to the μ-oxo bridge. The presence of a H-bonded hydroperoxide species in oxyhemerythrin had been suggested previously as a possible explanation for the Mössbauer finding that the two irons are less chemically equivalent than in any of the met forms.[5] The involvement of the bridging oxo group as the H-bond acceptor would explain the unusual ν_s(Fe-O-Fe) frequency and resonance enhancement in oxyhemerythrin relative to the methemerythrins. Since several studies have shown that the oxygen affinity[40] and rate of oxygen binding[41] in hemerythrin are unaffected by changes in $[H^+]$ between pH 6 and 9, a proton attached to the bound peroxide would have to be derived from an appropriate donor in deoxyhemerythrin. A possible donor might be an Fe(II)-ligated hydroxo group[14,42] in the deoxygenated protein.

Acknowledgments:

The authors are grateful to John D. McCallum for contributing to the early phases of this investigation, and to Harry B. Gray, Donald M. Kurtz, Jr., Ralph G. Wilkins and Patricia C. Harrington for helpful discussions. This research was supported by the National Institutes of Health (GM 18865).

References and Notes

1. (a) Oregon Graduate Center. (b) Portland State University.
2. Sanders-Loehr, J.; Loehr, T.M. Adv. Inorg. Biochem. 1979, 1, 235-252.
3. Wilkins, R.G.; Harrington, P.C. Adv. Inorg. Biochem. 1983, 5, 52-85
4. Sanders-Loehr, J.; Loehr, T.M.; Mauk, A.G.; Gray, H.B. J. Am. Chem. Soc. 1980, 102, 6992-6996.
5. Garbett, K.; Darnall, D.W.; Klotz, I.M.; Williams, R.J.P. Arch. Biochem. Biophys. 1969, 135, 419-434.
6. Dunn, J.B.R.; Shriver, D.F.; Klotz, I.M. Proc. Natl. Acad. Sci. USA 1973, 70, 2582-2584.
7. Dunn, J.B.R.; Addison, A.W.; Bruce, R.E.; Sanders-Loehr, J; Loehr, T.M. Biochemistry 1977, 16, 1743-1749.
8. Dawson, J.W.; Gray, H.B.; Hoenig, H.E.; Rossman, G.R.; Schredder, J.M.; Wang, R.H. Biochemistry 1972, 11, 461-465.
9. (a) Armstrong, W.H.; Lippard, S.J. J. Am. Chem. Soc. 1983, 105, 4837-4838; (b) Wieghardt, K.; Pohl, K.; Gebert, W. Angew. Chem. Int. Ed. Eng., 1983, 22, 727.
10. Stenkamp, R.E.; Jensen, L.H. Adv. Inorg. Biochem. 1979, 1, 219-233.
11. Ward, K.B.; Hendrickson, W.A.; Klippenstein, G.L. Nature 1975, 257, 818-821.
12. Stenkamp, R.E.; Sieker, L.C.; Jensen, L.H.; Sanders-Loehr, J. Nature 1981, 291, 263-264.
13. Freier, S.M.; Duff, L.L.; Shriver, D.F.; Klotz, I.M. Arch. Biochem. Biophys. 1980, 205, 449-463.
14. Stenkamp, R.E.; Sieker, L.C.; Jensen, L.H.; McCallum, J.D.; Sanders-Loehr, J. unpublished results.
15. Gay, R.R.; Solomon, E.I. J. Am. Chem. Soc. 1978, 100, 1972-1973.

16. (a) Elam, W.T.; Stern, E.A.; McCallum, J.D.; Sanders-Loehr, J. J. Am. Chem. Soc. 1982, 104, 6369-6373. (b) Hendrickson, W.A.; Co, M.S.; Smith, J.L.; Hodgson, K.O.; Klippenstein, G.L. Proc. Natl. Acad. Sci. USA 1982, 79, 6255-6259.

17. Kurtz, D.M.; Shriver, D.F.; Klotz, I.M. Coord. Chem. Rev. 1977, 24, 145-178.

18. York, J.L.; Bearden, A.J. Biochemistry 1970, 9, 4549-4554.

19. Clark, P.E.; Webb, J. Biochemistry 1981, 20, 4628-4632.

20. Klotz, I.M.; Klotz, T.A.; Fiess, H.A. Arch. Biochem. Biophys. 1957, 68, 284-299.

21. Loehr, T.M.; Keyes, W.E.; Pincus, P.A. Anal. Biochem. 1979, 96, 456-463.

22. (a) Dunn, J.B.R.; Shriver, D.F. Appl. Spectrosc. 1974, 28, 319-323; (b) Strekas, T.C.; Adams, D.H.; Packer, A.; Spiro, T.G. ibid. 1974, 28, 324-327.

23. Olivas, E.; deWaal, D.J.A.; Wilkins, R.G. J. Inorg. Biochem. 1979, 11, 205-212.

24. Bradic, Z.; Harrington, P.C.; Wilkins, R.G.; Yoneda, G. Biochemistry 1980, 19, 4149-4155.

25. Burke, J.M.; Kincaid, J.R.; Spiro, T.G. J. Am. Chem. Soc. 1978, 100, 6077-6083.

26. Solbrig, R.M.; Duff, L.L.; Shriver, D.F.; Klotz, I.M. J. Inorg. Biochem. 1982, 17, 69-74.

27. Armstrong, W.H.; Spool, A,; Papaefthymiou, G.C.; Frankel, R.B.; Lippard, S.J., personal communication.

28. Sjöberg, B.-M.; Loehr, T.M.; Sanders-Loehr, J. Biochemistry 1982, 21, 96-102.

29. Plowman, J.E.; Loehr, T.M.; Schauer, C.K.; Anderson, O.P. submitted (1983).

30. Lord, R.C.; Yu, N-T. J. Mol. Biol. 1970, 50, 509-524.

31. Stenkamp, R.E.; Sieker, L.C.; Jensen, L.H. J. Am. Chem. Soc. 1984, 106, 618-622.

32. Wing, R.M.; Callahan, K.P. Inorg. Chem. 1969, 8, 871-874.

33. Solomon, E.I.; Eickman, N.C.; Gay, R.R.; Penfield, K.W.; Himmelwright, R.S.; Loomis, L.D. in Invertebrate Oxygen Binding 1981, pp 487, J. Lamy and J. Lamy, Eds., Marcel Dekker, New York.

34. Schugar, H.J.; Rossman, G.R.; Barraclough, C.G.; Gray, H.B. J. Am. Chem. Soc. 1972, 94, 2683-2690.

35. Schmidtke, H.H. Theor. Chim. Acta 1971, 20, 92-104.

36. Jezowska-Trzebiatowska, B. Pure Appl. Chem. 1971, 27, 89-111.

37. Kurtz, Jr., D.M. Ph.D. Dissertation, Northwestern University 1977.

38. Taylor, R.C.; Cross, P.C. J. Chem. Phys. 1956, 24, 41-44.

39. Kitagawa, T.; Ondrias, M.R.; Rousseau, D.L.; Ikeda-Saito, M.; Yonetani, T. Nature 1982, 298, 869-871.

40. Kubo, M. Bull. Chem. Soc. Japan 1953, 26, 189-192.

41. Bradic, Z.; Wilkins, R.G. personal communication.

42. Elam, W.T.; Stern, E.A.; McCallum, J.D.; Sanders-Loehr, J. J. Am. Chem. Soc. 1983, 105, 1919-1923.

Table I. Vibrational frequencies (in cm^{-1}) for the symmetric and asymmetric stretching modes of the Fe-O-Fe cluster in hemerythrins and model compounds.

	ν_s(Fe-O-Fe)[a]		ν_{as}(Fe-O-Fe)[e]		δ(Fe-O-Fe)[a]	
Sample	$H_2{}^{16}O$	$H_2{}^{18}O$	$H_2{}^{16}O$	$H_2{}^{18}O$	$H_2{}^{16}O$	$H_2{}^{18}O$
Hemerythrin						
Oxy	486	475	~753	720	n.o.	n.o.
Azidomet	507	493	768	733	292	286
Thiocyanatomet	514	498	780	742	~300	n.d.
Met	510	496	~750	~715	n.o.	n.d.
Hydroxomet	508	498	780	~750	n.o.	n.d.
Cyanatomet	509	493[f]	782	n.d.	n.o.	n.d.
Cyanomet	512	499[f]	773	n.d.	n.o.	n.d.
Model Compound						
$Fe_2O(CH_3COO)_2(HBpz_3)_2$ [b]	528	511	751	721	283	269
$[Fe_2O(phen)_4(H_2O)_2]^{4+}$ [c]	395	390	827	788	n.o.	n.o.
$[Fe_2OCl_6]^{2-}$ [d]	458	440	870	826	203	198

[a] Values obtained by Raman spectroscopy (n.d. = not determined; n.o. = not observed). The ν_s(Fe-O-Fe) values for the methemerythrins in H_2O are similar (± 1 cm^{-1}) to those reported previously.[13]

[b] Ref. 27.

[c] Ref. 29.

[d] Ref. 26.

[e] Values for hemerythrin obtained by Raman spectroscopy. Values for model compounds obtained by ir spectroscopy. Uncertainty in frequencies (indicated by ~) due to the interference of the 757 cm^{-1} protein peak.

[f] Ref. 13.

Figure Legends

Figure 1. Resonance Raman spectrum of oxyhemerythrin in $H_2{}^{16}O$ (upper) and $H_2{}^{18}O$ (lower). Protein concentration ≈1.2 mM in monomer; 363.8-nm excitation, 20 mW; scan rate, 1.0 cm^{-1}/s; slit width, 8.0 cm^{-1}. The peak at 981 cm^{-1} is due to 0.3 M $SO_4{}^{2-}$ used as an internal standard.

Figure 2. Resonance Raman enhancement profiles for oxyhemerythrin. Upper: electronic absorption spectrum of oxyhemerythrin. Middle: enhancement profile for the symmetric vibration at 486 cm^{-1}. Lower: enhancement profiles for the vibrations of the bound peroxide: O-O stretch at 844 cm^{-1}; Fe-O_2 stretch at 503 cm^{-1}. Enhancement measured as the height of the Raman peak relative to the height of ν_1 of 0.3 M $SO_4{}^{2-}$ at 981 cm^{-1} and normalized to the ν(Fe-O_2) height obtained with 530.9 nm excitation.

Figure 3. Resonance Raman enhancement profiles for azidomethemerythrin. Upper: electronic spectrum of azidomethemerythrin. Middle: enhancement profile for the symmetric Fe-O-Fe vibration at 507 cm^{-1}. Lower: enhancement profiles for the Fe-N(azide) stretch at 375 cm^{-1}, N-N(azide) stretch at 2048 cm^{-1}, and Fe-O-Fe deformation at 292 cm^{-1}. Enhancement measured as in Fig. 3, but normalized to the ν(Fe-N_3) height obtained with 496.5 nm excitation.

Figure 4. Resonance Raman spectrum of azidomethemerythrin in $H_2{}^{18}O$ (upper), H_2O (middle) and D_2O (lower). Experimental conditions: 530.9-nm excitation, 40 mW; scan rate 0.5 cm^{-1}/s; slit width, 6.5 cm^{-1}; ~1 mM in hemerythrin monomer.

Figure 5. Resonance Raman spectrum of oxyhemerythrin in H_2O (middle) and in D_2O (lower). Upper curve: computer-generated difference spectrum of middle minus lower spectrum. Frequencies of the Raman peaks (± 1 cm^{-1}) are reported relative to ν_1 of SO_4^{2-} at 981 cm^{-1}. Experimental conditions: 530.9-nm excitation, 25 mW; scan rate, 0.2 cm^{-1}/s; slit width, 8 cm^{-1}; ~1 mM in hemerythrin monomer.

Figure 6. Proposed structure of the binuclear iron center of oxyhemerythrin based on x-ray absorption spectroscopy[16], x-ray crystallography[14], and the present investigation.

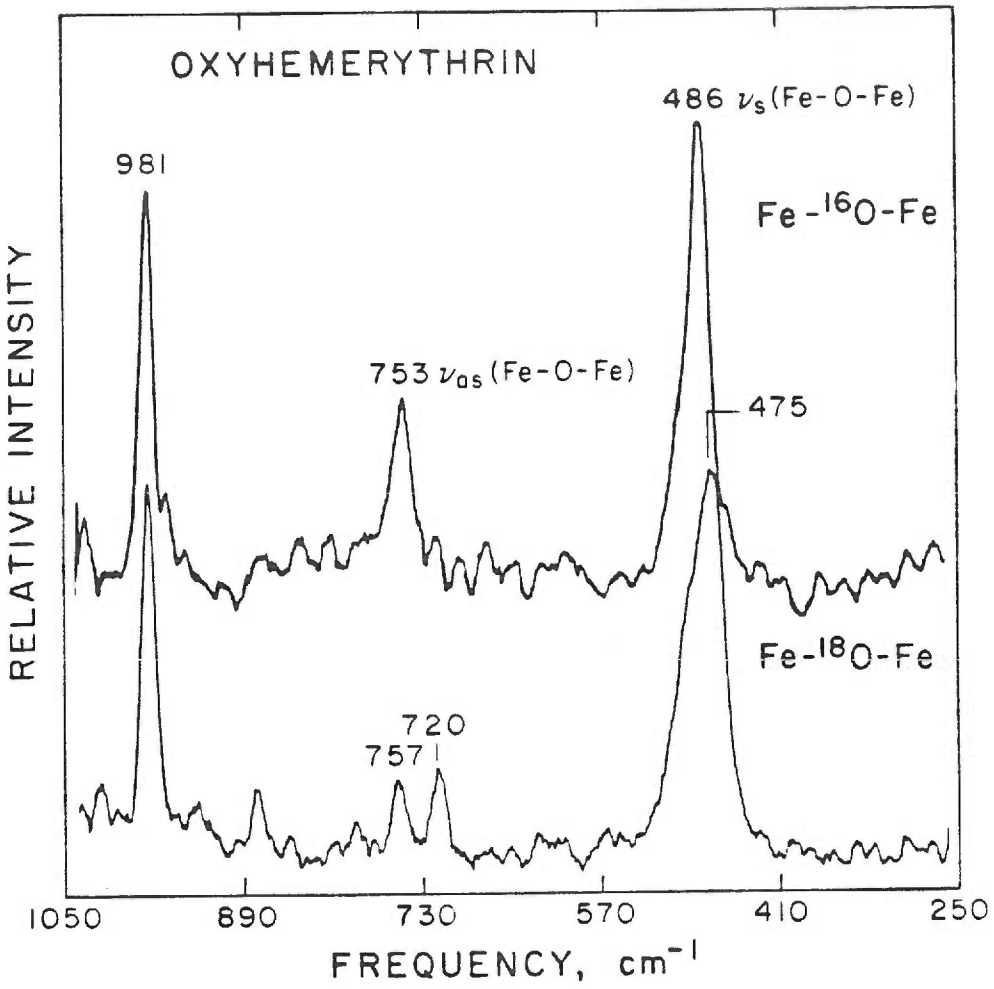
OXYHEMERYTHRIN
486 ν_s(Fe-O-Fe)
981
Fe-^{16}O-Fe
753 ν_{as}(Fe-O-Fe)
475
Fe-^{18}O-Fe
720
757
RELATIVE INTENSITY
1050
890
730
570
410
250
FREQUENCY, cm^{-1}

Figure 1

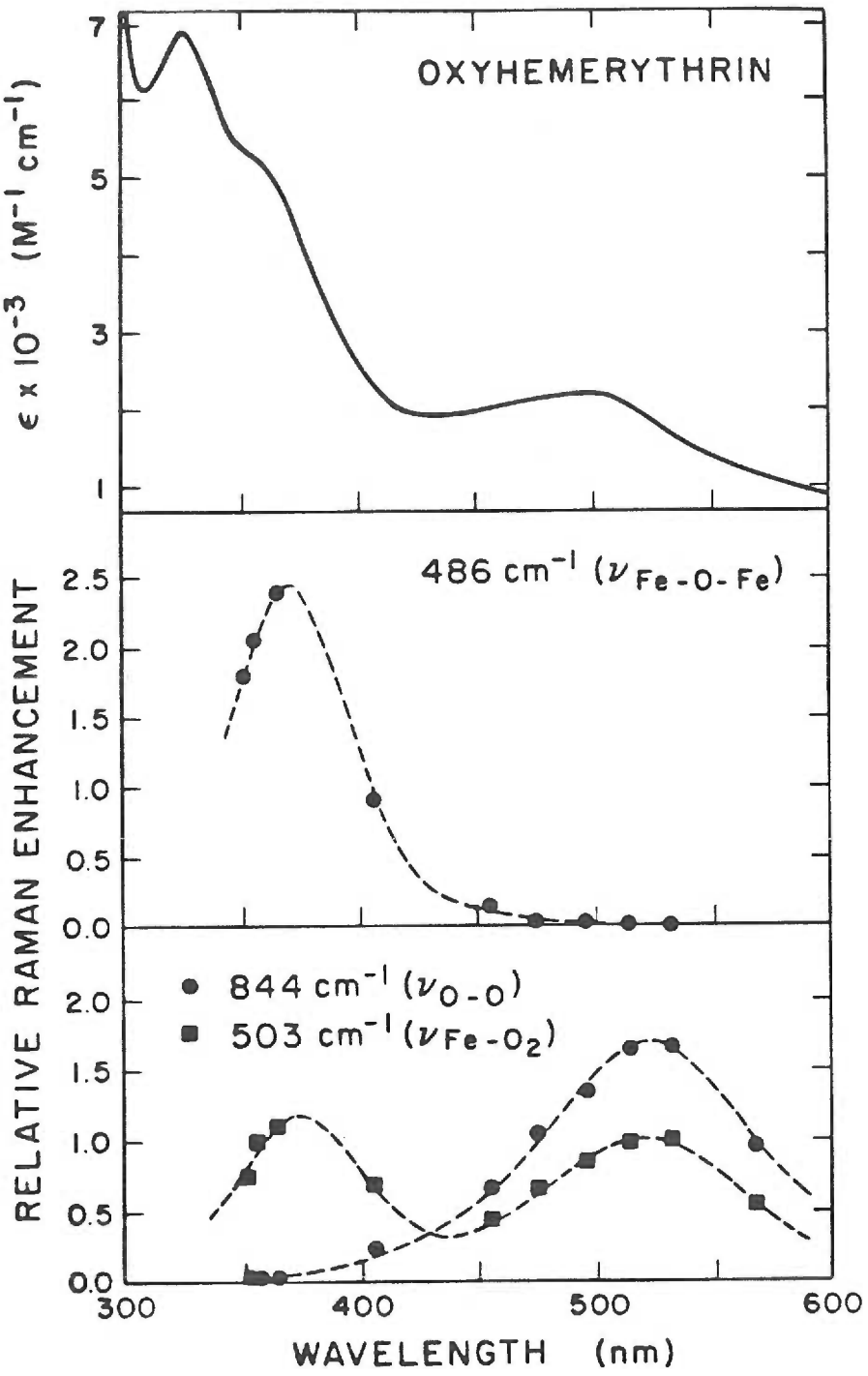
OXYHEMERYTHRIN
$\epsilon \times 10^{-3}$ (M^{-1} cm^{-1})
7
5
3
1
486 cm^{-1} ($\nu_{Fe-O-Fe}$)
RELATIVE RAMAN ENHANCEMENT
2.5
2.0
1.5
1.0
0.5
0.0
844 cm^{-1} (ν_{O-O})
503 cm^{-1} (ν_{Fe-O_2})
300
400
500
600
WAVELENGTH (nm)

Figure 2

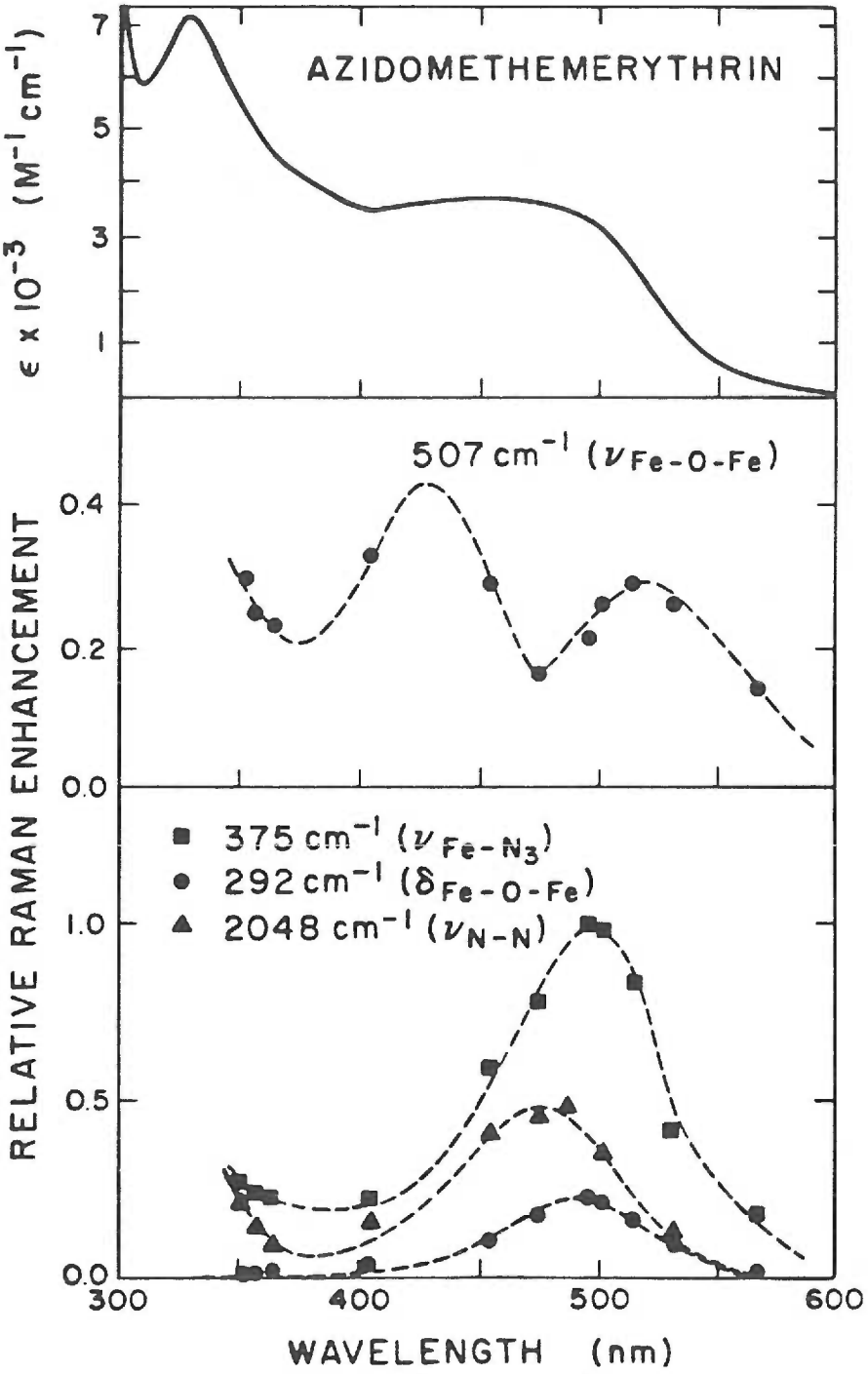
AZIDOMETHEMERYTHRIN
ε x 10⁻³ (M⁻¹ cm⁻¹)
7
5
3
1
507 cm⁻¹ (ν Fe-O-Fe)
RELATIVE RAMAN ENHANCEMENT
0.4
0.2
0.0
375 cm⁻¹ (ν Fe-N3)
292 cm⁻¹ (δ Fe-O-Fe)
2048 cm⁻¹ (ν N-N)
1.0
0.5
0.0
300
400
500
600
WAVELENGTH (nm)

Figure 3

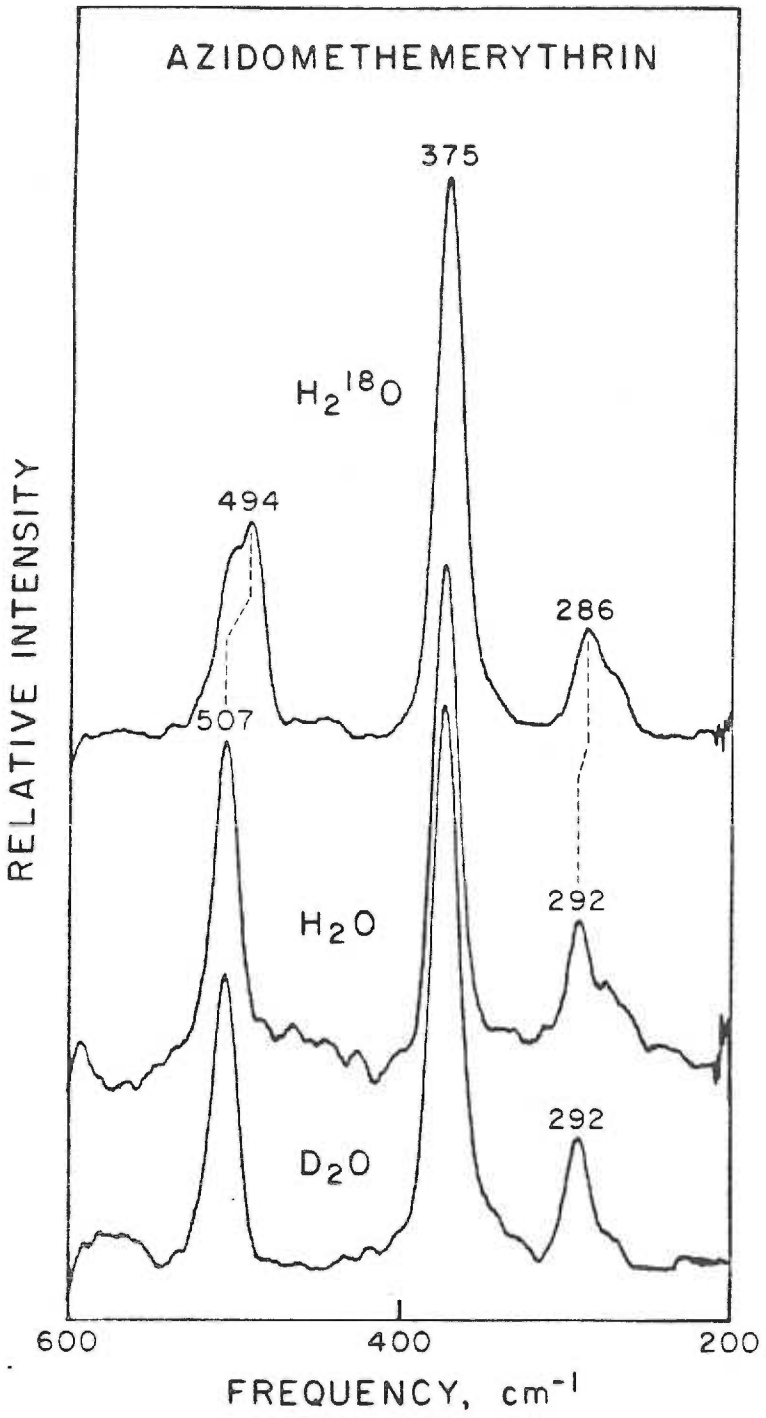
AZIDOMETHEMERYTHRIN
375
$H_2{}^{18}O$
494
286
507
H_2O
292
292
D_2O
RELATIVE INTENSITY
600
400
200
FREQUENCY, cm^{-1}

Figure 4

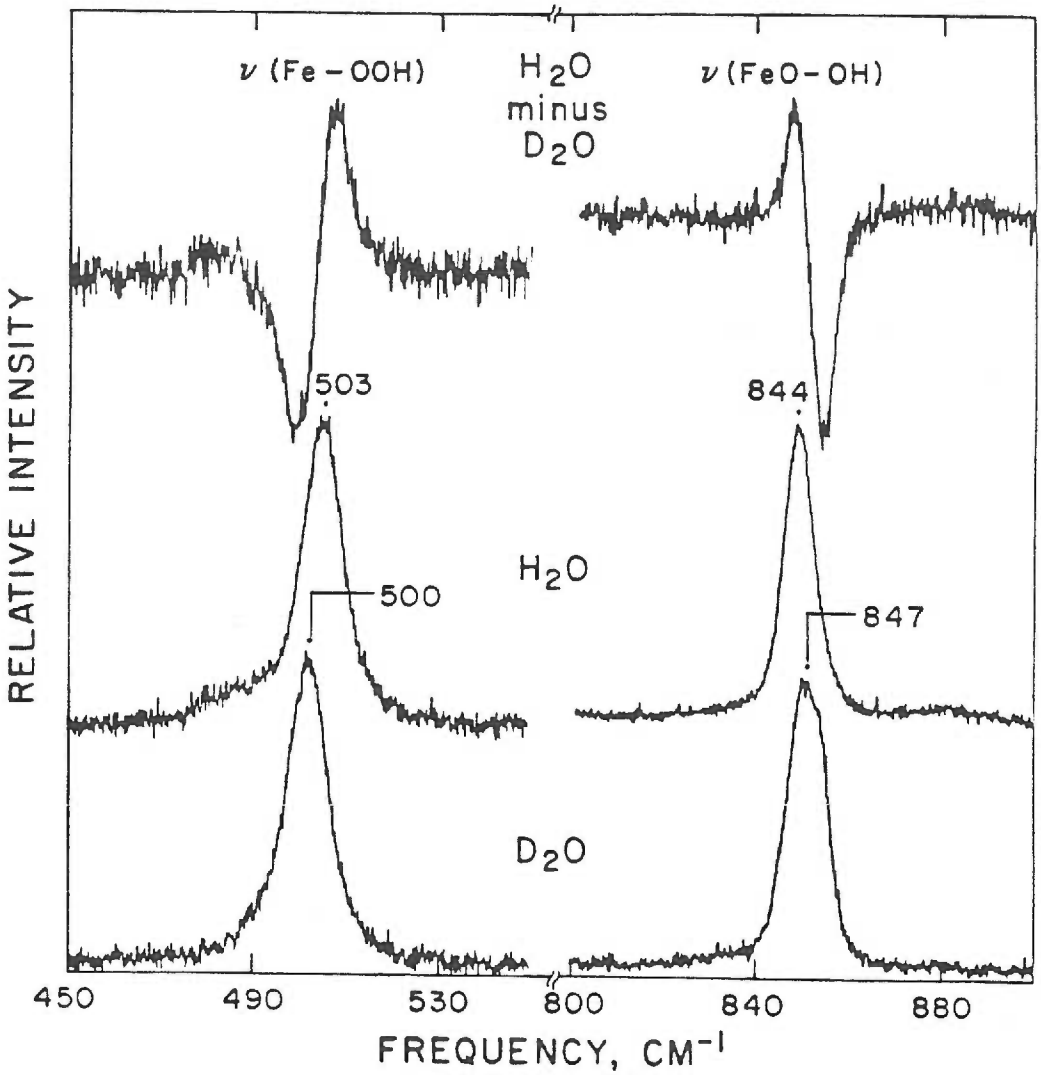
ν (Fe – OOH)
H2O
minus
D2O
ν (FeO – OH)
503
844
500
847
H2O
D2O
RELATIVE INTENSITY
450
490
530
800
840
880
FREQUENCY, CM-1

Figure 5

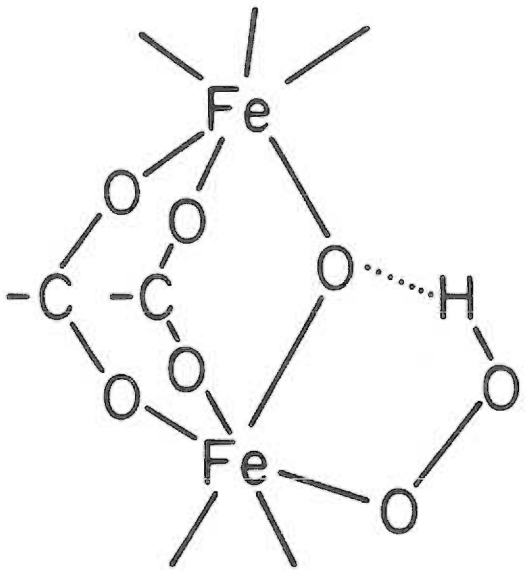

Figure 6

CHAPTER IV

A Resonance Raman Study of Oxyhemerythrin and Hydroxomethemerythrin. Evidence for Hydrogen Bonding of Ligands to the Fe-O-Fe Center

Andrew K. Shiemke, Thomas M. Loehr, and Joann Sanders-Loehr

Accepted for Publication in the Journal of the American Chemical Society, November, 1985

Abstract

Hydrogen bonding in the ligand binding site of the respiratory protein hemerythrin has been investigated by resonance Raman spectroscopy. Evidence for hydrogen bond interactions between the oxo bridge of the Fe-O-Fe moiety and the exogenous ligand has been found for both oxy and hydroxomethemerythrin. In the latter case peaks are observed at 492 and 506 cm^{-1} which shift upon ^{18}O bridge substitution to 477 and 491 cm^{-1}, respectively. These are assigned as ν_s(Fe-O-Fe) modes of two distinct Fe-OH conformations: the cis conformer has an intramolecular hydrogen bond between the bound hydroxide and the oxo bridge which is lacking in the trans conformer. This proposal is supported by the observation of a temperature-dependent equilibrium between the conformers with the cis conformer becoming more prevalent at low temperature as indicated by the increased intensity at 492 cm^{-1} relative to 506 cm^{-1}. The variation in the intensity as a function of temperature yields a ΔH° of -0.4 kcal/mol for the trans to cis conversion, consistent with the formation of a weak intramolecular hydrogen bond. The low frequency of ν_s(Fe-O-Fe) for cis-hydroxomethemerythrin relative to other methemerythrins is caused by weakening of the bridge bonds when the oxo group acts as a hydrogen bond acceptor. A similarly low ν_s(Fe-O-Fe) frequency of 486 cm^{-1} is observed for oxyhemerythrin indicating that the bound hydroperoxide ligand also has the ability to hydrogen bond to the oxo bridge. This hydrogen bond is considerably stronger than that of the hydroxide adduct such that only a single ν_s(Fe-O-Fe) peak is observed for oxyhemerythrin between 90 and 300 K. This peak undergoes a shift of +4 cm^{-1} in D_2O, an effect

specific to oxyhemerythrin, owing to a weakening of the hydrogen bond upon deuterium exchange. An effect of deuterium exchange is also observed for cis-hydroxomethemerythrin, although in this case the shift is due to coupling between ν_s(Fe-O-Fe) and the Fe-O-D bending vibration. An additional peak located at 565 cm^{-1} in hydroxomethemerythrin is assigned as the Fe-OH stretch based on its shift to 538 cm^{-1} in $^{18}OH_2$. The relative intensity of this peak is independent of temperature indicating that hydrogen bonding has little or no effect on the Fe-OH vibration.

INTRODUCTION

Hemerythrin is a non-heme iron-containing respiratory protein found in many marine invertebrates. The coelomic protein from the sipunculid Phascolopsis gouldii has an octameric quaternary structure, as does the protein from most other sources.[1] Each protein monomer contains one dioxygen binding site involving two iron atoms which, in the deoxy form of hemerythrin, are in the ferrous state.[1,2] Upon binding dioxygen the iron atoms are oxidized to the ferric state with concomitant reduction of O_2 to peroxide, resulting in the formation of oxyhemerythrin.[2-5] An additional form of the protein, methemerythrin, also contains ferric iron but does not bind O_2. Instead, methemerythrin avidly binds small anions such as N_3^-, SCN^-, OCN^-, CN^-, and Cl^-.[3]

Crystallographic studies of methemerythrin, azidomethemerythrin, azidometmyohemerythrin and oxyhemerythrin have shown that the dioxygen (and anion) binding site contains a μ-oxo bridged binuclear iron cluster.[6-8] The two face sharing octahedral iron atoms are also bridged by carboxyl groups of aspartate and glutamate (Figure 1), with the remaining coordination sites being filled by imidazole nitrogens of histidine side chains and the exogenous ligand. This oxo-bridged iron cluster is responsible for many of the noteworthy spectroscopic and magnetic properties of the protein, including the strong antiferromagnetic coupling of the ferric iron atoms,[9] the unusually high intensity of the iron ligand field transitions,[2,10] the near-UV electronic transitions,[3,10,11] and the resonance enhanced Raman spectra of active site vibrational modes.[4,5,12] Based on comparisons with model compounds, the near-UV bands in the electronic spectrum of hemerythrin

have long been suspected to be $O^{2-} \rightarrow Fe^{3+}$ charge transfer transitions.[3,11] Direct evidence for this assignment is the strong, selective enhancement of symmetric (ν_s) and asymmetric (ν_{as}) Fe-O-Fe vibrations in the hemerythrin resonance Raman (RR) spectra obtained with excitation into these near-UV transitions.[13] We have recently discovered that Fe-O-Fe vibrational modes are quite sensitive to exogenous ligand binding and this has afforded an opportunity for a more detailed study of oxy- and hydroxomethemerythrin.

In the case of oxyhemerythrin our previous RR studies indicated that dioxygen is coordinated as the hydroperoxide anion.[13] Furthermore, we proposed the existence of a hydrogen bond between the bound hydroperoxide ligand and the oxo bridge, as shown in Figure 1. Support for this structure came from an x-ray crystallographic study of oxyhemerythrin which showed that the hydroperoxide ligand is nearer to the iron-oxo bridge vector than is the azide ligand in azidomethemerythrin.[8] However, in our earlier Raman work we failed to observe any effect of D_2O on the oxo bridge vibrations.[13] We have now found that the ν_s(Fe-O-Fe) of oxyhemerythrin is sensitive to deuterium isotope substitution in a manner consistent with the oxo bridge acting as a hydrogen bond acceptor.

Methemerythrin, which has no bound exogenous ligand, undergoes a pH dependent transformation between acid and base forms, with a pKa of 7.6.[14-16] The high pH form, hydroxomethemerythrin, is derived by hydroxide-ion binding to methemerythrin through a simple associative mechanism.[17] As shown in the present study the RR spectrum of hydroxomethemerythrin is unique in that it exhibits two Fe-O-Fe vibrational modes at 492 and 506 cm^{-1}, whereas only a single such mode

appears in this region in all other ligated methemerythrins.[12] The occurrence of one of the Fe-O-Fe modes of hydroxomethemerythrin at a frequency considerably lower than that for all other methemerythrins, as well as the temperature dependence of the relative intensity of the two hydroxomethemerythrin modes leads us to propose the existence of two conformers in hydroxomethemerythrin, with structures illustrated in Figure 2. The two conformers are distinguished by the presence of a hydrogen bond between the bound hydroxide ligand and the oxo bridge in the cis conformer and the absence of this hydrogen bond in the trans conformer. The 492 cm^{-1} feature was previously misassigned as an Fe-OH stretching mode on the basis of its marked, but somewhat anomalous shift to higher energy when the protein was prepared in D_2O.[17] We have now obtained evidence that this deuterium-induced shift arises from a coupling between the Fe-O-Fe stretching mode and the Fe-O-D bending mode of at least one of the hydroxomethemerythrin conformers. In addition, a new peak has been located at 565 cm^{-1} and identified as the Fe-OH stretching mode of the bound hydroxide ligand.

EXPERIMENTAL SECTION

Hemerythrin. P. gouldii marine worms were obtained from the Marine Biological Laboratory, Woods Hole, MA. Hemerythrin was isolated from the coelomic fluid using the procedure of Klotz et al.[18] The protein (predominantly in the oxy form) was purified by crystallization via dialysis against 15% (v/v) ethanol in water. The crystals were dissolved in Raman buffer: 0.05 M Tris, 0.21 M sulfate (pH 8.0) and stored as a sterile solution at 5°C. The isolated protein was converted to hydroxomethemerythrin by addition of solid potassium ferricyanide in a

4-fold molar excess per hemerythrin monomer, followed by extensive dialysis against Raman buffer (pH 9.8). Preparation of samples with 6.2 < pH < 9.8 was accomplished by dialysis of methemerythrin against either 0.05 M MES (pH 6-7) or 0.05 M Tris (pH 7-10) containing 0.2 M sodium sulfate and adjusted to the desired pH with H_2SO_4.

Deoxyhemerythrin was prepared by anaerobic dialysis of methemerythrin against a 4-fold molar excess of sodium dithionite (British Drug Houses) and equimolar potassium thiocyanate. Excess reagents were removed by further anaerobic dialysis against Raman buffer (pH 8.0). Raman spectra of oxyhemerythrin were obtained within 2 days of oxygenation of the deoxy protein to minimize spectral contributions of methemerythrin. Anion adducts of methemerythrin were prepared by adding solid potassium or sodium salts of the various anions to methemerythrin to a final concentration of 0.1 to 0.5 M, with the following exceptions. The formate adduct of methemerythrin was prepared by addition of solid sodium formate to methemerythrin in Raman buffer (pH 6.0), until no further changes occurred in the optical spectrum. The following extinction coefficients (in M^{-1} cm^{-1} per monomer) were determined: ε_{480} = 600, ε_{362} = 6000, ε_{331} = 6200. An ~1500-fold molar excess of formate was required for complete conversion. Deuterated sodium formate (99 atom % D) was obtained from Merck, Sharp & Dohme, Ltd., Montreal. Cyanomethemerythrin was prepared by adding solid KCN to hydroxomethemerythrin (pH 9.8) to a final concentration of 0.3 M. Protein concentrations were determined spectrophotometrically using published extinction coefficients.[3,19]

$^{18}OH_2$ and $^{18}OD_2$ Buffer Exchange. $^{18}OH_2$ buffer was prepared by addition of 6.0 mg Tris base and 28.4 mg Na_2SO_4 to 1.0 mL of $^{18}OH_2$ (95

atom %, Monsanto Co., Miamisburg, OH) to give 0.05 M Tris, 0.2 M sulfate. The solution was titrated with conc. sulfuric acid to pH 10. Crystalline methemerythrin (obtained by dialysis against 15% ethanol) was dissolved in the $^{18}OH_2$ buffer to a final concentration of 1.6 mM protein monomer. Solid Tris base (~2.0 mg) was then added to raise the pH to 9.8.

A similar procedure was used to prepare $^{18}OD_2$ buffer. The buffer was prepared by adding 7.2 mg Tris and 34.1 mg Na_2SO_4 to 1.2 mL of $^{18}OD_2$ (97 atom % ^{18}O, 98 atom % D, KOR Isotopes, Cambridge, MA), to give 0.05 M Tris, 0.2 M Na_2SO_4, and conc. sulfuric acid was added to obtain a solution pH of 10.2. Hydroxomethemerythrin (in H_2O) was concentrated to ~0.1 mL, 15 mM in protein monomer, using a Centricon 10 filtration device (Amicon). To this protein solution was added 0.4 mL of $^{18}OD_2$ buffer. This concentration-dilution procedure was repeated 3 times with the $^{18}OD_2$ buffer and the final solution was concentrated to ~0.2 mL, 7 mM in protein monomer.

^{18}O Bridge Exchange. Substitution of ^{18}O into the oxo-bridge position of hemerythrin was carried out by our previously published procedure,[13] but with a slight modification. Because the protein crystals contain ~50% water, dissolution in $^{18}OH_2$ buffer causes dilution of the label. To mitigate this problem, the deoxyhemerythrin crystals were centrifuged and suspended in 0.5 mL of unbuffered $^{18}OH_2$. Very little of the protein dissolved. This suspension was tightly stoppered and stored at 5°C overnight. This procedure was repeated a second time before the deoxyhemerythrin crystals were finally dissolved in 1.0 mL of $^{18}OH_2$ buffer (pH 8.0) and stored for 2 days at 5°C. All manipulations of deoxyhemerythrin were performed anaerobically. Deoxyhemerythrin was oxygenated by exposing it to the atmosphere for 6 hours while in the

$^{18}OH_2$ buffer. The sample was then dialyzed vs. $^{16}OH_2$ Raman buffer (pH 8.0) for 20 hours followed immediately by acquisition of the oxyhemerythrin Raman spectrum. This sample of oxyhemerythrin containing an ^{18}O bridge was later converted to hydroxomethemerythrin by addition of solid potassium ferricyanide followed by dialysis in Raman buffer (pH 9.8).

Deuterium Exchange. D_2O buffer was prepared by addition of solid Na_2SO_4 and solid Tris to D_2O (99.7 atom %, Merck, Sharpe, & Dohme, Ltd., Montreal) to give 0.05 M Tris, 0.2 M Na_2SO_4. The D_2O solution was titrated with conc. sulfuric acid to a pD of 8.4 or 10.2 for oxy and hydroxomethemerythrin, respectively. Deuterium exchange of the proteins was achieved by successive cycles of concentration and dilution. Crystalline protein (either met or oxyhemerythrin) was dissolved in 2-3 mL of the appropriate D_2O buffer. The solutions were concentrated to 0.2 mL with a Centricon 10, then diluted to ~2 mL with D_2O buffer. This procedure was repeated at least 3 times and the samples were left overnight in the D_2O buffer at 5°C prior to obtaining Raman spectra.

Spectroscopy. Resonance Raman spectra were collected on a computer-interfaced Jarrell-Ash spectrophotometer[20] equipped with Spectra-Physics 164-05 (Ar) and 164-01 (Kr) lasers, an RCA C31034A photomultiplier tube, and an ORTEC Model 9302 amplifier/discriminator. Both lasers are equipped with ultra-high-field magnets to enhance ultraviolet output. Spectra of hemerythrin at low temperature were obtained by backscattering from a capillary sample tube held in either a copper cold-finger and Dewar[21] cooled with liquid N_2 (sample temperature 90 K), or a Varian E-4540 variable temperature controller using a stream of cold N_2 gas to maintain the sample temperature (100-250 K). Sample

temperatures for the variable temperature experiment were measured using an iron-constantan thermocouple and a Rubicon Instruments potentiometer. The voltages were corrected relative to 0°C, and the temperature determined from standard tables of thermoelectric voltage vs. temperature. Solution spectra were measured using a flow cell[13] in a 90-degree scattering geometry with a sample reservoir of 2-3 mL held at -2°C or 35°C. Sample concentrations were typically 1.5-2 mM in hemerythrin monomer for the solution spectra and 5-8 mM for the frozen samples. Spectra of isotopically labeled samples intended for comparison were run consecutively, on the same day, with identical instrumental and sample conditions. In all cases ν_1 of sulfate (981 cm^{-1} in solution, 990 cm^{-1} when frozen) was used as an internal frequency standard. Reported peak positions are accurate within 1 cm^{-1}. The frequency of isolated peaks was determined by comparison to the internal standard. Where overlapping peaks occur, positions were determined from a computer generated fit of the spectrum. Unless otherwise stated, fits were performed with a 90% Lorentzian-10% Gaussian peak shape and an 18 cm^{-1} band width (full width at half height). Absorption spectra were obtained on a Perkin Elmer Lambda 9 spectrometer.

RESULTS and DISCUSSION

Temperature Dependence of Fe-O-Fe Vibrations in Hydroxomethemerythrin. The RR spectra of most ligated methemerythrins exhibit a single strong peak between 507 and 516 cm^{-1} (Table I), which has been assigned to the symmetric stretching frequency of the Fe-O-Fe cluster.[5,12] In contrast to this straightforward behavior, the RR

spectrum of hydroxomethemerythrin exhibits two features in this region (Figure 3a).[12,17] Curve resolution of the spectrum in Figure 3a indicates that these two peaks are centered at 492 and 506 cm^{-1} with an intensity ratio of 3:1. When the oxo bridge is replaced by ^{18}O, the 492 and 506 cm^{-1} features shift to 477 and 491 cm^{-1}, respectively (Figure 3c), thus proving that both of these peaks arise from ν_s(Fe-O-Fe) vibrations. The components at 477 and 491 cm^{-1} also show a 3:1 intensity ratio. The contribution of residual peaks at 492 and 506 cm^{-1} to the spectrum in Figure 3c is consistent with the presence of 15% ^{16}O-bridged hydroxomethemerythrin in this sample. The latter was verified by converting this sample to the thiocyanate form and observing that its ν_s(Fe-^{18}O-Fe) and ν_s(Fe-^{16}O-Fe) spectral features at 498 and 514 cm^{-1}, respectively, were present in an intensity ratio of 5.5 to 1.

The two observed ν_s(Fe-O-Fe) modes (Fig. 3a) must arise from two different conformations of hydroxomethemerythrin since their relative intensities are independent of pH. The ratio of the 492 to 506 cm^{-1} peak areas remains constant between pH 9.2 and 10.0, despite a 6.3-fold increase in OH^- concentration. The ν_s(Fe-O-Fe) of ligand-free methemerythrin at 512 cm^{-1} appears only with decreasing pH, corresponding to a pKa of 7.9 (Figure 7), in agreement with the acid/base equilibrium constant determined by other methods.[14-16] Thus, any contribution of methemerythrin to the 506 cm^{-1} peak may be excluded, and both peaks must be due to vibrational modes of the hydroxide adduct. In addition, the effect of pH on the RR spectra of various hemerythrin derivatives was found to be insignificant, indicating that pH-induced alterations of protein structure (if any occur) are not important to the existence of two ν_s(Fe-O-Fe) modes in hydroxomethemerythrin.

The assignment of the two Fe-O-Fe modes to distinct conformations of hydroxomethemerythrin is further supported by the temperature dependence of the relative intensities of the two peaks. When the temperature is lowered to 90 K there is a sharpening of all spectral peaks and an ~2 cm^{-1} decrease in frequencies (Fig. 4a). The intensity of the 504 cm^{-1} peak is only 1/12 that of the 490 cm^{-1} peak at 90 K compared to 1/3 at 278 K. The observed temperature dependence is in the direction expected for the proposed hydrogen bond interaction. A hydrogen bond between the bound hydroxide ion and the oxo group generates the cis form and disruption of this hydrogen bond generates the trans form (Fig. 2). Accordingly, the 492 cm^{-1} Fe-O-Fe mode arises from the cis conformer which is more prevalent at low temperature owing to the stabilizing influence of the hydrogen bond, whereas the 506 cm^{-1} mode arises from the trans conformer whose concentration increases at higher temperatures due to the disruption of this hydrogen bond.

The energy of the hydrogen bond in hydroxomethemerythrin can be quantitated using the temperature dependence of the equilibrium between the two conformers according to the relationship:

$$\ln K_{eq} = -\Delta H^\circ/RT + \Delta S^\circ/R \qquad (1)$$

The concentrations of the cis and trans conformers are proportional to the integrated intensities of the 492 cm^{-1} and 506 cm^{-1} peaks, respectively:

$$[\underline{\text{cis}}] = I_{492}/S_c \qquad (2)$$

$$[\underline{\text{trans}}] = I_{506}/S_t \qquad (3)$$

where S_c and S_t are the molar scattering coefficients of *cis* and *trans* hydroxomethemerythrin, respectively. For the conversion of *trans* to *cis*:

$$K_{eq} = [\underline{cis}]/[\underline{trans}] = \{I_{492}/I_{506}\}\{S_t/S_c\} \quad (4)$$

Combining equations (1) and (4) yields:

$$\ln\{I_{492}/I_{506}\} = -\Delta H^\circ/RT + \Delta S^\circ/R - \ln\{S_t/S_c\} \quad (5)$$

The variation in the intensity ratio (equation 5) over a 90-300 K temperature range is plotted in Figure 5. The linear relationship (correlation coefficient = 0.98) indicates that ΔH° corresponds to a conversion between two discrete states. The slope of the line yields an enthalpy change of -0.4 kcal/mol for the formation of the hydrogen bond between the hydroxide ligand and the oxo bridge. The presence of molar scattering coefficients in equation 5 precludes the determination of ΔS°. If the molar scattering coefficients of the two conformers were equivalent, ΔS° could be determined from the ordinate intercept in Figure 5. However, the extent of resonance enhancement of the two conformers is not identical. Freier et al.[12] observed 492 and 506 cm^{-1} peaks of nearly equal intensity with 457.9 nm excitation (at 276 K) whereas with 363.8 nm excitation (Figure 3a) their intensity ratio is ~3:1. Since temperature restrictions prevent the determination of the relative scattering coefficient for either conformer, the ΔS° for the formation of the hydrogen bond must remain unknown.

Fe-OH Vibration in Hydroxomethemerythrin. We have now identified the Fe-OH stretching mode as a weak feature at 565 cm^{-1} (Figure 3a) that shifts to 538 cm^{-1} upon ^{18}O hydroxide substitution (Figure 3b). The frequency observed in $^{18}OH_2$ is very close to the 540 cm^{-1} expected for an Fe-^{18}OH stretching vibration calculated from a simple harmonic oscillator model. The 5 cm^{-1} shift in D_2O is rather small compared to other metal-hydroxide complexes whose M-OH vibrations typically shift 10-25 cm^{-1} upon deuteration.[22] This explains our previous failure to assign the 565-cm^{-1} peak in hydroxomethemerythrin to the Fe-OH stretch.[17]

It is of interest that only a single Fe-OH stretching frequency is observed, even in samples containing a substantial amount of trans conformer (e.g., Figure 3a). Furthermore, the intensity of the 565 cm^{-1} peak remains constant at 13% (± 2%) of the combined intensities of the ν_s(Fe-O-Fe) peaks between 90-300 K. This indicates that the 565 cm^{-1} peak contains contributions from both the cis and trans conformers and that ν(Fe-OH) is not sensitive to the hydrogen bond to the oxo bridge. In view of the unusually small deuterium isotope dependence of this vibration, its lack of sensitivity to hydrogen bonding is not surprising.

Deuterium Effects on Fe-O-Fe Vibrations in Hydroxomethemerythrin. Given the presence of the hydrogen bond in the cis conformer of hydroxomethemerythrin one might expect the 492 cm^{-1} peak to exhibit a deuterium isotope effect, whereas the 506 cm^{-1} peak should be unaffected. As shown in Figure 3d and Table I, deuterium exchange has a marked influence on the RR spectrum of hydroxomethemerythrin. Comparing the spectral data for the H_2O with the D_2O solution, the major peak at 492 cm^{-1} appears to have shifted to 518 cm^{-1}, a shoulder near 500 cm^{-1} remains that may be derived from the original 506 cm^{-1} peak, and a new

unresolved feature appears at ~465 cm^{-1}. The poor resolution in Figure 3d (due to extensive overlap of bands) makes it difficult to determine the exact number of components in this spectral envelope. The spectrum of hydroxomethemerythrin in D_2O solution becomes much more distinct when the temperature is reduced to 90 K (Figure 4b). This spectrum has three well resolved features centered at 518, 495, and 463 cm^{-1}, with band widths of 19, 17, and 16 cm^{-1} respectively. The improved resolution of this spectrum stems from the narrower band widths and the reduced contribution of the trans conformer at this temperature.

The appearance of three intense spectral features at 518, 495, and 463 cm^{-1} in D_2O (Figure 4b) when only one was present at 490 cm^{-1} in H_2O (Figure 4a) is indicative of coupled vibrational modes in the deuterated protein. All three features must have Fe-O-Fe character because they shift to lower energy when the bridge is replaced by ^{18}O (Figure 4c). In addition, they must also have some Fe-OD character from the bound hydroxide ligand since they all shift to slightly lower energy and alter their relative intensities when the D_2O solvent is replaced by $D_2{}^{18}O$ (Figure 4d). In contrast, the Fe-OD stretch at 557 cm^{-1} is essentially unaffected by ^{18}O substitution in the bridge and is, therefore, likely to be an isolated vibration. Fermi resonance coupling can arise when there is coincidence in the symmetries and energies of fundamental vibrations.[23a] The most likely candidate for a mode which involves a solvent-exchangeable hydrogen and which may occur near 500 cm^{-1} and, hence, be able to couple with ν_s(Fe-O-Fe) is the Fe-O-D bend.

The bending vibrations of metal hydroxides are typically found between 600-1200 cm^{-1} and are subject to shifts of several hundred cm^{-1} upon deuteration.[23b] Thus, the δ(Fe-O-D) could easily occur near 500

cm^{-1} in hydroxomethemerytirn. If this mode were to undergo a Fermi resonance with ν_s(Fe-O-Fe) at 490 cm^{-1}, the result would be the appearance of two resonance-enhanced peaks which have diverged in frequency.[23a] This is the likely origin of the peaks at 463 and 518 cm^{-1} in D_2O (Fig. 4b) and at 456 and 511 cm^{-1} for the ^{18}O-bridged sample in D_2O (Fig. 4c). The variability in intensity with isotopic composition is indicative of differences in the relative energies in the fundamentals and, hence, the strength of the coupling interactions. The remaining weak peaks at 495 cm^{-1} (Fig. 4b) and 478 cm^{-1} (Fig. 4c) may well be due to the coupling of ν_s(Fe-O-Fe) of the trans conformer with δ(Fe-O-D). Such an occurrence would indicate that there is substantially more trans conformer present at 90 K in D_2O than in H_2O (Fig. 4a), a finding which would imply that deuterium substitution weakens the hydrogen-bonding interaction of the bound hydroxide with the μ-oxo bridge.

Deuterium Effect on the Fe-O-Fe Vibration in Oxyhemerythrin. The ν_s(Fe-O-Fe) of oxyhemerythrin is observed at 486 cm^{-1} (Figure 6a) and shifts 14 cm^{-1} to lower energy when the bridge is replaced by ^{18}O (Figure 6b).[13] Comparison with the behavior of the ν_s(Fe-O-Fe) of hydroxomethemerythrin (Table I) indicates that the vibrational frequency in oxyhemerythrin is characteristic of a hydrogen-bonded Fe-O-Fe. Moreover, the spectrum of oxyhemerythrin shows no evidence for an additional ν_s(Fe-O-Fe) near 510 cm^{-1} which would be expected for a non-hydrogen-bonded form of the protein (Table I). All of the intensity at 503 cm^{-1} can be accounted for as the Fe-O_2 stretch,[4,13] and no changes in relative peak intensities are observed when the sample is cooled to 90 K. Thus, the hydrogen bond between hydroperoxide and the oxo bridge in

oxyhemerythrin must be considerably more stable than that between hydroxide and the oxo bridge in hydroxomethemerythrin.

Definitive evidence for this hydrogen bond in oxyhemerythrin comes from the effect of deuterium isotope exchange on ν_s(Fe-O-Fe) (Figure 6c). Curve resolution of the spectra reveals peaks centered at 486 and 503 cm^{-1} in H_2O solution (Fig. 6a) that shift to 490 and 500 cm^{-1}, respectively, in D_2O solution (Fig. 6c). The shift of ν(Fe-O_2) to 500 cm^{-1} in D_2O agrees with our previously published results.[13] However, the effect of D_2O on ν_s(Fe-O-Fe) was missed. Observation of this shift in the present experiments is due to the almost total exclusion of methemerythrin from the sample and more complete substitution of deuterium on the hydroperoxide ligand. The fit of the spectrum in Figure 6c indicates <5% contamination by the met forms of hemerythrin, whereas previous spectra showed close to 20%.[13]

The RR spectra of many derivatives of hemerythrin have been investigated in D_2O, with shifts of ν_s(Fe-O-Fe) being observed only for oxy and hydroxomethemerythrin (Table I). This lack of an influence following general protein exchange indicates that the spectral shift in oxyhemerythrin is due specifically to perturbation of the hydrogen bond interaction at the ligand binding site. Although the observed shift of ν_s(Fe-O-Fe) to higher energy in D_2O is opposed to the expected mass effect, this type of shift is not unusual in hydrogen-bonded systems. In cases where the deuterium bond is weaker than the corresponding hydrogen bond, the vibrational frequency of the hydrogen bond acceptor, e.g., ν_s(Fe-O-Fe), will be less affected by deuterium than by hydrogen. A similar type of behavior occurs with 2-methoxyethanol which contains an intramolecular hydrogen bond between the alcohol and ether moieties.[24]

We observe by infrared spectroscopy that while deuteration causes ν(C-OH) to shift from 1060 to 1041 cm^{-1}, a 19 cm^{-1} decrease, ν_{as}(C-O-C) shifts from 1126 to 1129 cm^{-1}, a 3 cm^{-1} increase. In contrast, the weak asymmetric Fe-O-Fe stretches of oxyhemerythrin and hydroxomethemerythrin at 753 and 782 cm^{-1}, respectively, do not appear to shift upon deuteration of the hydrogen bond donor, despite the fact that they drop by ~35 cm^{-1} upon substitution of the oxo bridge with ^{18}O.[13]

The 55% decrease in the intensity of $\nu(Fe-O_2)$ when ν_s(Fe-O-Fe) shifts to lower energy upon ^{18}O bridge substitution (Fig. 6a,b) is suggestive of coupling between these modes. The absence of an effect on the frequency of the 503 cm^{-1} peak indicates little or no mixing of the excited state wave functions such as occurs in Fermi resonance. Rather, the observed behavior is characteristic of an "intensity borrowing" type of coupling whereby the $\nu(Fe-O_2)$ peak gains intensity simply owing to its proximity to the strongly enhanced ν_s(Fe-O-Fe) mode. Similar coupling has been observed in the RR spectra of O_2 adducts of cobalt porphyrins[25] in which axial base modes borrow intensity from the strongly enhanced O-O stretch. In the latter case the shift of the O-O vibration, through substitution of $^{18}O_2$, causes a marked decrease in the intensity of the axial base vibrational mode but little effect on its frequency. The enhancement of $\nu(Fe-O_2)$ in oxyhemerythrin by intensity borrowing from ν_s(Fe-O-Fe) also explains why $\nu(Fe-O_2)$ shows an excitation profile maximum in the near UV region while the ν(O-O) at 844 cm^{-1} does not.[13]

Rationale for Fe-O-Fe Frequencies. The majority of hemerythrin derivatives have ν_s(Fe-O-Fe) frequencies between 506 and 516 cm^{-1} (Table I). The slight variation in these frequencies does not appear to be related to properties of the exogenous ligand (e.g., size, ligand field

strength, or π-donating ability), and probably stems from minor variations in Fe-O-Fe angle, which is known to affect Fe-O-Fe vibrational frequencies.[27] Since it is unlikely that a hydroperoxide or hydroxide ligand would cause a significant increase in the bridge angle, the 20-30 cm^{-1} shift to lower energy for the ν_s(Fe-O-Fe) vibrations of oxyhemerythrin and cis-hydroxomethemerythrin is more readily ascribed to hydrogen bonding. The only other protonated anions that are known to bind to methemerythrin are formate ($HCOO^-$) and cyanamide ($NCNH^-$), but these adducts show no evidence of hydrogen bonding to the oxo bridge (Table 1). Whereas the non-polar character of its proton precludes hydrogen bonding by formate, the proton of cyanamide is reasonably polar (pKa = 11).[28] However, it appears that cyanamide is coordinated to the iron via its trigonal, protonated nitrogen, because ν(Fe-N) of cyanamidomethemerythrin shifts 5 cm^{-1} to lower energy upon deuteration of the ligand.[29] In this case the proton could be oriented away from the oxo bridge and, thereby, be unavailable for hydrogen bonding.

Due to the electron withdrawal caused by hydrogen bonds, a significant decrease in vibrational frequency is the expected behavior for a group when acting as a hydrogen bond acceptor. This phenomenon has been observed in the spectra of α-hydroxy ketones where the C=O stretch at ~1700 cm^{-1} in the non-hydrogen bonded derivatives shifts 10-15 cm^{-1} to lower energy in compounds exhibiting intramolecular hydrogen bonding.[30] In horseradish peroxidase (HRP) compound II, a hydrogen bond between a distal histidine and the Fe(IV)=O group has been suggested to be responsible for the ~10 cm^{-1} reduction in the frequency of the Fe(IV)=O vibration at pH values below 7.[31] In addition, the O-O stretch of O_2 complexes of cobalt porphyrins occurs at ~1150 cm^{-1},[25] which is ~20 cm^{-1}

higher than the analogous vibrations of cobalt substituted hemoglobin and myoglobin.[32] The lower vibrational frequencies in the proteins could be due in part to hydrogen bonding between the distal histidine and the bound dioxygen as observed in crystal structures of oxyhemoglobin and oxymyoglobin.[33] Similarly, the frequency reduction of ν_s(Fe-O-Fe) in oxyhemerythrin and cis-hydroxomethemerythrin is indicative of a weakening of the Fe-O(bridge) bonds as is expected for an oxo group acting as a hydrogen bond acceptor. The decrease in Fe-O bond strength is probably also responsible for the reduced antiferromagnetic coupling of oxyhemerythrin ($-J = 77\ cm^{-1}$) compared to methemerythrin ($-J = 134\ cm^{-1}$).[9]

Although there is some uncertainty as to whether H or D forms stronger hydrogen bonds,[34] there are numerous examples of the bond to hydrogen being stronger than the analogous bond to deuterium.[34-36] In the latter case, the vibrational frequency of the hydrogen bond acceptor will actually undergo a smaller decrease in energy upon hydrogen bonding to a deuterium donor than to a hydrogen donor. The result is that the deuterated species will exhibit a higher vibrational frequency than the protonated species because there is less withdrawal of electron density in bonding to D than to H. Such effects have been observed in a number of the systems mentioned above. For example, the O-O stretch of the bound dioxygen in cobalt-substituted myoglobin and hemoglobin shifts 2-5 cm^{-1} to higher frequency in D_2O.[32] Similarly, the hydrogen bonded Fe(IV)=O stretch of HRP compound II shifts from 775 cm^{-1} in H_2O to 779 cm^{-1} in D_2O.[31] Also, the ν_{as}(C-O-C) of 2-methoxyethanol shifts from 1126 to 1129 cm^{-1} upon deuteration of the intramoplecularly hydrogen bonded OH group. The shift of the ν_s(Fe-O-Fe) of oxyhemerythrin from 486 cm^{-1} in

H_2O to 490 cm^{-1} in D_2O is certainly in line with this behavior. Our previous observation of a 6 cm^{-1} increase in the ν_s(Fe-O-Fe) of ribonucleotide reductase in D_2O may also be due to hydrogen bonding of a protein functional group to the μ-oxo bridge.[21]

Rationale for Hydrogen-Bonded Structures. Although we have established that the oxo bridge acts as a hydrogen bond acceptor in both oxy and hydroxomethemerythrin, it is more difficult to definitively establish that the protonated ligands (Figs. 1 and 2) are indeed the hydrogen bond donors. In the case of oxyhemerythrin there is crystallographic evidence that the bound hydroperoxide is hydrogen bonded to the oxo bridge.[8] Furthermore, the shift in the O-O stretch of oxyhemerythrin from 844 cm^{-1} in H_2O to 848 cm^{-1} in D_2O is commensurate with a protonated peroxide.[13] Crystallographic data are not available for hydroxomethemerythrin and the effects of deuterium substitution on ν(Fe-OH) are ambiguous. However, since hydrogen bonding is unique to oxy and hydroxomethemerythrin, and since there are no other suitable bond donors in the vicinity of the ligand binding site of hemerythrin,[37] OH^- and OOH^- ligands are strongly implicated as the hydrogen donating groups.

Crystallographic studies of ligand-free methemerythrin have revealed the presence of additional electron density near the oxo bridge, possibly from a non-ligated water molecule.[38] However, this water molecule appears to be displaced upon perchlorate or exogenous ligand binding to methemerythrin as judged by both Raman[29] and crystallographic[37] results. It is, therefore, not likely to participate in the hydrogen bonding of oxyhemerythrin or hydroxomethemerythrin.

The strength of hydrogen bonds ($\Delta H°$) has been determined for many small molecules and has been found to vary depending on the type of

hydrogen-bonding interaction.[39,40] Whereas $\Delta H°$ for most intermolecular hydrogen bonds ranges from -3 to -10 kcal/mol, $\Delta H°$ for intramolecular hydrogen bonds typically ranges from -1 to -4 kcal/mol and some have values as low as that for hydroxomethemerythrin ($\Delta H°$ = -0.4 kcal/mol). Examples of the latter are 2-nitroethanol ($\Delta H°$ = -0.40 kcal/mol), 2-fluoro-6-chlorophenol (-0.18 kcal/mol), ethanolamine (-0.70 kcal/mol), and 2-benzylphenol (-0.33 kcal/mol).[40] The bond energy determined for cis-hydroxomethemerythrin is thus commensurate with the existence of a very weak intramolecular hydrogen bond. This is similar to the situation in hemoglobin where the hydroxide ligand of hydroxomethemoglobin is hydrogen-bonded to the distal histidine.[41]

In oxyhemerythrin, only the cis conformation is observed. This indicates that the hydrogen bond in oxyhemerythrin is considerably stronger than in cis hydroxomethemerythrin and is likely to be in the -1 to -4 kcal/mol range of the more typical intramolecular hydrogen bonds. For oxyhemerythrin, assuming reasonable angles and distances for the coordinate and covalent bonds,[42] we estimate a hydrogen bond distance (μ-O···HOO) of 1.7 Å and a hydrogen bond angle of 130°. The distance is that of a fairly strong hydrogen bond; the angle is within the range generally observed for intramolecular hydrogen bonds in proteins.[43] The bond angle for intramolecular hydrogen bonds in protein and small molecules can actually occur anywhere between 90° and 180° depending on the constraints of the covalent structure and, thus, is far less uniform than intermolecular hydrogen bond angles which tend to be closer to 180°.[43,30a] Since the cyclic hydrogen-bonded structure in cis-hydroxomethemerythrin contains only 4 atoms, it is certain to be a rather strained system. This is reflected in somewhat narrower covalent

bond angles,[42] an estimated hydrogen bond distance (μ-O...HO) of 2.3 Å, and a hydrogen bond angle of 95°. These latter two values are close to the limits for hydrogen-bonded atoms in proteins[43] and, thus, are in agreement with the low enthalpy of the cis to trans interconversion in hydroxomethemerythrin.

The hydrogen bonding of the dioxygen ligand to the oxo bridge has some interesting implications for the chemistry of oxyhemerythrin. As previously proposed,[8,13] the structure in Figure 1 would be expected to facilitate the rapid conversion of deoxyhemerythrin to oxyhemerythrin, with the peroxide proton originating from the hydroxide bridge of deoxyhemerythrin. This model is consistent with the absence of a pH effect on the rate of oxygenation.[44] In contrast, the displacement of peroxide by other anions is acid-catalyzed,[45] reflecting the need for further protonation in achieving the release of H_2O_2. The fact that the release of peroxide from oxyhemerythrin (autooxidation) is slow[45] indicates that hydrogen bonding to the oxo bridge may exert a stabilizing influence on the peroxide complex. The copper-containing respiratory protein, oxyhemocyanin, is even more resistant to autooxidation because both ends of the peroxide are metal coordinated in the structure Cu-O-O-Cu.[46]

In addition to being stable towards autooxidation, the peroxide complex in oxyhemerythrin also does not produce intermediate redox states. This is in marked contrast to mononuclear complexes such as the peroxide adduct of Fe(III)EDTA which undergoes rapid decomposition due to the formation of Fe(II) and superoxide.[47] Presumably, a binuclear metal center can be of considerable help in this regard. A species which is more reminiscent of oxyhemerythrin in its stability and structure is a

cyanide-bridged binuclear cobalt complex, Co(III)-CN-Co(III)-O_2^{2-}, with a side-on bonded peroxide.[48] As in oxyhemerythrin, this peroxide also results from an oxidative addition, utilizing the two-electron transfer potential of the binuclear metal site. Side-on binding of peroxide as in the cobalt compound is the general rule in metal complexes,[49] and this also appears to be the case in the Fe(III)EDTA peroxo complex.[50] Thus, the end-on binding observed in oxyhemerythrin is clearly facilitated by the hydrogen-bonding capability of the Fe-O-Fe site. In an analogous fashion, hydrogen bonding to the proton of a distal donor is believed to be an important factor in stabilizing the dioxygen complexes of hemoglobin and myoglobin[33] and of model systems containing iron and cobalt porphyrins.[51]

Acknowledgements

The authors would like to thank Dr. Edward N. Baker for helpful discussions regarding hydrogen bonds in proteins and A. Grant Mauk for suggesting the use of temperature dependence to identify the conformers of hydroxomethemerythrin, and Salman Ahmad for performing the experiments on 2-methoxyethanol. This research was supported by the National Institutes of Health (GM 18865).

REFERENCES

(1) (a) Sanders-Loehr, J.; Loehr, T. M. Adv. Inorg. Biochem. **1979**, 1, 235-252. (b) Klotz, I. M.; Kurtz, D. M., Jr. Acc. Chem. Res. **1984**, 17, 16-22. (c) Wilkins, R. G.; Harrington, P. C. Adv. Inorg. Biochem. **1983**, 5, 52-85.

(2) Sanders-Loehr, J.; Loehr, T. M.; Mauk, A. G.; Gray, H. B. J. Am. Chem. Soc. **1980**, 102, 6992-6996.

(3) Garbett, K.; Darnall, D. W.; Klotz, I. M.; Williams, R. J. P. Arch. Biochem. Biophys. **1969**, 135, 419-434.

(4) Dunn, J. B. R.; Shriver, D. W.; Klotz, I. M. Proc. Natl. Acad. Sci. USA **1973**, 70, 2582-2584.

(5) Kurtz, D. M., Jr.; Shriver, D. W.; Klotz, I. M. Coord. Chem. Rev. **1977**, 24, 145-178.

(6) (a) Stenkamp, R. E.; Sieker, L. C.; Jensen, L. H. J. Inorg. Biochem. **1983**, 19, 247-253. (b) Stenkamp, R. E.; Sieker, L. C.; Jensen, L. H. J. Am. Chem. Soc. **1984**, 106, 618-622.

(7) Sheriff, S.; Hendrickson, W. A.; Smith, J. L. Life Chem. Rep. Suppl. Series **1983**, 1, 305-308.

(8) Stenkamp, R. E.; Sieker, L. C.; Jensen, L. H.; McCallum, J. D.; Sanders-Loehr, J. Proc. Natl. Acad. Sci. USA **1985**, 82, 713-716.

(9) Dawson, J. W.; Gray, H. B.; Hoenig, H. E.; Rossman, G. R.; Schredder, J. M.; Wang, R. H. Biochemistry **1972**, 11, 461-465.

(10) Schugar, H. J.; Rossman, G. R.; Barraclough, C. G.; Gray, H. B. J. Am. Chem. Soc. **1972**, 94, 2683-2690.

(11) Solomon, E. I.; Eickman, N. C.; Gay, R. R.; Penfield, K. W.; Himmelwright, R. S.; Loomis, L. D. In "Invertebrate Oxygen-Binding Proteins: Structure, Active Site and Function"; Lamy, J.; Lamy, J., Eds.; Marcel Dekker: New York, 1981; pp 487-502.

(12) Freier, S. M.; Duff, L. L.; Shriver, D. F.; Klotz, I. M. Arch. Biochem. Biophys. 1980, 205, 449-463.

(13) Shiemke, A. K.; Loehr, T. M.; Sanders-Loehr, J. J. Am. Chem. Soc. 1984, 106, 4951-4956.

(14) Garbett, K.; Darnall, D. W.; Klotz, I. M. Arch. Biochem. Biophys. 1971, 142, 455-470.

(15) Gorman, E. G.; Darnall, D. W.; Biochemistry 1981, 20, 38-43.

(16) Bradić, Z.; Wilkins, R. G. Biochemistry 1983, 22, 5396-5401.

(17) McCallum, J. D.; Shiemke, A. K.; Sanders-Loehr, J. Biochemistry 1984, 23, 2819-2825.

(18) Klotz, I. M.; Klotz, T. A.; Fiess, H. A. Arch. Biochem. Biophys. 1957, 68, 284-299.

(19) Dunn, J. B. R.; Addison, A. W.; Bruce, R. E.; Sanders-Loehr, J.; Loehr, T. M. Biochemistry 1977, 16, 1743-1749.

(20) Loehr, T. M.; Keyes, W. E.; Pincus, P. A. Anal. Biochem. 1979, 96, 456-463.

(21) Sjöberg, B.-M.; Loehr, T. M.; Sanders-Loehr, J. Biochemistry 1982, 21, 96-102.

(22) (a) Loehr, T. M.; Plane, R. A. Inorg. Chem. 1968, 7, 1708-1714. (b) Hewkin, D. J.; Griffith, W. P. J. Chem. Soc. A 1966, 472-475. (c) Cox, L. E.; Peters, D. G. Inorg. Chem. 1970, 9, 1927-1930. (d) Griffith, W. P.; Wickens, T. D. J. Chem. Soc. A 1966, 1087-1090. (e) Griffith, W. P. J. Chem. Soc. 1964, 245-249.

(23) (a) Herzberg, G. "Infrared and Raman Spectroscopy"; D. Van Nostrund: Princeton, 1945. (b) Nakamoto, K. In "Infrared Spectra of Inorganic and Coordination Compounds"; Wiley-Interscience: New York, 3rd Ed., 1978.

(24) Kuhn, L. P.; Wires, R. A. J. Am. Chem. Soc. **1964**, 86, 2161-2165.

(25) Bajdor, K.; Kincaid, J. R.; Nakamoto, K. J. Am. Chem. Soc. **1984**, 106, 7741-7747.

(26) Spiro, T. G. Acc. Chem. Res. **1974**, 7, 339-344.

(27) Plowman, J. E.; Loehr, T. M.; Schauer, C. K.; Anderson, O. P. Inorg. Chem. **1984**, 23, 3553-3559.

(28) "Cyanamide"; American Cyanamid Corp., Process Chemicals Dept., 1963, Wayne, New Jersey.

(29) Shiemke, A. K. Ph.D. Dissertation, Oregon Graduate Center, in preparation.

(30) (a) Tichy, M. Adv. Org. Chem. **1965**, 5, 115-297. (b) Duculot, C. C. R. Acad. Sci. **1955**, 241, 1738-1741. (c) Jones, N. R.; Humphries, P.; Herling, F.; Dobriner, K. J. Am. Chem. Soc. **1952**, 74, 2820-2828. (d) Dorval, C.; Zeegers-Huyskens, T. Spectrochim. Acta **1973**, 29A, 1805-1814.

(31) Sitter, A. J.; Reczek, C. M.; Terner, J. J. Biol. Chem. **1985**, 260, 7515-7522.

(32) Kitagawa, T.; Ondrias, M. R.; Rousseau, D. L.; Ikeda-Saito, M.; Yonetani, T. Nature (London) **1982**, 298, 869-871.

(33) (a) Shaanan, B. Nature (London) **1982**, 296, 683-684. (b) Phillips, S. E. V.; Schoenborn, B. P. Nature (London) **1982**, 292, 81-82.

(34) (a) Buckingham, A. D.; Fan-Chen, L. Int. Rev. Phys. Chem. **1981**, 1, 253-269. (b) Eisenberg, D.; Kauzman, W. In "The Structure and Properties of Water"; Oxford University Press: New York, 1969.

(35) (a) Novak, A. Struct. Bonding (Berlin) **1974**, 18, 177-216. (b) Emsley, J. Struct. Bonding **1984**, 57, 147-191.

(36) Hamilton, W. C.; Ibers, J. A. "Hydrogen Bonding in Solids"; W. A. Benjamin: New York, 1968, Chapter 3.

(37) Stenkamp, R. E., personal communication.

(38) Stenkamp, R. E.; Sieker, L. C.; Jensen, L. H. J. Mol. Biol. **1978**, 126, 457-466.

(39) Joesten, M. D.; Schaad, L. J. "Hydrogen Bonding"; Marcel Dekker: New York, 1974, p 2.

(40) Murthy, A. S. N.; Rao, C. N. R. Appl. Spectrosc. Rev. **1968**, 2, 69-191.

(41) Takano, T. J. Mol. Biol. **1977**, 110, 537-568.

(42) The estimated bond distances and angles for (Fe_1- O-Fe_2-O-O-H) in oxyhemerythrin were: μO-Fe_2, 1.8 Å; Fe_2-O, 2.0 Å; O-O, 1.5 Å; O-H, 1.0 Å; μO-Fe_2-O, 90°; Fe_2-O-O, 110°; O-O-H, 110°. The analogous parameters for (Fe_1-μO-Fe_2-O-H) in cis-hydroxomethemerythrin were: μO-Fe_2, 1.8 Å; Fe_2-O, 2.1 Å; O-H, 1.0 Å; μO-Fe_2-O, 85°; Fe2-O-H, 105°.

(43) Baker, E. N.; Hubbard, R. E. Prog. Biophys. Mol. Biol. **1984**, 44, 97-179.

(44) deWaal, D. J. A.; Wilkins, R. G. J. Biol. Chem. **1976**, 251, 2339-2343.

(45) Bradic, Z.; Conrad, R.; Wilkins, R. G. J. Biol. Chem. **1977**, 252, 6069-6075.

(46) Solomon, E. I. In "Copper Proteins"; Spiro, T. G., Ed.; John Wiley: New York, 1981, Chapter 2.

(47) (a) Bull, C.; McClune, G. J.; Fee, J. A. J. Am. Chem. Soc. **1983**, 105, 5290-5300. (b) Francis, K. C.; Cummins, D.; Oakes, J. J. Chem. Soc. Dalton Trans. **1985**, 493-501.

(48) Halpern, J.; Goodall, B. L.; Khare, G. P.; Lim, H. S.; Pluth, J. J.; Pluth, J. A. J. Am. Chem. Soc. **1975**, 97, 2301-2303.

(49) (a) Lever, A. B. P.; Gray, H. B. Acc. Chem. Res. **1978**, 11, 348-355. (b) Valentine, J. S.; McCandlish, E. In "Electron Transport and Oxygen Utilization"; C. Ho, Ed.; Elsevier-North Holland: 1982, pp 229-235.

(50) McCallum, J. D.; Shiemke, A. K.; Sanders-Loehr, J.; Loehr, T. M.; Appelman, E. H., unpublished results.

(51) (a) Lavelette, D.; Tetreau, C.; Mispelter, J.; Momenteau, M.; Lhoste, J.-M. Eur. J. Biochem. **1984**, 145, 555-565. (b) Walker, F. A.; Bowen, J. J. Am. Chem. Soc. **1985**, submitted.

Table I. Vibrational Frequencies for the Symmetric Fe-O-Fe Vibration in Various Forms of Hemerythrin[a]

Ligand	ν_s(Fe-O-Fe) in H_2O	ν_s(Fe-O-Fe) in $H_2{}^{18}O$	Shift in D_2O
Non-H-bonded			
N_3^-	507	493	0
SCN^-	514	498	0
CN^-	512	498	0
OCN^-	509	497	0
Cl^-	510	496	0
None (Met)	512	496	0
None (ClO_4^-)	512	496	0
$HNCN^-$	508	495	0
$HCOO^-$	513	497	0[b]
OH^- (*trans*)	506	491	0[c]
H-bonded			
OH^- (*cis*)	492	477	+26[d]
OOH^- (Oxy)	486	472	+4

[a]All spectra taken on liquid samples in flow cell at 278 K with near-UV excitation; frequencies in cm^{-1}. [b]Hemerythrin derivative prepared from deuterated sodium formate ($DCOO^-$) as well as in D_2O. [c]Curve fitting of spectrum in Figure 3d indicates that a peak near 506 cm^{-1} is still present in the deuterated protein. [d]Upward shift of most intense spectral feature due to coupling of ν_s(Fe-O-Fe) with δ(Fe-O-D).

FIGURE CAPTIONS

Figure 1. Proposed structure of the ligand binding site of oxyhemerythrin.[8,13] The hydroperoxide ligand is derived from O_2, the oxo bridge from solvent, the carboxylate bridges are from Asp and Glu, and the remaining ligands are N(His).

Figure 2. Proposed structures of the ligand binding site of hydroxomethemerythrin in the (a) cis conformation, (b) trans conformation. The hydroxide ligand is derived from solvent, other ligands are identical to those in Figure 1.

Figure 3. Resonance Raman spectra of hydroxomethemerythrin at 278 K. Excitation at 363.8 nm, 20 mW at the sample, 90° scattering geometry, protein concentration of 1.5-2.0 mM in monomer. Each spectrum represents the accumulation of 10-15 scans with a slit width of 7 cm^{-1} and scan rate of 0.5 cm^{-1}/sec. Isotopic composition of the bridge oxygen and the solvent is listed to the right of each spectrum. Data have been submitted to a 17-point Savitsky-Golay smoothing routine.

Figure 4. Resonance Raman spectra of hydroxomethemerythrin at 90 K. Excitation at 406.7 nm, 17 mW at the sample, 5-10 mM protein concentration and 180° scattering geometry. Spectra are the accumulation of 15-20 scans with a slit width of 8 cm^{-1} and scan rate of 1 cm^{-1}/sec. A 17-point smoothing routine was used.

Figure 5. Temperature dependence of the relative intensity of the two ν_s(Fe-O-Fe) modes of hydroxomethemerythrin. Each data point represents the average of two separate determinations (the average of three at 90 K) using conditions as in Figure 4.

Figure 6. Resonance Raman spectra of oxyhemerythrin in solution at 278 K. Conditions are the same as for Figure 3.

Figure 7. pH titration for the conversion of methemerythrin to hydroxomethemerythrin. the ordinate represents the amount of hydroxomethemerythrin as a fraction of the total amount of protein, as determined from the relative intensities of symmetric Fe-O-Fe vibrations. The solid line is the theoretical curve for a pK_a of 7.9. Instrumental and sample conditions as in Figure 3.

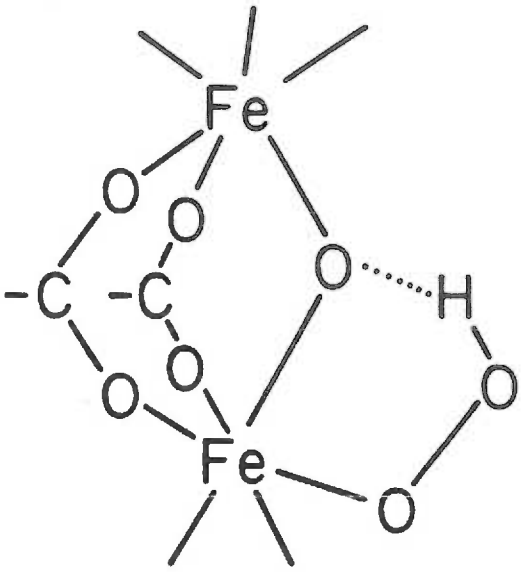

FIGURE 1

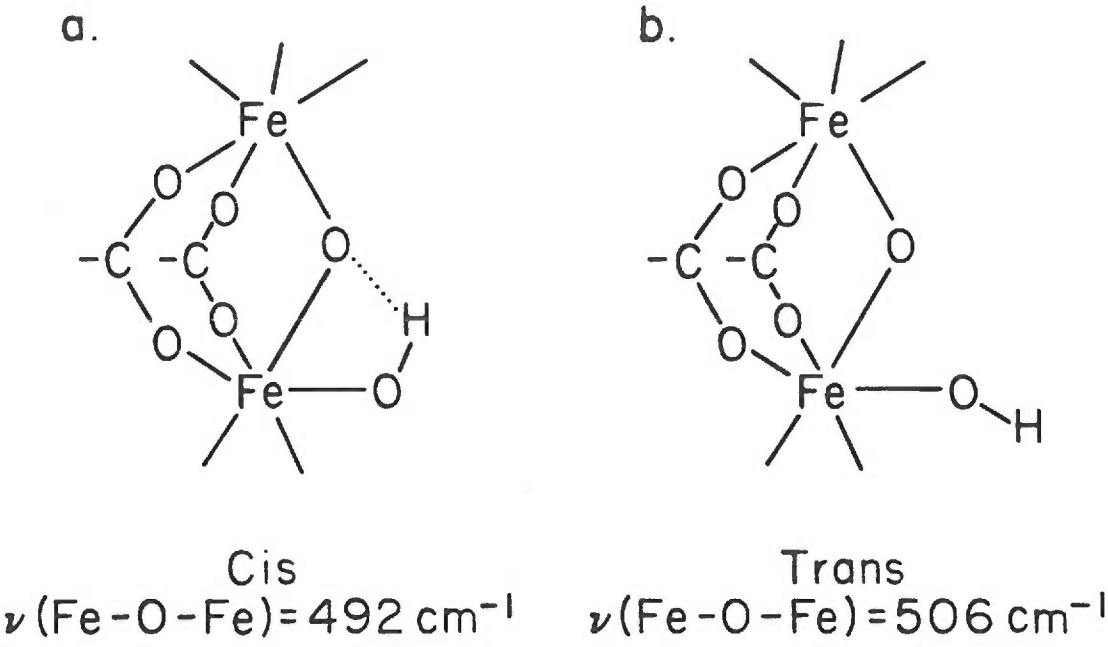

Cis
ν(Fe-O-Fe)=492 cm^{-1}

Trans
ν(Fe-O-Fe)=506 cm^{-1}

Figure 2

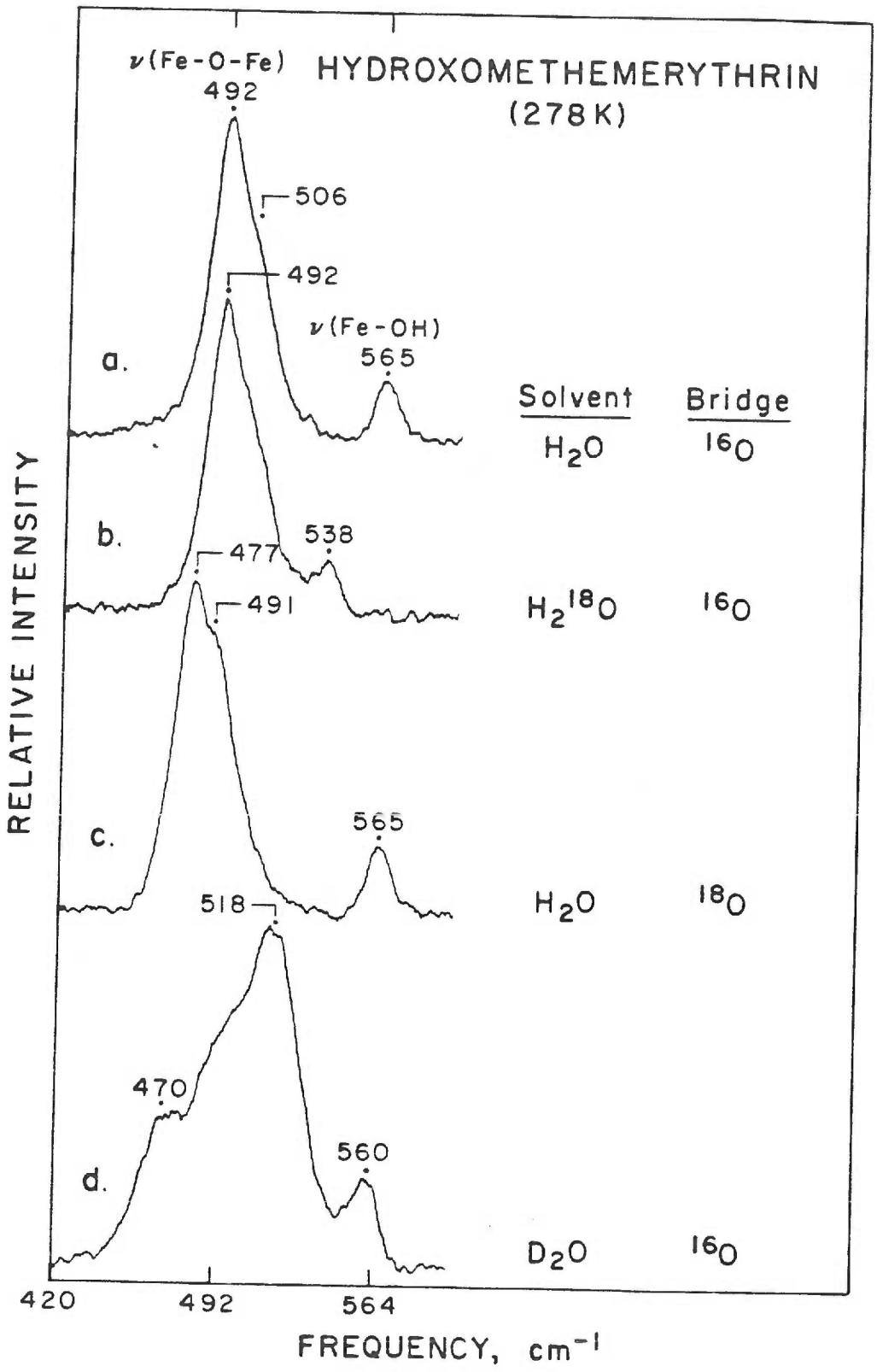
ν(Fe-O-Fe)
492
HYDROXOMETHEMERYTHRIN
(278 K)
506
492
ν(Fe-OH)
565
a.
Solvent
Bridge
H2O
16O
b.
477
538
491
H2 18O
16O
c.
565
518
H2O
18O
470
560
d.
D2O
16O
RELATIVE INTENSITY
420
492
564
FREQUENCY, cm-1

FIGURE 3

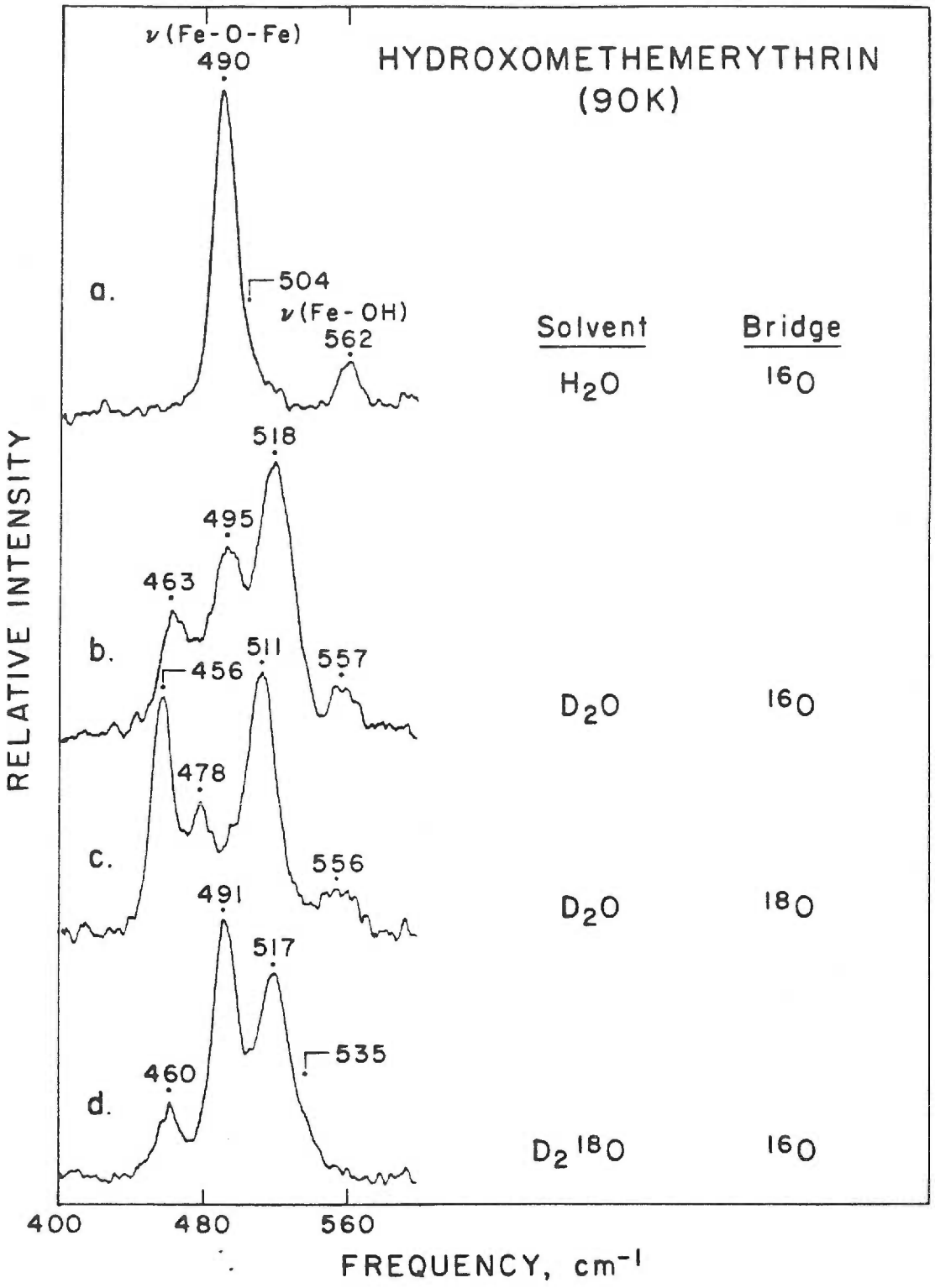
ν(Fe-O-Fe)
490
HYDROXOMETHEMERYTHRIN
(90K)
a.
504
ν(Fe-OH)
562
Solvent
Bridge
H2O
16O
518
495
463
b.
511
456
557
D2O
16O
478
c.
556
491
D2O
18O
517
535
460
d.
D2 18O
16O
RELATIVE INTENSITY
400
480
560
FREQUENCY, cm-1

FIGURE 4

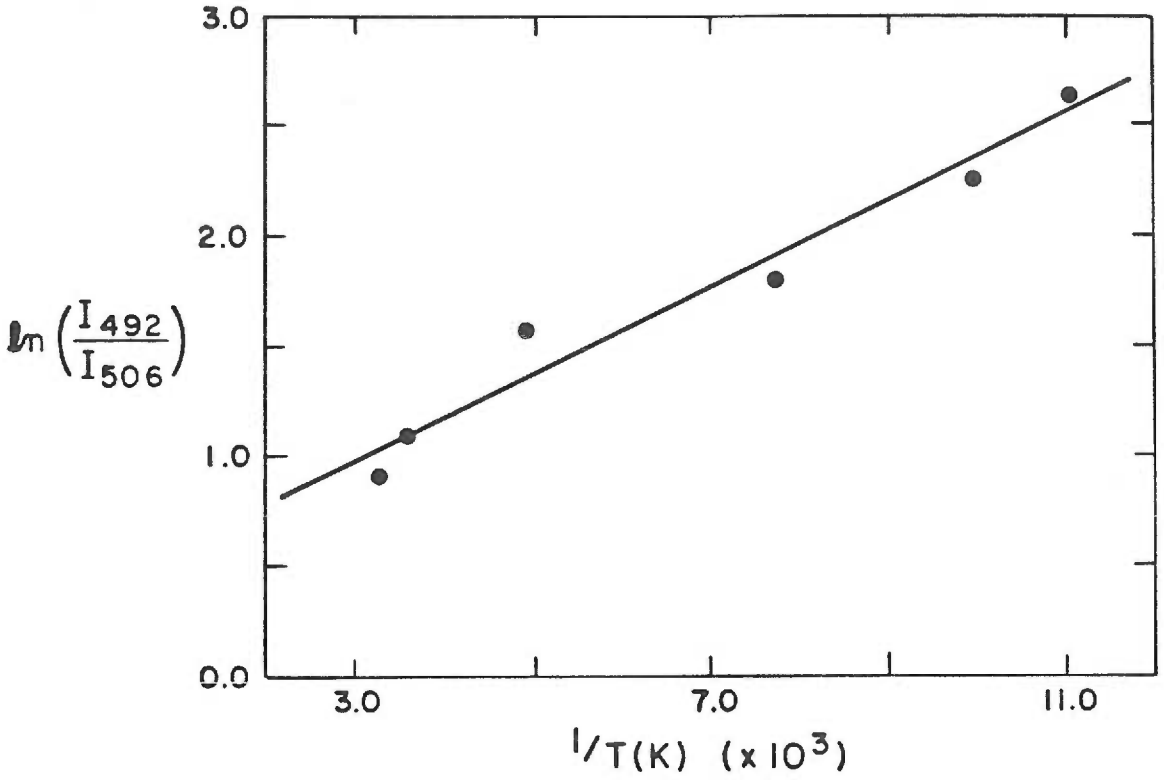

FIGURE 5

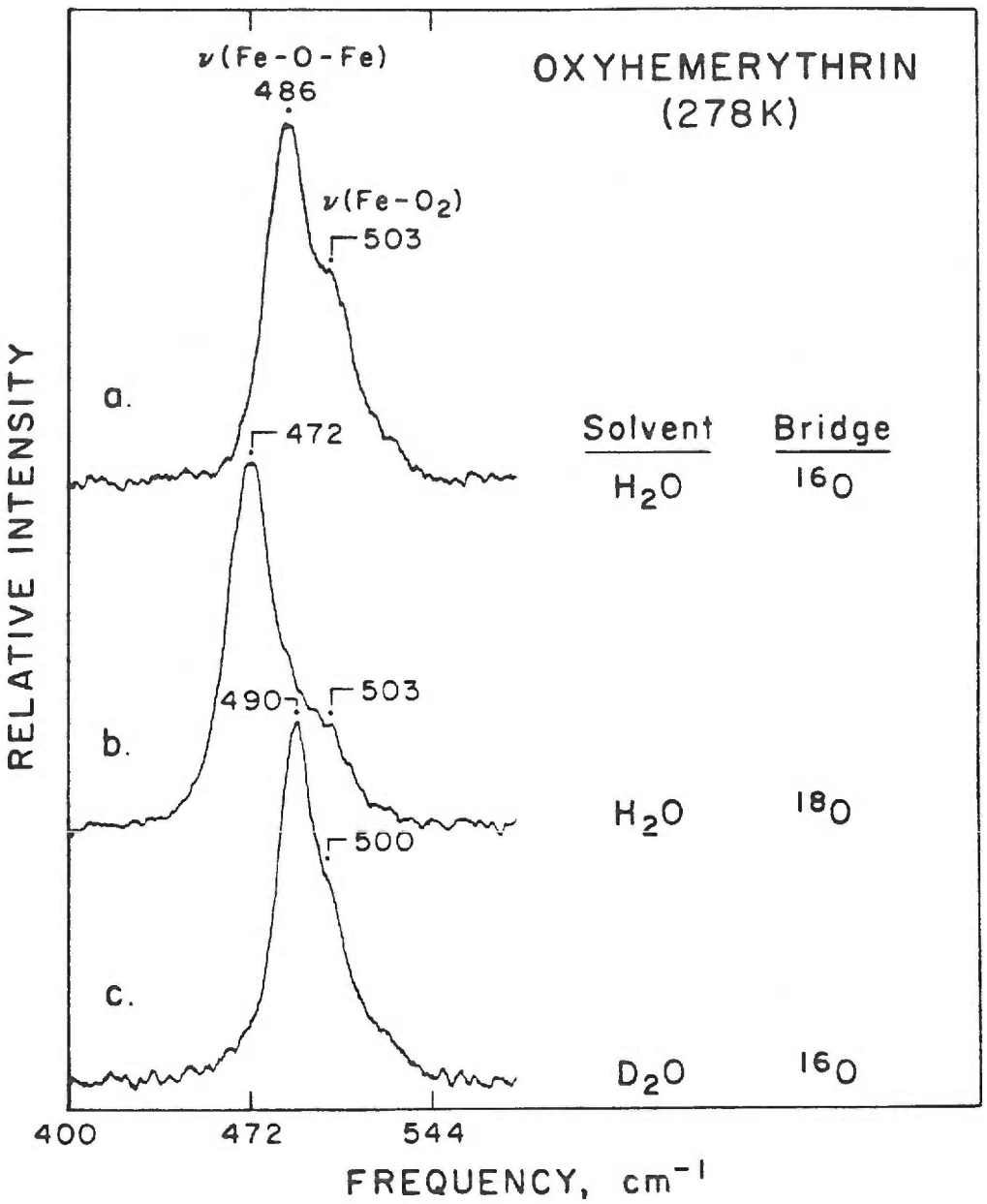
ν(Fe-O-Fe)
486
OXYHEMERYTHRIN
(278K)
ν(Fe-O2)
503
a.
472
Solvent
Bridge
H2O
16O
490
503
b.
H2O
18O
500
c.
D2O
16O
RELATIVE INTENSITY
400
472
544
FREQUENCY, cm-1

FIGURE 6

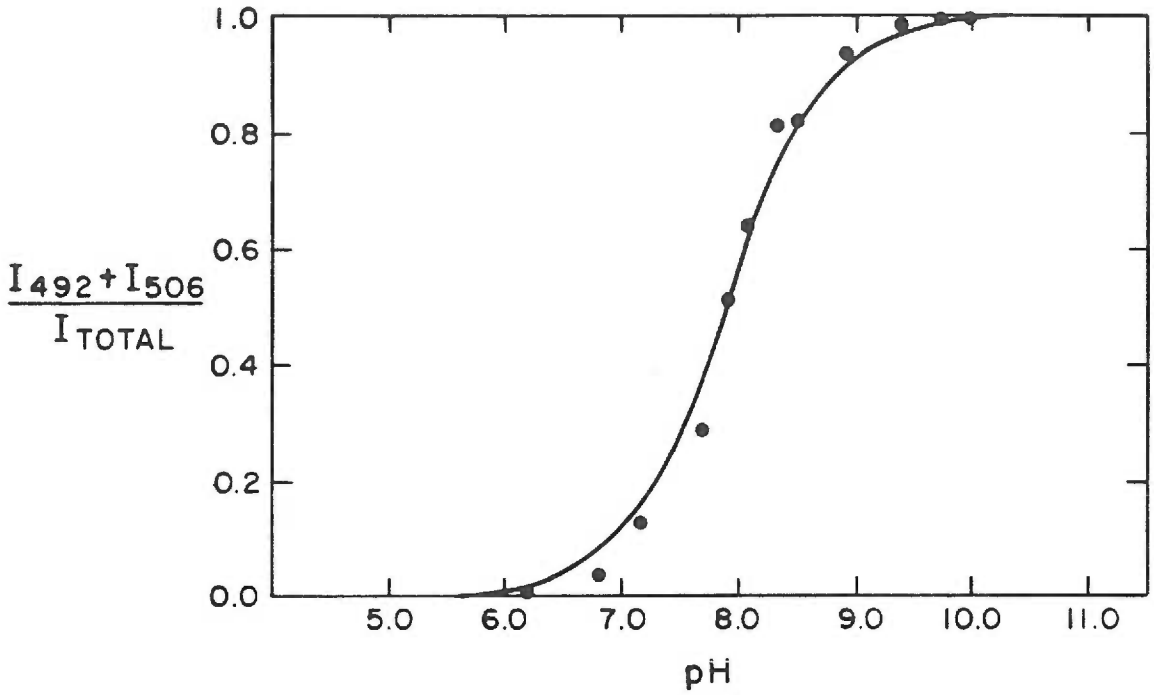

FIGURE 7

CHAPTER V

Resonance Raman Study of Ligand-Free Methemerythrin. Evidence for Multiple Conformations of the Fe-O-Fe Center at Low Temperatures

INTRODUCTION

The ferric forms of hemerythrin, which include the oxy and the ligated methemerythrin derivatives, have been the subject of extensive physical studies.[1] Their similar spectral and physical properties indicate that the binuclear iron centers of these forms of hemerythrin possess a common structure having face-sharing octahedral ferric ions.[2-5] The structure of the iron center of azidomethemerythrin (Fig. 1a) shows that all but three of the coordination sites are filled by endogenous imidazole (His) and carboxylate (Asp and Glu) ligands. Two of the remaining sites are occupied by the bridging oxo group, leaving a single position for the binding of the exogenous ligand. Considerable evidence from spectroscopy and x-ray diffraction indicates that all of the small anionic ligands of hemerythrin bind in a manner analogous to that of azide.[1-5]

The binding site structures of oxy (i.e. hydroperoxo) and hydroxomethemerythrin differ slightly from those of the prototypic azidomethemerythrin in that hydrogen bonding occurs between the exogenous ligand and the oxo bridge. These structural differences were delineated by resonance Raman spectroscopy and presented in the previous two chapters. Recent x-ray diffraction studies, however, show that the binuclear iron center of unligated methemerythrin is structurally unique.[3] Unlike most other spectral techniques, the resonance Raman spectral features of methemerythrin reflect this unique structure.

Methemerythrin is the oxidized form of the protein that exists at low pH (<7) in the absence of added coordinating anions. This

derivative, previously referred to as aquomethemerythrin, undergoes a pH-dependent transformation between acid and base forms with a pK_a of 7.6 which can be detected by small changes in the optical spectrum between 370 and 380 nm.[6,7] The titration behavior had been interpreted as the deprotonation of a ligated water molecule in the acid form to a hydroxo ion in the base form.[7-9] However, refinement of the crystal structure revealed that the ligand binding site is vacant in the low pH form of methemerythrin.[3b] This species has, therefore, been renamed "methemerythrin" rather than "aquomethemerythrin". Although the gross structural features of the binuclear iron center are maintained in methemerythrin (Figure 1b), the absence of an exogenous ligand leads to a new coordination geometry for Fe_b having a pentacoordinate trigonal bipyramidal structure.[3b] The distortion is effected primarily by displacement of Fe_b away from the ligand binding pocket, as illustrated by the negative electron density in the difference density map (F_0azide - F_0met) shown in Figure 2.

Despite the altered binding site structure of methemerythrin, only slight differences in its Mossbauer,[10] circular dichroism, and optical spectra[11] are observed. However, resonance Raman spectra show features which are unique to methemerythrin. In particular, the asymmetric Fe-O-Fe vibration of methemerythrin is observed at 752 cm^{-1}, some 30 cm^{-1} lower in energy than the analogous vibration of ligated methemerythrins. In addition, methemerythrin spectra have a feature at ~530 cm^{-1} appearing as a shoulder on the strong 512 cm^{-1} ν_s(Fe-O-Fe) band which is peculiar to this derivative, and at low temperatures (<200 K), an entirely new peak appears at 490 cm^{-1}. The identification of the 490-cm^{-1} peak as an Fe-O-Fe vibration from isotopic bridge exchange suggests the presence of

two conformations of methemerythrin in this temperature range. This behavior is attributed to a temperature-dependent interconversion of the ligand-binding iron between trigonal bipyramidal and octahedral geometries. We also have evidence that this effect on the binuclear iron center is related to a protein conformational change.

EXPERIMENTAL SECTION

Hemerythrin. Phascolopsis gouldii marine worms were obtained from the Marine Biological Laboratory, Woods Hole, MA. Hemerythrin was isolated from the coelomic fluid of the worms using the procedure of Klotz et al.[12] The protein from P. gouldii was purified by crystallization via dialysis against 15% (V/V) ethanol. The crystalline protein, predominantly in the oxy form, was washed at least three times with fresh 15% ethanol, then dissolved in 0.05 M Tris, 0.21 M sulfate (pH 8.0) and stored as a sterile solution at 5°C. This purified protein was converted to methemerythrin by addition of $K_3Fe(CN)_6$ in a 4-fold molar excess per hemerythrin monomer, followed by extensive dialysis against Raman buffer: 0.05 M MES, 0.2 M sulfate (pH 6.2). Methemerythrin-perchlorate was prepared by addition of solid $NaClO_4$ to methemerythrin in Raman buffer. Final ClO_4^- concentration was 0.2 M.

Deoxyhemerythrin was prepared by anaerobic dialysis of methemerythrin against a 4-fold molar excess of sodium dithionite (Gallard-Schlesinger Corp., Carle Place, NY) and equimolar potassium thiocyanate. Excess reagents were removed by further anaerobic dialysis against 0.05 M Tris, 0.2 M sulfate (pH 8.0). Substitution of ^{18}O into the oxo bridge position was carried out by incubating deoxyhemerythrin in

$H_2{}^{18}O$ according to our previously published procedure.[13] The exchange of solvent for D_2O (0.05 M MES, 0.2 M sulfate, pD 6.4) or $H_2{}^{18}O$ buffer (0.05 M MES, 0.2 M sulfate, pH 6.2) was accomplished by several cycles of concentration and dilution with the labeled buffer, as published.[13]

Spectroscopy. Resonance Raman spectra were collected on a computer interfaced Jarrell-Ash spectrometer[14] equipped with Spectra-Physics 164-05 (Ar) and 164-01 (Kr) lasers, a cooled RCA C31034A photomultiplier tube, and an ORTEC Model 9302 amplifier/discriminator. Both lasers are equipped with ultra-high-field magnets to enhance ultraviolet output. Spectra of hemerythrin at low temperature were obtained by backscattering from a frozen sample in a capillary tube. Sample temperatures were maintained and measured according to previously published methods.[13] Spectra of samples in solution were obtained using a flow cell (sample temperature of ~5°C) as described elsewhere.[13,15] Protein concentrations were typically 1.5-2 mM in hemerythrin monomer for the solution spectra and 5-10 mM for the low temperature spectra. The spectra of isotopically labeled samples intended for comparison were run consecutively, on the same day, under identical instrumental and sample conditions. Reported peak positions are accurate within 1 cm^{-1}. The frequency of isolated peaks was determined by comparison to the internal standard (ν_1 of sulfate). Where overlapping peaks occur, positions and relative intensities were determined from curve-resolved components using computer-generated peaks for a best fit of the spectrum. Fitting was performed with 90% Lorentzian-10% Gaussian peak shapes and 18-cm^{-1} band widths (full width at half height) for solution samples or 14-cm^{-1} band widths for frozen samples. Protein concentrations were determined from their absorption spectra using published extinction coefficients.[11]

Absorption spectra were obtained on a Perkin-Elmer Lambda 9 spectrophotometer.

RESULTS and DISCUSSION

Methemerythrin Spectra at 278 K. All of the ferric hemerythrins (oxy and met) are characterized by intense transitions in the near-UV region of the optical spectrum.[11] These transitions have been assigned as O^{2-}(bridge) $\rightarrow$ Fe(III) charge transfer on the basis of polarized, single-crystal optical spectra.[16] Consistent with this assignment is the strong, selective enhancement of Fe-O-Fe Raman vibrations (both symmetric and asymmetric) with near-UV excitation.[13,15] The near-UV excited Raman spectrum of (ligand-free) methemerythrin in solution exhibits peaks at 512 (with a shoulder at ~530 cm^{-1}) and 752 cm^{-1} (Figures 3a and 4a). Upon substitution of the oxo bridge with ^{18}O, the 512 and 752 cm^{-1} peaks shift to 498 and 716 cm^{-1} (Figures 3c and 4b), establishing these spectral bands as the symmetric (ν_s) and asymmetric (ν_{as}) Fe-O-Fe vibrations, respectively. Similarly, the peak at 1014 cm^{-1} in Figure 4a can be assigned as the 2 x ν_s(Fe-O-Fe) overtone on the basis of its shift to lower energy in the Fe-^{18}O-Fe species (Fig. 4b). This overtone band has also been observed in the resonance Raman spectra of the triply-bridged model compound $Fe_2O(CH3COO)_2(HBpz_3)_2$,[22a] as well as many other ligated methemerythrins (with UV excitation).

The ν_{as}(Fe-O-Fe) frequency for (ligand-free) methemerythrin is some 20-30 cm^{-1} lower than the analogous vibration of other (ligated) methemerythrins.[17] Such a frequency decrease could conceivably stem from a decrease in the Fe-O-Fe angle[18] since the crystal structures of

the T. dyscrita proteins reveal an Fe-O-Fe angle of 127° in methemerythrin versus 135° in azidomethemerythrin. However, a decrease in the bridge angle should increase ν_s(Fe-O-Fe),[18] but ν_s(Fe-O-Fe) of methemerythrin at 512 cm^{-1} is similar to that of most other (ligated) methemerythrins (506-516 cm^{-1}).[17] Alternatively, the low value for ν_{as}(Fe-O-Fe) in methemerythrin could be due to a reduction in the force constants of the Fe-O (oxo bridge) bonds, but this would be expected to lower ν_s(Fe-O-Fe) as well (as is observed for oxy and hydroxomethemerythrin).[13] Thus, changes in both the oxo bridge force constants and the bridge angle are required to account for the low ν_{as}(Fe-O-Fe) and "normal" ν_s(Fe-O-Fe) frequencies of methemerythrin. The structural distortion of methemerythrin relative to the ligated derivatives which decreases the Fe-O-Fe angle[3b] by ~8° is also likely to alter the force constants. Thus, the anomalous Fe-O-Fe vibrational frequencies of methemerythrin presumably stem from its distinctive structure.

The appearance of shoulders at ~519 and 530 cm^{-1} (Fig. 3a and 5a) are also unique to methemerythrin. These peaks do not shift in frequency when ^{18}O is present in the bridge (Fig. 3c and 5c), indicating that they are not Fe-O-Fe vibrations. Thus, the presence of the additional bands in (ligand-free) methemerythrin is not analogous to hydroxomethemerythrin, whose two peaks at 492 and 506 cm^{-1} are both ν_s(Fe-O-Fe) vibrations.[13] Furthermore, the spectrum of methemerythrin is totally unaffected by exposure to $H_2{}^{18}O$ solvent (Fig. 3b and 5b), thereby excluding H_2O or OH^- as ligands responsible for the 519 and 530 cm^{-1} features. This is in contrast to hydroxomethemerythrin where an $H_2{}^{18}O$-sensitive Fe-OH stretch at 565 cm^{-1} is clearly observed.[13]

These Raman results are thus entirely consistent with the conclusions from x-ray crystallography that methemerythrin lacks an exogenous ligand.[3]

Bridge substitution by ^{18}O, however, does affect the intensity of the 519 and 530-cm^{-1} shoulders, causing a ~50% decrease as ν_s(Fe-O-Fe) shifts from 512 to 498 cm^{-1} (Figures 3a and 3c). The change in intensity is indicative of weak coupling to ν_s(Fe-O-Fe). Coupling can arise when vibrational modes belonging to the same symmetry species have similar frequencies;[19] this type of configuration interaction (Fermi resonance) results in marked frequency shifts of the coupled modes upon isotope substitution. In the present case, however, where only intensities are affected in response to the isotope-induced perturbation, the coupling may be described as intensity borrowing. Similar coupling is observed between the 486 cm^{-1} ν_s(Fe-O-Fe) and 503 cm^{-1} ν(Fe-O_2) of oxyhemerythrin,[13] and the O-O stretch and axial base vibrations of O_2 adducts of cobalt porphyrins.[20] In all these cases, a strongly-enhanced vibration lends intensity to a nearby mode which does not participate in the excited state distortion and, therefore, would not otherwise be observed. Consistent with this picture is the observation that the intensity of the 530-cm^{-1} mode of methemerythrin decreases much faster than does ν_s(Fe-O-Fe) as the incident light moves off resonance (to longer wavelength). This rapid decrease in enhancement explains why Freier et al. failed to observe the 530-cm^{-1} peak with 457.9-nm excitation.[21]

The coupling between the modes at 519 and 530 cm^{-1} and ν_s(Fe-O-Fe) implies a structural connection between the atoms involved in the separate vibrations.[19] The peaks in question must therefore be due to

vibrations of endogenous iron ligands, i.e., either imidazole from His or carboxylate from Asp or Glu. However, the frequencies of these features are too high for either Fe-N(imidazole) or Fe-O(carboxylate) vibrations, which occur at ~250 and ~360 cm^{-1}, respectively,[23,24] and must therefore arise from internal vibrations. The only internal imidazole vibration occurring near 500 cm^{-1}, the N-H out-of-plane bend, typically shows a 50-cm^{-1} decrease in D_2O.[25] There is a definite loss of intensity at ~519 cm^{-1} upon deuteration (Fig. 3d, 5d), suggesting that this peak may be assigned to the imidazole bend. The failure to observe a new peak at lower frequency is expected since a vibration at that energy would no longer be coupled to the Fe-O-Fe mode.

The 530-cm^{-1} peak is clearly not affected by deuteration and, therefore, can be assigned as an internal vibration of one or both of the carboxylate bridges, i.e., the O-C-O bend (δ(O-C-O)). In free acetate, δ(O-C-O) is observed at 650 cm^{-1} and at 690 cm^{-1} in the copper acetate dimer.[24,26] In the resonance Raman spectrum of the triply-bridged model $Fe_2O(CH3COO)_2(TACN)_2$ a feature observed at 581 cm^{-1} is probably the δ(O-C-O) of the bridging carboxylates.[22b] In the latter example there appears to be coupling similar to that in methemerythrin: the 581-cm^{-1} mode undergoes a ~40% decrease in intensity when ^{18}O-bridge substitution shifts ν_s(Fe-O-Fe) from 540 to 525 cm^{-1}.[22b]

Methemerythrin Spectra at 90 K. The resonance Raman spectrum of methemerythrin at 90 K is shown in Figure 5. The 512 and 530 cm^{-1} peaks are somewhat sharper and slightly shifted in frequency, effects that are typical of low temperature spectra.[13] In addition, a strong new feature appears at 490 cm^{-1}. Substitution of the oxo bridge with ^{18}O causes the 490 cm^{-1} peak to shift to 474 cm^{-1} (Fig. 5c), identifying it as a

ν_s(Fe-O-Fe) vibration. The 510-cm^{-1} feature (corresponding to the 512-cm^{-1} peak in the solution spectra, Fig. 3 and 4) is shifted 14 cm^{-1} to lower energy by this substitution, as expected. The appearance of these two ν_s(Fe-O-Fe) peaks (490 and 510 cm^{-1}) indicates the presence of two conformations of methemerythrin at low temperature which we ascribe to an intramolecular isomerization in the protein. The fact that the 519 and 530-cm^{-1} features have not lost any intensity relative to the peak at 510 cm^{-1} upon change in temperature indicates that they are associated with the 510-cm^{-1}, but not the 490-cm^{-1} Fe-O-Fe conformation.

The appearance of the 490-cm^{-1} peak takes place rapidly as the sample temperature is reduced below 200 K. This temperature dependence was quantitated in a manner analogous to that used for the cis-trans isomerization of hydroxomethemerythrin.[13] For methemerythrin the intensity ratio of the 490 and 510 cm^{-1} peaks is taken to be proportional to the equilibrium constant for the isomerization. This intensity ratio was measured at various temperatures (by fitting the observed spectra) to give the van't Hoff plot of Figure 6. In contrast with the results for hydroxomethemerythrin,[13] the present van't Hoff plot is clearly non-linear, and indicates that the enthalpy and entropy changes for the isomerization are temperature dependent. In other words, the heat capacities of reactants and products are different. Changes in heat capacity are characteristic of protein conformational changes.[27]

In this particular case, the heat capacity of the conformation with ν_s(Fe-O-Fe) at 490 cm^{-1} is decreased relative to the solution conformation. Although it is difficult to quantitate the difference in heat capacity of the two conformations (this requires differentiating ΔH° with respect to temperature), it is estimated to be on the order of 10

cal mole^{-1} K^{-1} at atmospheric pressure.[28] This is at least two orders of magnitude less than the change in heat capacity that occurs upon denaturation of proteins.[27] The specific structural differences between these two methemerythrin conformations must therefore be limited to changes in a few protein residues rather than gross changes in secondary structure.

The intensity of the 490-cm^{-1} peak also depends on the age of the protein, consistent with a dependence on protein conformation. This low frequency ν_s(Fe-O-Fe) mode has been observed in fresh methemerythrin samples from four different preparations of P. gouldii protein and one preparation of T. dyscrita protein. However, it was not seen in samples that were more than 3 months old, but in which the 510-cm^{-1} peak is retained. Apparently, as the protein ages, it is no longer able to undergo the conformational change responsible for the appearance of the 490-cm^{-1} ν_s(Fe-O-Fe) mode. Similar behavior has been documented for ligand binding reactions of methemerythrin: as the protein ages it loses its ability to bind anions such as N_3^- or OH^-.[29]

Multiple Protein Conformations. Kinetics studies of Harrington and Wilkins[30] support the existence of multiple protein conformations in methemerythrin. Many reactions of hemerythrin, such as binding of exogenous ligands have a rate constant of ~10^{-3} s^{-1} that is independent of the concentrations of the reactants. This has led to the suggestion that the rate determining step is a protein conformational change. A minimum of two distinct protein conformations may be proposed (hereafter referred to as non-reactive (N) and reactive (R) conformations) having an equilibrium constant such that N predominates near room temperature. According to this scheme (illustrated in Fig. 7) the N conformation

reacts very slowly with hydroxide,[9] thiocyanate,[9] and dithionite.[9] When the protein is in the R form, it reacts rapidly; the rate-determining step is the conversion from N to R with a first-order rate constant of 10^{-3} s^{-1}. A similar conformational change may also be involved in the oxidation of semi-methemerythrin with ferricyanide,[31] the disproportionation of semi-met hemerythrin[32] and the conversion between $(semi\text{-}met)_R$ and $(semi\text{-}met)_O$,[31] since the latter three processes also occur at a rate of $\sim 10^{-3}$ s^{-1}.

It is likely that these same two protein conformations give rise to the distinctive vibrations observed in the low temperature resonance Raman spectrum of methemerythrin. The conformation with ν_s(Fe-O-Fe) at 510 cm^{-1} predominates near room temperature and, therefore, corresponds to the N conformation. With decreasing temperature, the equilibrium between the two conformations shifts such that the R form with ν_s(Fe-O-Fe) at 490 cm^{-1} can be observed below 220 K. We propose that the change in protein conformation from N to R results in a change in the geometry of the binuclear iron center. In the N conformation, the ligand-binding iron (Fe_b) is in a trigonal bipyramidal arrangement as shown in Figure 1b. In the R conformation, the ligand-binding iron has been converted to an octahedral geometry similar to the azidomethemerythrin structure (Fig. 1a), but with an empty coordination site. The binding of exogenous ligands such as N_3^-, SCN^-, OCN^-, $HCOO^-$, and Cl^- stabilizes the R conformation. Thus, only a single ν_s(Fe-O-Fe) peak is observed for these ligated methemerythrins, regardless of sample temperature.

Further information about the N to R conformational change comes from studies of the effect of perchlorate ion on methemerythrin. Unlike

the small anions which bind at the binuclear iron center, perchlorate has been shown to bind to the surface of the protein at a site ~15 Å from the Fe-O-Fe cluster.[5] The spectral properties of the perchlorate adduct are identical to those of methemerythrin, and difference density maps ($F_o$met-perchlorate - $F_o$met) indicate that the binuclear iron center is essentially identical to that of methemerythrin (Fig. 1b).[5] Yet the chemistry of these two derivatives is very different. Both ligand binding and redox reactions that take place at the Fe-O-Fe site, as well as disulfide and mercurial binding at the protein periphery are retarded in the presence of perchlorate.[8,9,30,31] The most reasonable explanation for these results is that perchlorate binding stabilizes the N conformation, thereby making it more difficult for the protein to undergo the reactions which depend on the change in conformation. This interpretation is supported by resonance Raman studies which show that methemerythrin-perchlorate at 90 K fails to exhibit the 490-cm^{-1} peak characteristic of the R conformation (Fig. 8).

The proposed change in the geometry of Fe_b coincident with the N to R conformation change would reasonably be expected to alter the force constants and angle of the Fe-O-Fe center and thereby bring about the observed reduction in ν_s(Fe-O-Fe) frequency. Because the angle and force constants are not independent of each other (as discussed above), the specific changes in each parameter that cause this frequency reduction cannot be identified. The lower frequency of ν_s(Fe-O-Fe) in the R form is in the expected direction for a wider Fe-O-Fe angle (135°) in an octahedral site (as in azidomethemerythrin[3b]) compared to the 127° angle in the N form of methemerythrin[3b] with its trigonal bipyramidal site. Since binding of exogenous ligands to the R form is not expected to have

much further effect on the geometry, the increase in ν_s(Fe-O-Fe) from 490 cm^{-1} in R to 507-515 cm^{-1} in ligated methemerythrin must be due primarily to changes in Fe-O bond force constants.

An alternative explanation for a ν_s(Fe-O-Fe) at 490 cm^{-1} might have been hydrogen bonding to the oxo bridge such as has been observed to result in ν_s(Fe-O-Fe) frequencies at 486 cm^{-1} in oxyhemerythrin and at 492 cm^{-1} in the cis conformer of hydroxomethemerythrin.[13] However, methemerythrin has no exogenous ligand which could act as a hydrogen bond donor and there are no protein groups within 6 Å of the Fe-O-Fe site which are capable of being hydrogen bond donors.[33] In addition, the 490-cm^{-1} ν_s(Fe-O-Fe) mode of methemerythrin is not sensitive to deuterium exchange (Fig. 5d). If the frequency reduction were related to hydrogen bonding we would expect ν_s(Fe-O-Fe) to shift to higher frequency in D_2O, as is observed for oxyhemerythrin.[13] Furthermore, the temperature dependence of the equilibrium between the two methemerythrin conformers cannot be described by a single $\Delta H°$, and is very different from the results for the cis-trans conversion of hydroxomethemerythrin.[13] The observed conformers of methemerythrin are, therefore, unlikely to arise from isomerization between hydrogen bonded and non-hydrogen bonded forms.

Despite the maintenance of the carboxylate bridges in all forms of hemerythrin, the δ(O-C-O) vibration appears to be observed only in the N conformer of methemerythrin. Comparison of azidomet and methemerythrin crystal structures indicates the Fe_b-O(Glu 58) bond distance is drastically reduced by ~0.30 Å in methemerythrin.[3b] This could conceivably lead to a reduction in the δ(O-C-O) frequency, thereby permitting it to couple to ν_s(Fe-O-Fe) at 512 cm^{-1}. The ligated methemerythrins and the R conformation do not share this binding site

distortion, thus their δ(O-C-O) frequencies would be closer to the more typical value of 600 cm^{-1}, too far from ν_s(Fe-O-Fe) for effective coupling.

CONCLUSIONS

The present Raman results have led to the proposal that a trigonal bipyramidal to octahedral change of the ligand binding iron in methemerythrin is part of the N to R conversion observed by other techniques. This structural rearrangement involves an equilibrium between two species whose non-linear van't Hoff plot is typical of a protein conformational change. However, much of the evidence is circumstantial and additional pieces of information would be helpful in verifying this proposal. For example, the the ν_s(Fe-O-Fe) enhancement profiles of the N and R state differ since the intensity of the 490-cm^{-1} peak decreases relative to 510 cm^{-1} with 457.9 nm excitation. Thus, it is possible that the optical spectrum of methemerythrin might change with temperature. We would expect the appearance of the R conformer at low temperature to contribute spectral features more similar to those of the ligated methemerythrins. Lastly, it would be informative to study myohemerythrin under these conditions (low temperature with near UV excitation) to see if it behaves the same as the octameric protein. In this way one could determine if interactions between subunits are involved in the conformational change. Some kinetics[1c] and resonance Raman results[34] indicate that conformational changes are important in the chemistry of this monomeric hemerythrin as well.

REFERENCES

1. (a) J. Sanders-Loehr and T. M. Loehr, Adv. Inorg. Biochem., **1**, 235 (1979). (b) D. M. Kurtz, Jr. and I. M. Klotz, Acc. Chem. Res., **17**, 16 (1984). (c) R. G. Wilkins and P. C. Harrington, Adv. Inorg. Biochem., **5**, 52 (1983). (d) D. M. Kurtz, Jr., D. F. Shriver, and I. M. Klotz, Coord. Chem. Rev., 24, 145 (1977). (e) J. Sanders-Loehr, "Binuclear Iron Proteins," in T. M. Loehr, A. B. P. Lever, and H. B. Gray, Eds., Iron Proteins, in press.
2. R. E. Stenkamp, L. C. Sieker, L. H. Jensen, J. D. McCallum, and J. Sanders-Loehr, Proc. Natl. Acad. Sci. USA, **82**, 713 (1985).
3. (a) R. E. Stenkamp, L. C. Sieker, and L. H. Jensen, J. Inorg. Biochem., **19**, 247 (1983). (b) R. E. Stenkamp, L. C. Sieker, and L. H. Jensen, J. Am. Chem. Soc., **106**, 618 (1984).
4. S. Sheriff, W. A. Hendrickson, and J. L. Smith, Life Chem. Rep. Suppl. Series, **1**, 305 (1983).
5. R. E. Stenkamp, L. C. Sieker, and L. H. Jensen, J. Mol. Biol., **126**, 457 (1978).
6. J. D. McCallum, A. K. Shiemke, and J. Sanders-Loehr, Biochemistry, **23**, 2819 (1984).
7. E. G. Gorman and D. W. Darnall, Biochemistry, **20**, 38 (1981).
8. K. Garbett, D. W. Darnall, and I. M. Klotz, Arch. Biochem. Biophys., **142**, 455 (1971).
9. Z. Bradic and R. G. Wilkins, Biochemistry, **22**, 5396 (1983).
10. K. Garbett, C. E. Johnson, I. M. Klotz, K. Y. Okamura, and R. J. P. Williams, Arch. Biochem. Biophys., **142**, 574 (1971).

11. K. Garbett, D. W. Darnall, I. M. Klotz, and R. J. P. Williams, Arch. Biochem. Biophys., **135**, 419 (1969).

12. I. M. Klotz, T. A. Klotz, and H. A. Fiess, Arch. Biochem. Biophys., **68**, 284 (1957).

13. A. K. Shiemke, T. M. Loehr, and J. Sanders-Loehr, J. Am. Chem. Soc., in press (1985). Chapter 4 of this dissertation.

14. T. M. Loehr, W. E. Keyes, and P. A. Pincus, Anal. Biochem., **96**, 456 (1979).

15. A. K. Shiemke, T. M. Loehr, and J. Sanders-Loehr, J. Am. Chem. Soc., **106**, 4951 (1984). Chapter 3 of this dissertation.

16. E. I. Solomon, N. C. Eickman, R. R. Gay, K. W. Penfield, R. S. Himmelwright, and L. D. Loomis, in J. Lamy and J. Lamy, Eds., Invertebrate Oxygen Binding Proteins: Structure, Active Site and Function, Marcel Dekker, New York, 1981, pp. 487-502.

17. See Table 1, Chapter 1 of this dissertation.

18. R. M. Wing and K. P. Callahan, Inorg. Chem., **8**, 871 (1969).

19. G. Herzberg, Infrared and Raman Spectroscopy, p. 218, D. Van Nostrand, Princeton, 1945.

20. K. Bajdor, J. R. Kincaid, and K. Nakamoto, J. Am. Chem. Soc., **106**, 7741 (1984).

21. S. M. Freier, L. L. Duff, D. F. Shriver, and I. M. Klotz, Arch. Biochem. Biophys., **205**, 449 (1980).

22. (a) W. H. Armstrong, A. Spool, G. C. Papaefthymiou, R. B. Frankel, and S. J. Lippard, J. Am. Chem. Soc., **106**, 365 (1984). (b) A. Spool, I. D. Williams, and S. J. Lippard, Inorg. Chem., **24**, 2156 (1985).

23. S. Salama and T. G. Spiro, J. Am. Chem. Soc., **100**, 1105 (1978).

24. Y. Mathey, D. R. Greig, and D. F. Shriver, Inorg. Chem., **21**, 3409 (1982).

25. M. Cordes and J. L. Walter, Spectrochim. Acta **24A**, 237 (1967).

26. K. Nakamoto, Infrared Spectra of Inorganic and Coordination Compounds, 3rd ed., Wiley-Interscience, New York, 1978.

27. C. R. Cantor and P. R. Schimmel, Biophysical Chemistry, W. H. Freeman and Co., San Francisco, Vol. 3, pp. 1078-1081.

28. This was estimated from the difference in ΔH° determined from the tangents to the curve (Fig. 6a) at 278 and 90 K.

29. J. D. McCallum, M.S. Thesis, Portland State University, 1982.

30. P. C. Harrington and R. G. Wilkins, Biochemistry, **24**, 210 (1985).

31. Z. Bradic, P. C. Harrington, R. G. Wilkins, and G. Yoneda, Biochemistry, **19**, 4149 (1980).

32. P. C. Harrington and R. G. Wilkins, J. Am. Chem. Soc., **103**, 1550 (1981).

33. R. E. Stenkamp, personal communication.

34. L. L. Duff, G. L. Klippenstein, D. F. Shriver, and I. M. Klotz, Proc. Natl. Acad. Sci. USA, **78**, 4138 (1981).

FIGURE LEGENDS

Figure 1. Structures of the binuclear iron centers in azidomethemerythrin (a) and methemerythrin (b) based on x-ray crystallography of T. dyscrita proteins at 2.0 Å resolution (from Ref. 3b).

Figure 2. Difference electron density map of azidomethemerythrin minus methemerythrin in the oxo bridge-Fe_b-N(azide) plane. Solid contours denote positive density and dashed contours denote negative electron density. Positions of atoms are according to the 2.0 Å azidomethemerythrin map.

Figure 3. Resonance Raman spectra of P. gouldii methemerythrin at 278 K. Excitation at 363.8 nm, 20 mW at the sample, 90° scattering geometry, protein concentrations of 1.5-2.0 mM in monomer. Each spectrum represents the accumulation of 10-15 scans with a slit width of 7 cm^{-1} and scan rate of 0.5 cm^{-1}/sec. Isotopic composition of the bridge oxygen and solvent is listed to the right of each spectrum. Data have been submitted to a 17-point Savitsky-Golay smoothing routine.

Figure 4. Resonance Raman spectra of methemerythrin at 278 K with normal isotopic composition in the bridge (a), and ^{18}O-substituted bridge (b). Instrumental and sample conditions are as in Figure 3, except the scan rate was 2 cm^{-1}/sec. Residual peak at 755 cm^{-1} in (b) due to protein tryptophans.[15]

Figure 5. Resonance Raman spectra of methemerythrin at 90 K. Excitation at 406.7 nm, 15 mW at the sample, 180° scattering geometry, protein concentration of 7-10 mM in monomer. Each spectrum represents

the accumulation of 15-20 scans with a slit width of 7 cm^{-1} and scan rate of 1.0 cm^{-1}/sec. Isotopic composition of the bridge oxygen and solvent is listed to the right of each spectrum. Data have been submitted to a 17-point Savitsky-Golay smooth.

Figure 6. Van't Hoff plots for the protein conformational change of methemerythrin. The ratio of peak intensities (490:510 cm^{-1}) was determined by fitting spectra obtained at the different temperatures. A. Data obtained in Dewar at atmospheric pressure. Each data point represents the average of two separate determinations (average of 4 at 90 K). B. Data obtained in Displex at <30 μm pressure (see Chapter 2). Instrumental and sample conditions as in Figure 5. The difference between curves A and B may be due to the difference in pressure in the two experiments.

Figure 7. Proposed scheme for the interconversion and relative reactivities of the different conformations of methemerythrin.

Figure 8. Resonance Raman spectra of methemerythrin-perchlorate at 278 K (a and b), and at 90 K (c and d). Instrumental and sample conditions as in Figure 3 (a and b), or Figure 5 (c and d). Isotopic composition of the solvent is listed to the right of each spectrum.

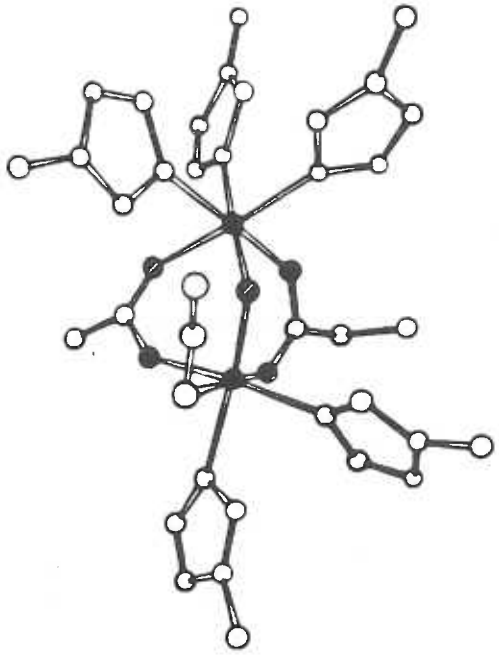

Azidomethemerythrin

a.

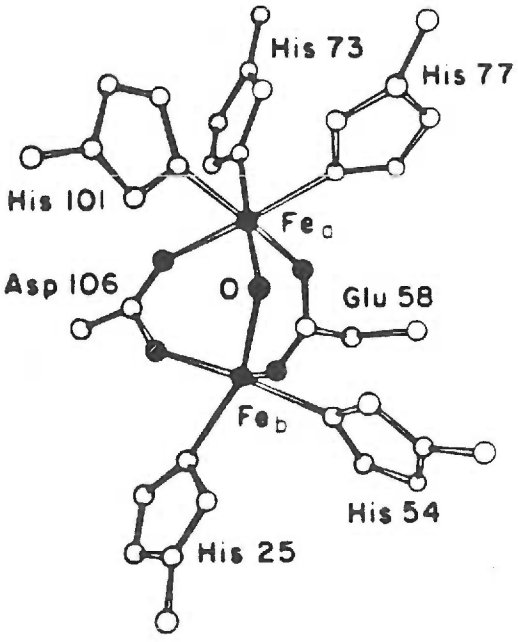

Methemerythrin

b.

FIGURE 1

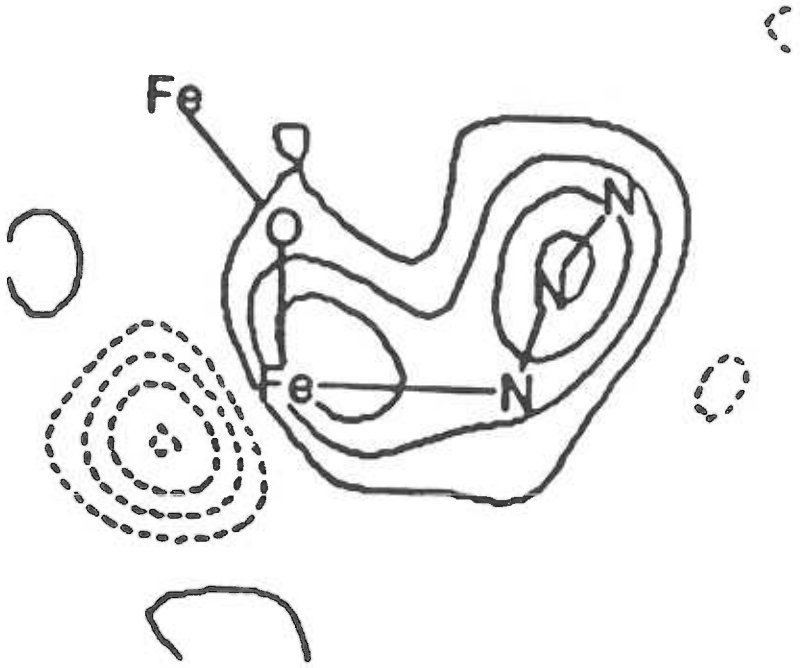

FIGURE 2

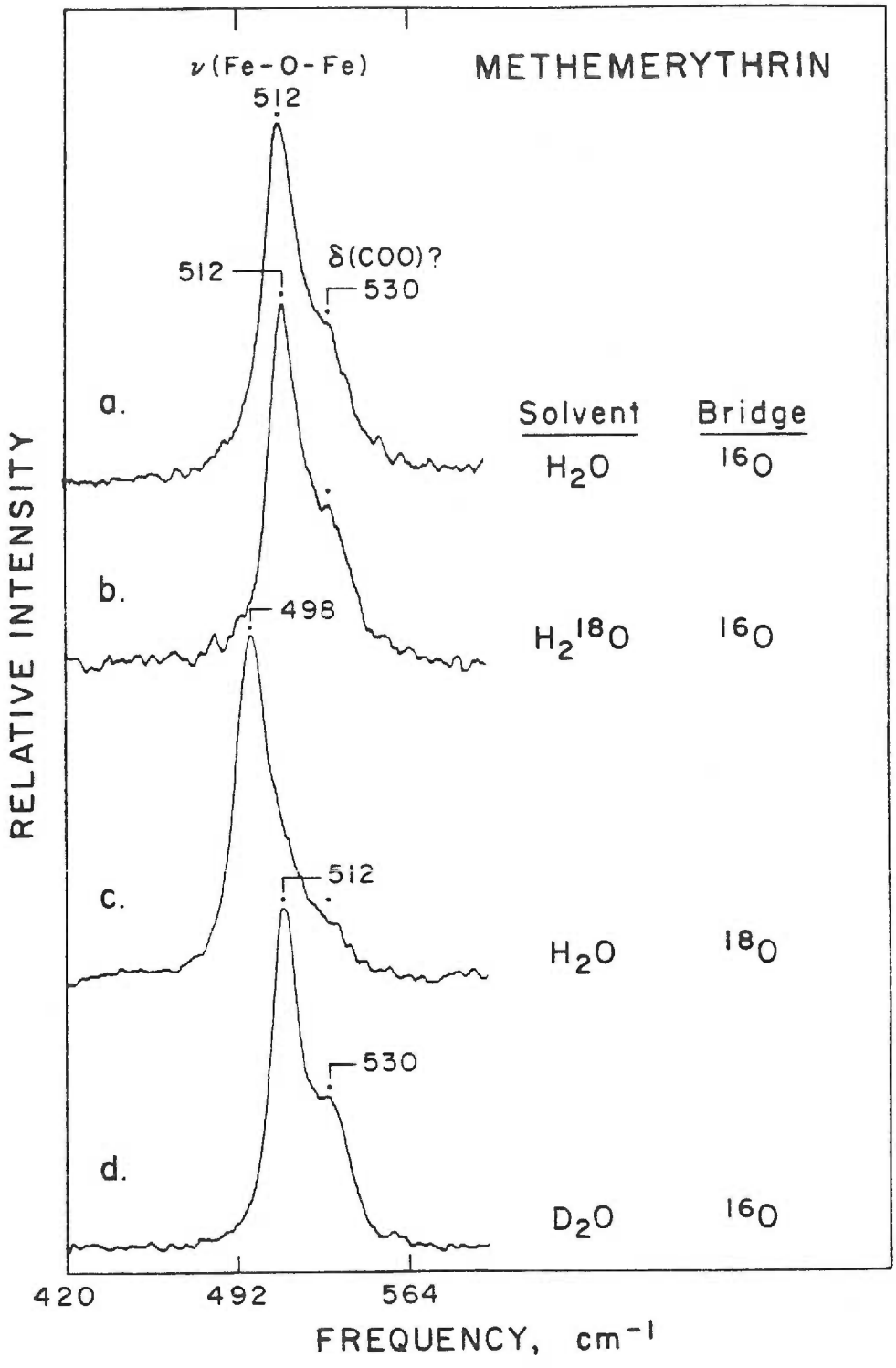
ν(Fe-O-Fe)
512
METHEMERYTHRIN
δ(COO)?
512
530
a.
Solvent
Bridge
H2O
16O
b.
498
H2 18O
16O
c.
512
H2O
18O
530
d.
D2O
16O
RELATIVE INTENSITY
420
492
564
FREQUENCY, cm-1

FIGURE 3

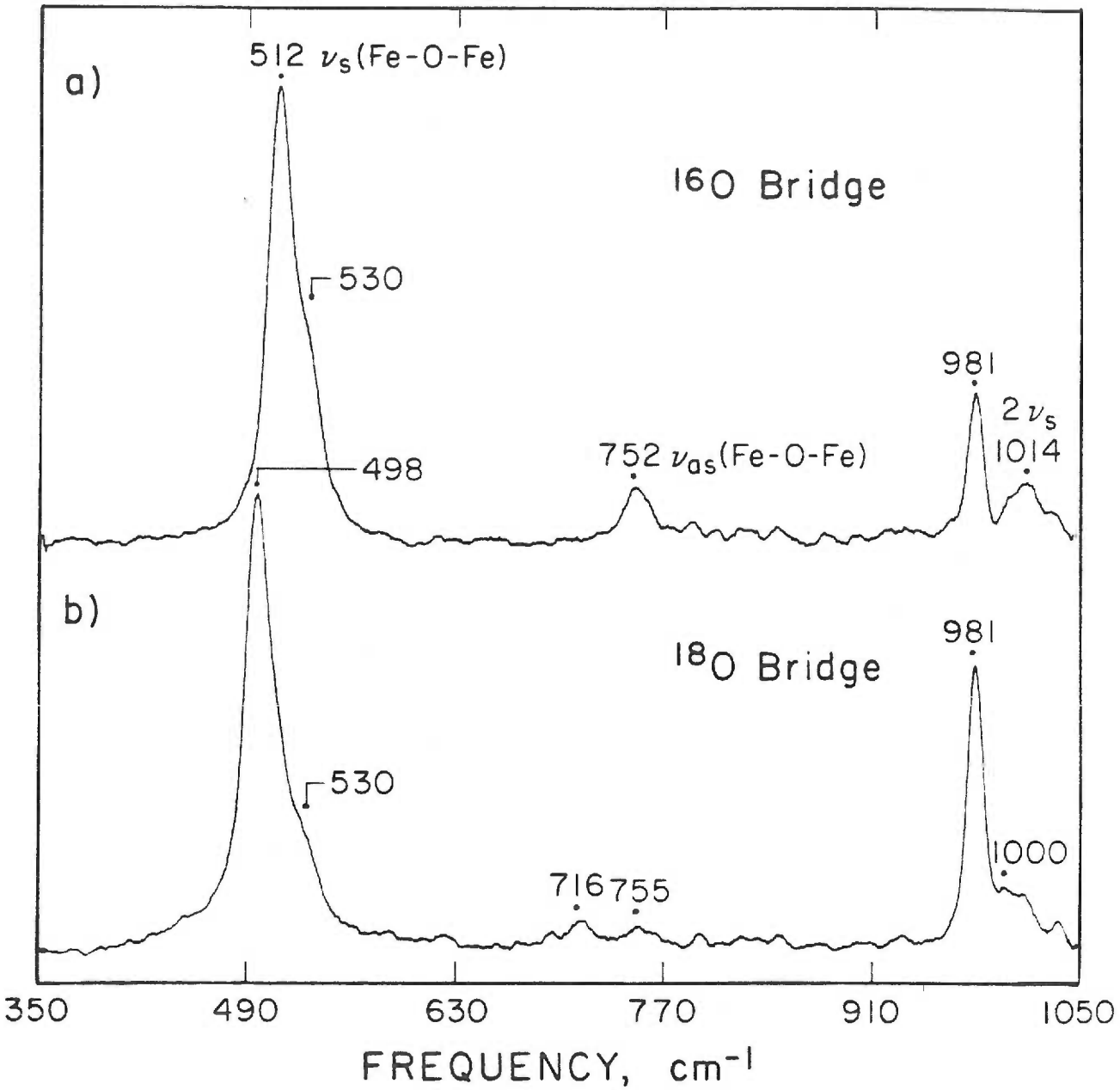
a)
512 ν_s(Fe-O-Fe)
^{16}O Bridge
530
498
752 ν_{as}(Fe-O-Fe)
981
2 ν_s
1014
b)
^{18}O Bridge
981
530
716
755
1000
350
490
630
770
910
1050
FREQUENCY, cm^{-1}

FIGURE 4

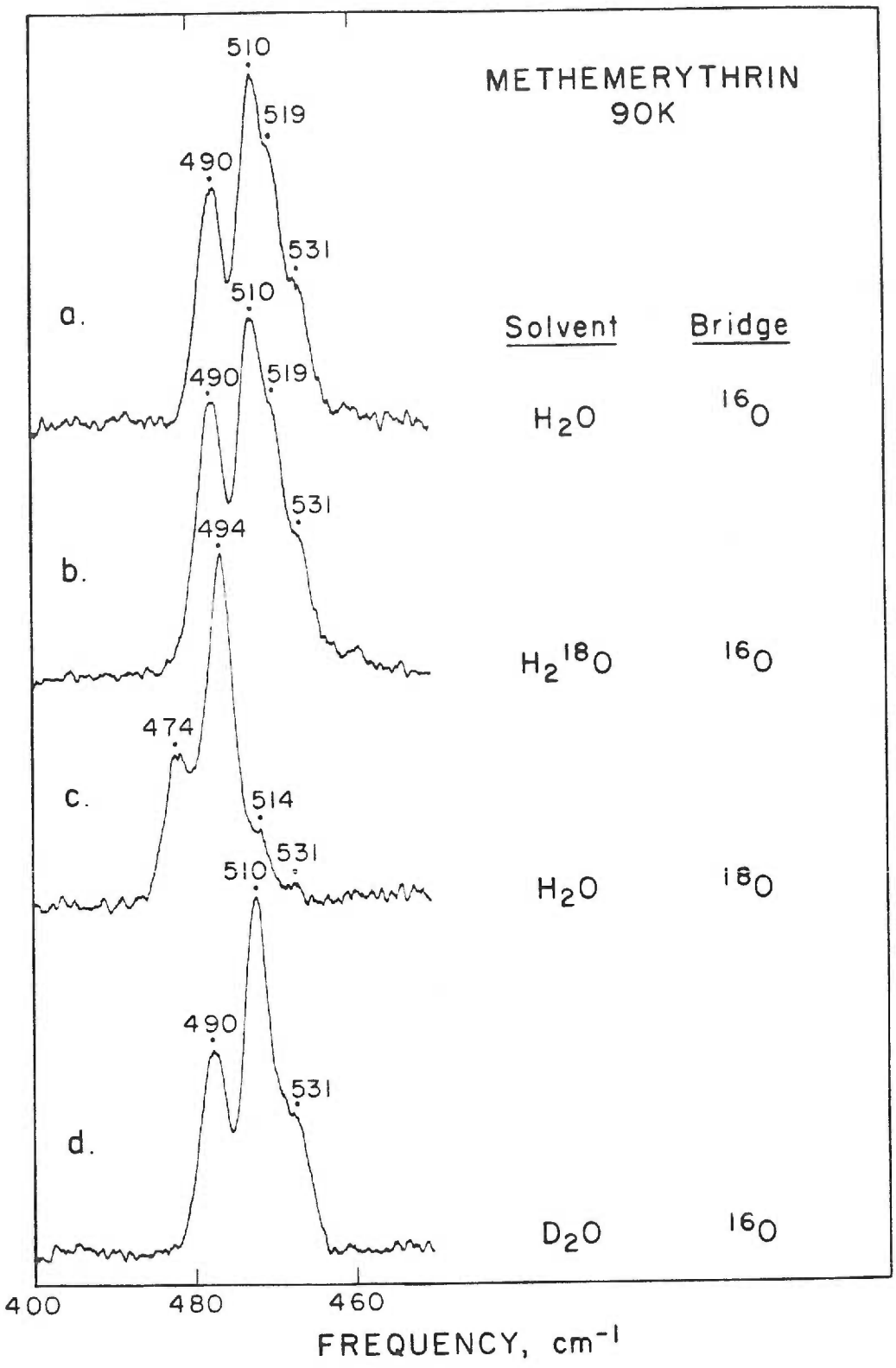
METHEMERYTHRIN
90K
Solvent
Bridge
a.
510
519
490
531
510
490
519
H2O
16O
b.
531
494
H2 18O
16O
474
c.
514
531
510
H2O
18O
490
d.
531
D2O
16O
400
480
460
FREQUENCY, cm-1

FIGURE 5

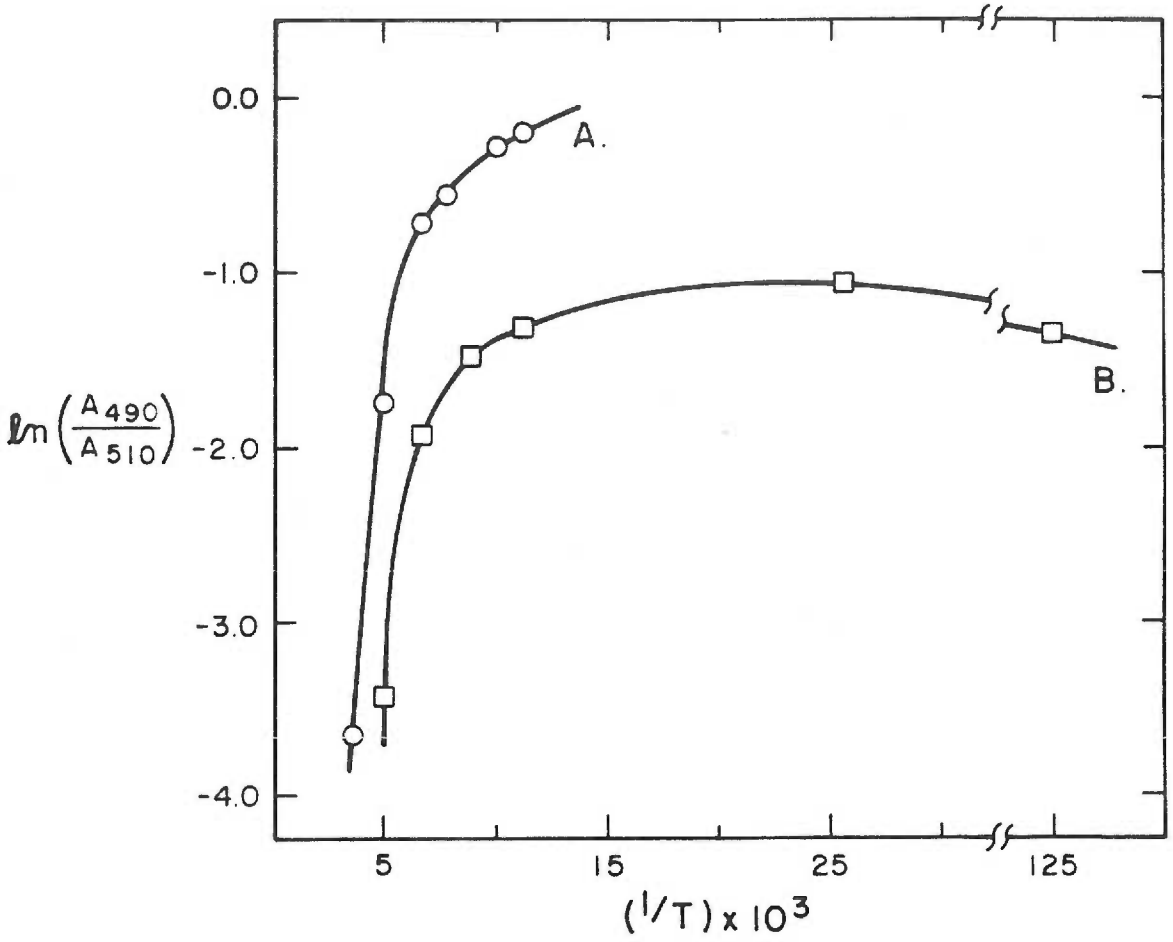

FIGURE 6

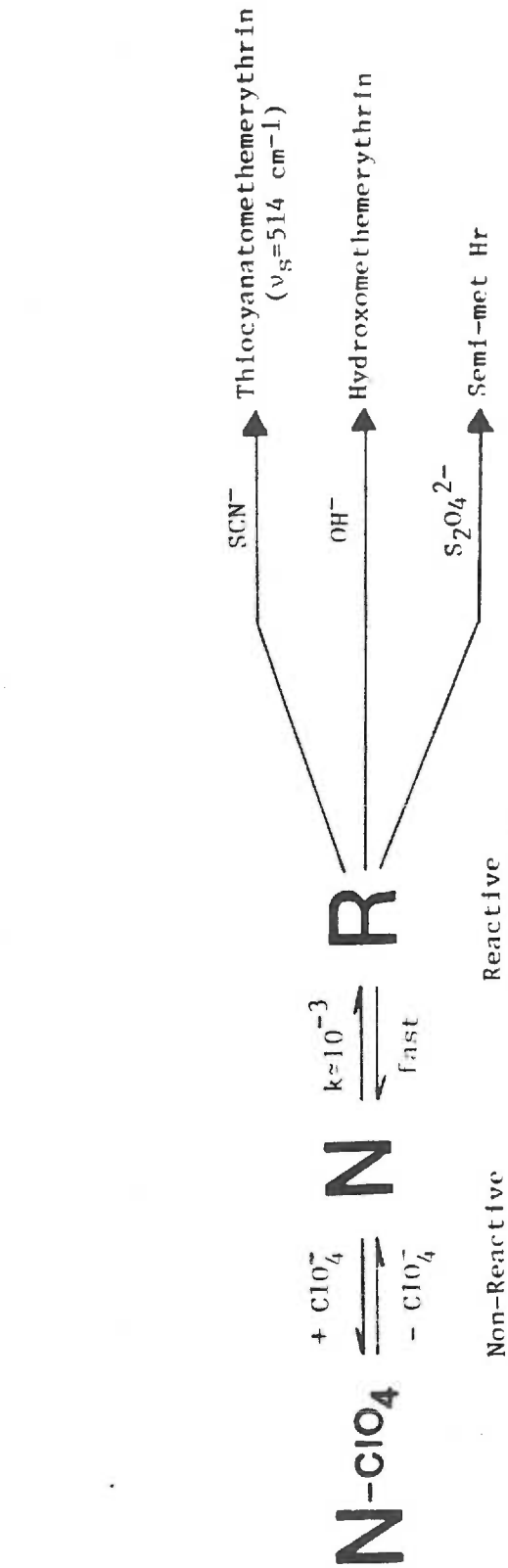
Thiocyanatomethemerythrin
(ν_s=514 cm^{-1})
Hydroxomethemerythrin
Semi-met Hr
SCN$^-$
OH$^-$
$S_2O_4^{2-}$
N-ClO$_4$
+ ClO$_4^-$
- ClO$_4^-$
N
k≈10^{-3}
fast
R
Non-Reactive
Conformation
(ν_s=510 cm^{-1})
Reactive
Conformation
(ν_s=490 cm^{-1})

FIGURE 7

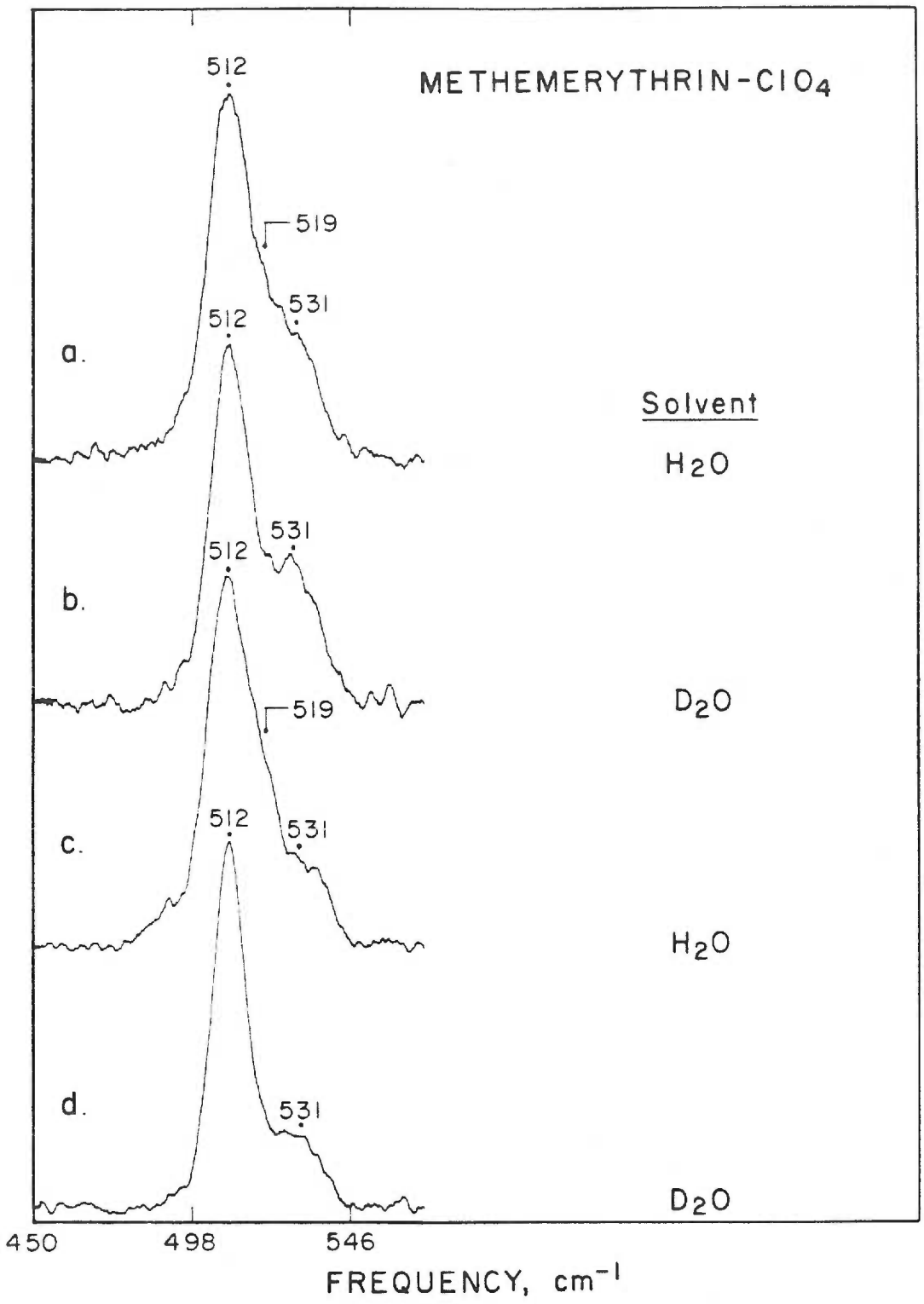
METHEMERYTHRIN-ClO4
512
519
531
a.
512
531
Solvent
H2O
512
531
b.
519
D2O
512
531
c.
H2O
531
d.
D2O
450
498
546
FREQUENCY, cm-1

FIGURE 8

Appendix I

Oxo Bridge Vibrations of Ligated Hemerytrins

At several points in the body of this thesis there are tables which summarize the vibrational fequencies of Fe-O-Fe vibrations (symmetric, asymmetric and bending modes) for many forms of hemerythrin. In most cases the effect of ^{18}O bridge substitution on these vibrations is also included in the table (see Table 1, chapter I; Table 1, chapter III; and Table 1, chapter IV). For many of these hemerythrin derivatives the spectra on which these tables are based have not been published. Those spectra are collected in this appendix.

In all the following figures the spectrum of the protein with normal isotopic composition of the bridge oxygen is shown on the bottom. Above that is shown the spectrum of the protein with the ^{18}O labeled bridge. The extent of incorporation of ^{18}O varies from 60 to 90% among these data, thus, in many cases the peaks due to residual Fe-^{16}O-Fe may be observed. The symmetric Fe-O-Fe vibrations occur between 486 and 516 cm^{-1} and are typically the strongest spectral features. The Fe-O-Fe deformation mode occurs at about 290 cm^{-1} (only observable in Figures 7-10) and is of moderate intensity. The asymmetric Fe-O-Fe vibration is a weak feature in all these spectra occuring between 750 and 785 cm^{-1}. In many cases the second overtone of the symmetric Fe-O-Fe stretch is observable as a weak feature near 1010 cm^{-1}. However this spectral region is often obscured by the strong 981 cm^{-1} peak of sulfate and a weaker peak near 1000 cm^{-1} due to tryptophan and phenylalanine side chains of the protein. The tryptophan side chains also contribute a weak peak near 750 cm^{-1} in many of these spectra. Other labeled peaks are due to exogenous ligand vibrations as listed in Table 3, chapter I. In the case of the cyanamidomethemerythrin spectra (Figure 9) the overtone of

the 382-cm^{-1} Fe-N stretch occurs near 750 cm^{-1}, further complicating this region of the spectrum. In Figure 8 a computer generated difference spectrum (^{18}O-^{16}O) is included to more clearly show the shift of the Fe-O-Fe deformation mode.

Figures 1-4 were obtained using the flow cell (Figure 6, chapter II) with sample temperature of 278 K and 363.8 nm excitation. Scan rates were 1.0 cm^{-1}/sec with a slit width of 8 cm^{-1}. The spectra represent accumulations of 12-20 scans and all data have been submitted to a 21-point Savitsky-Golay smoothing routine. The spectra in Figures 6 and 7 were obtained with 406.7 nm excitation on frozen samples at 90 K; other conditions as above. Conditions for the spectra in Figures 7, 9, and 10 are as in Figures 1-4 except 457.9 nm excitation was used. Spectra in Figure 8 were obtained on frozen samples at 90 K with 457.9 nm excitation and a 4 cm^{-1} slit width.

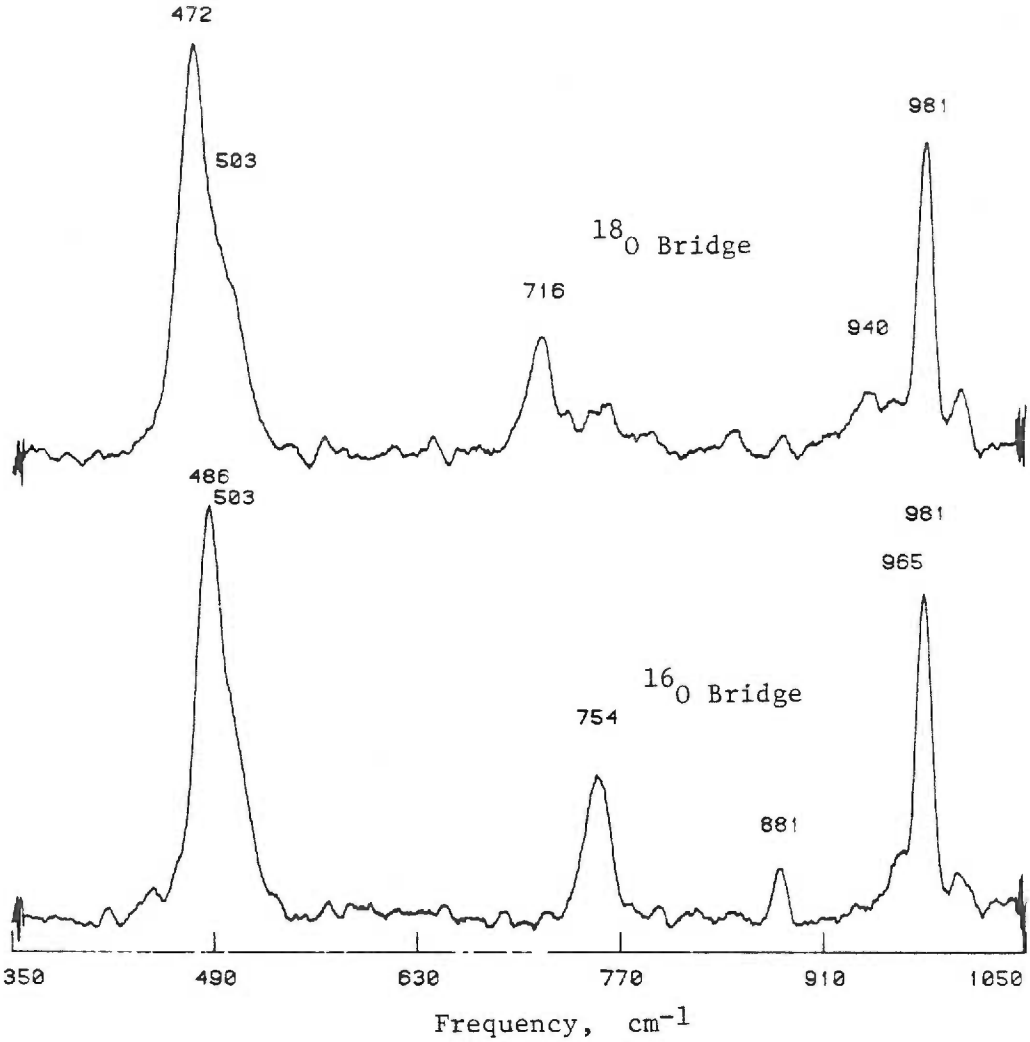

Figure 1. Oxyhemerythrin

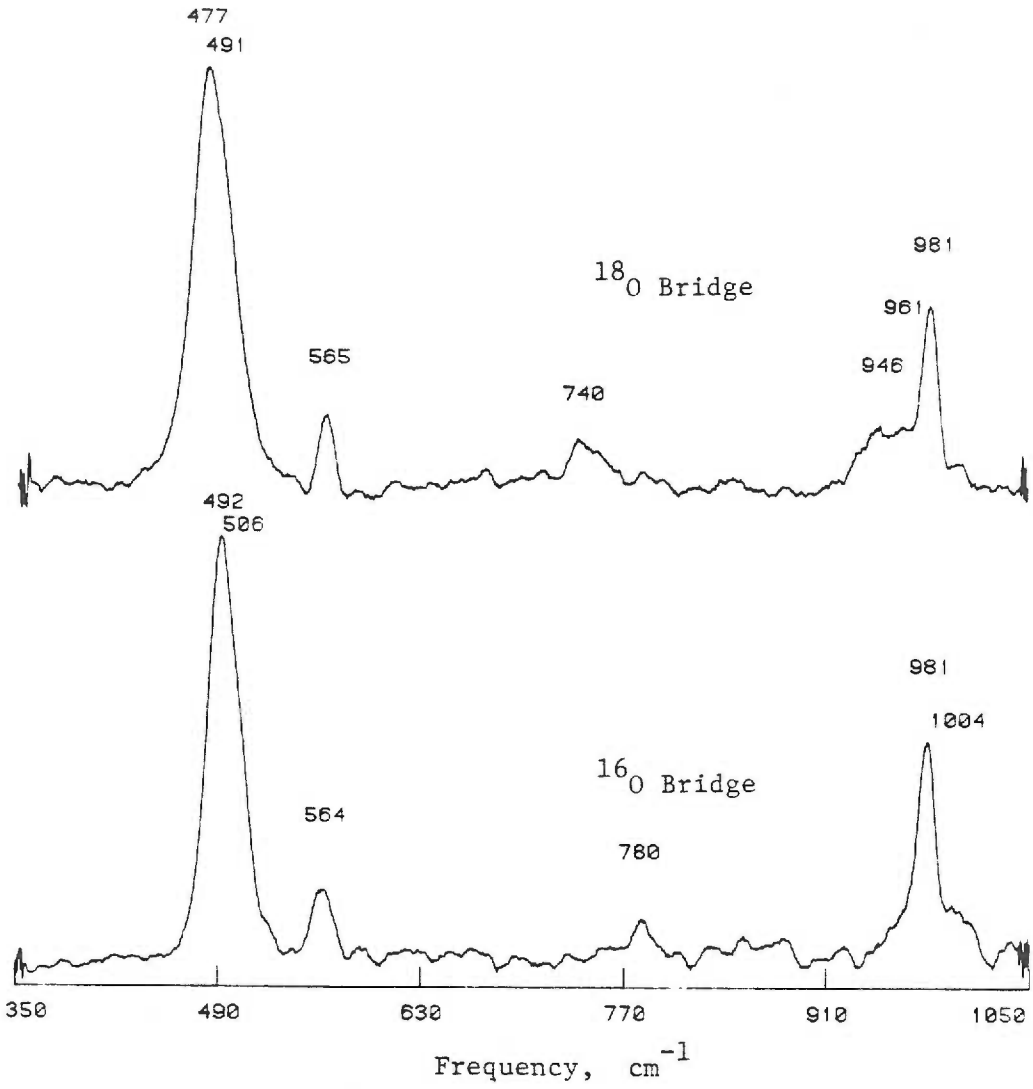

Figure 2. Hydroxomethemerythrin

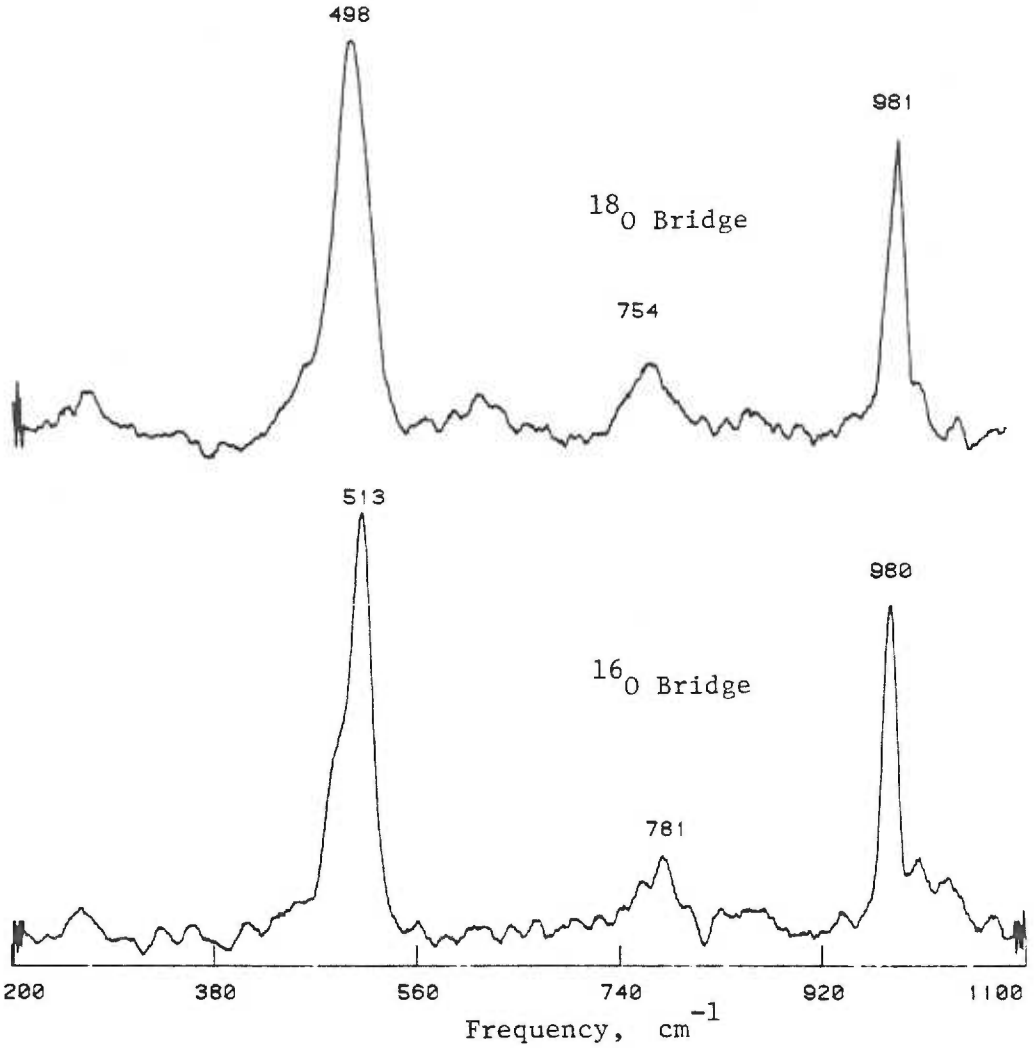

Figure 3. Cyanomethemerythrin

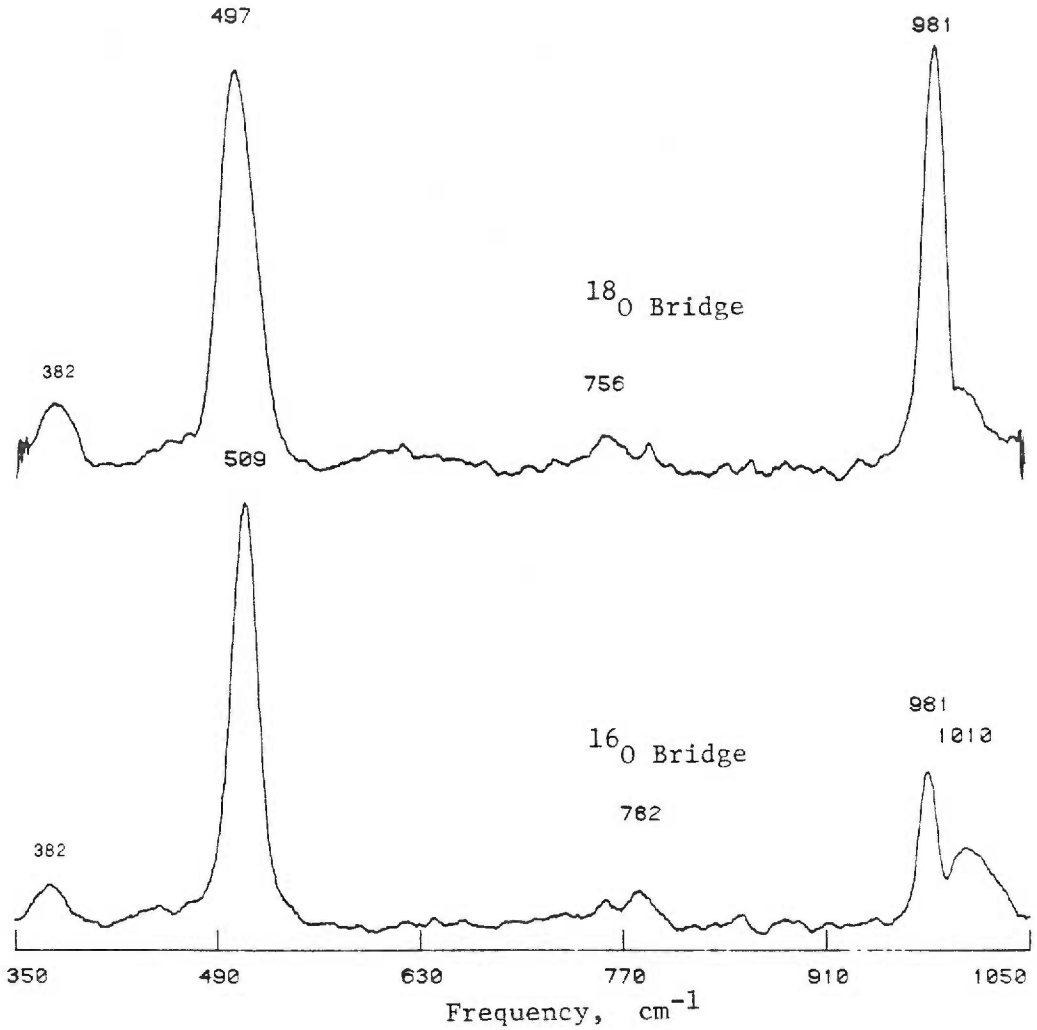

Figure 4. Cyanatomethemerythrin

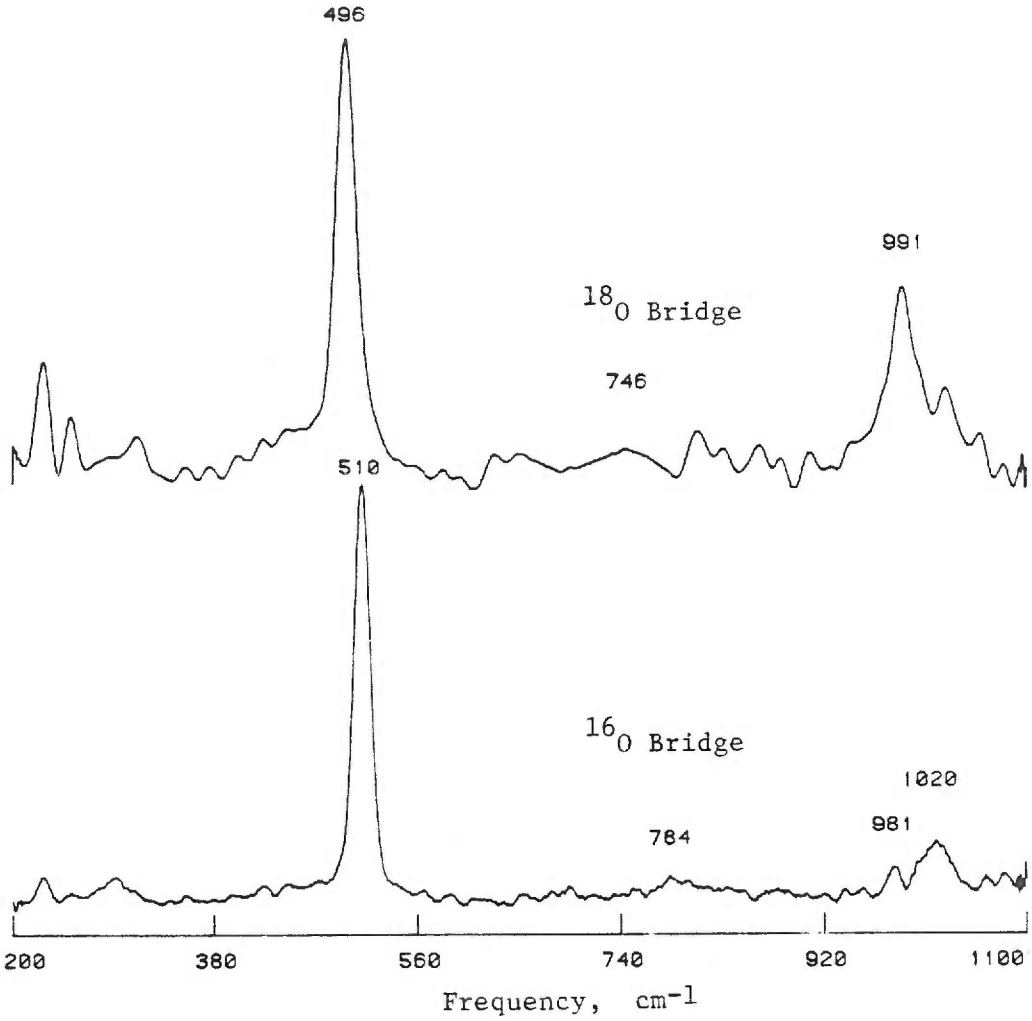

Figure 5. Chloromethemerythrin

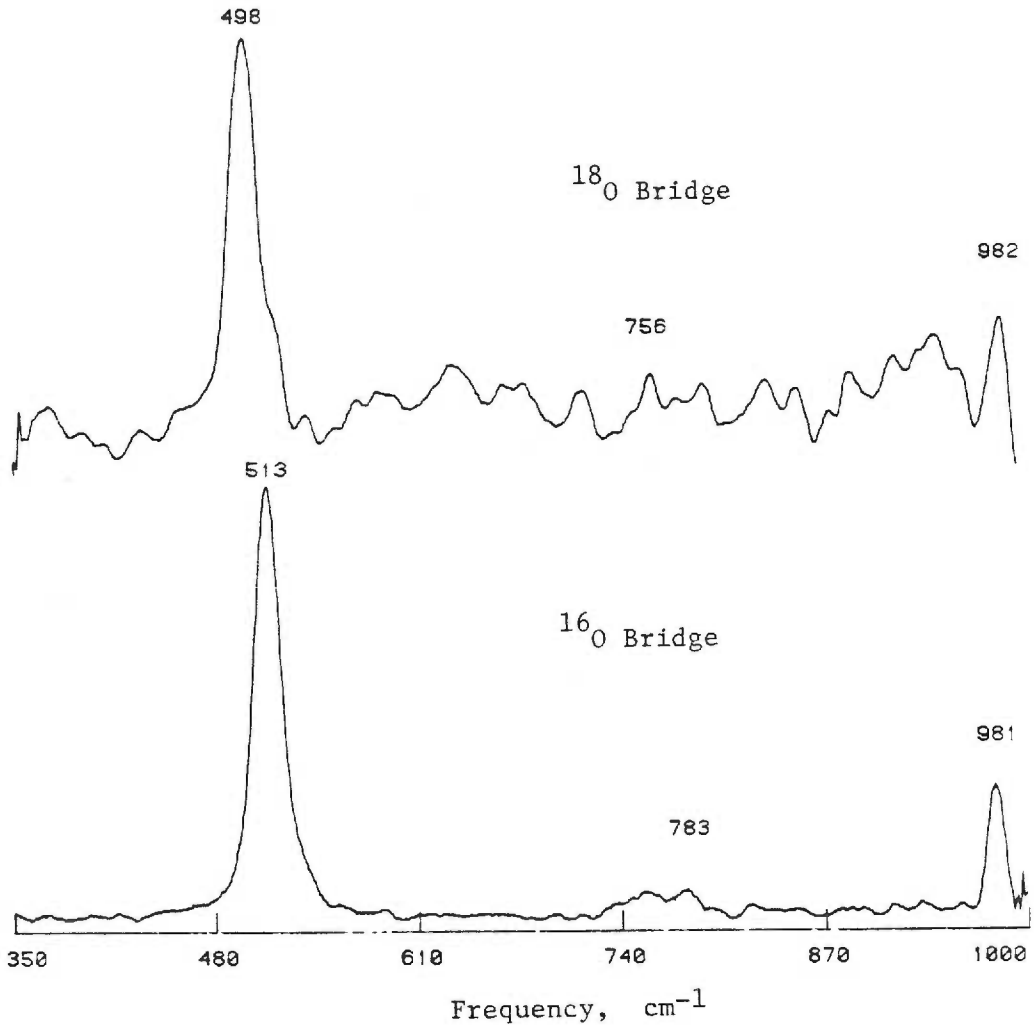

Figure 6. Formatomethemerythrin

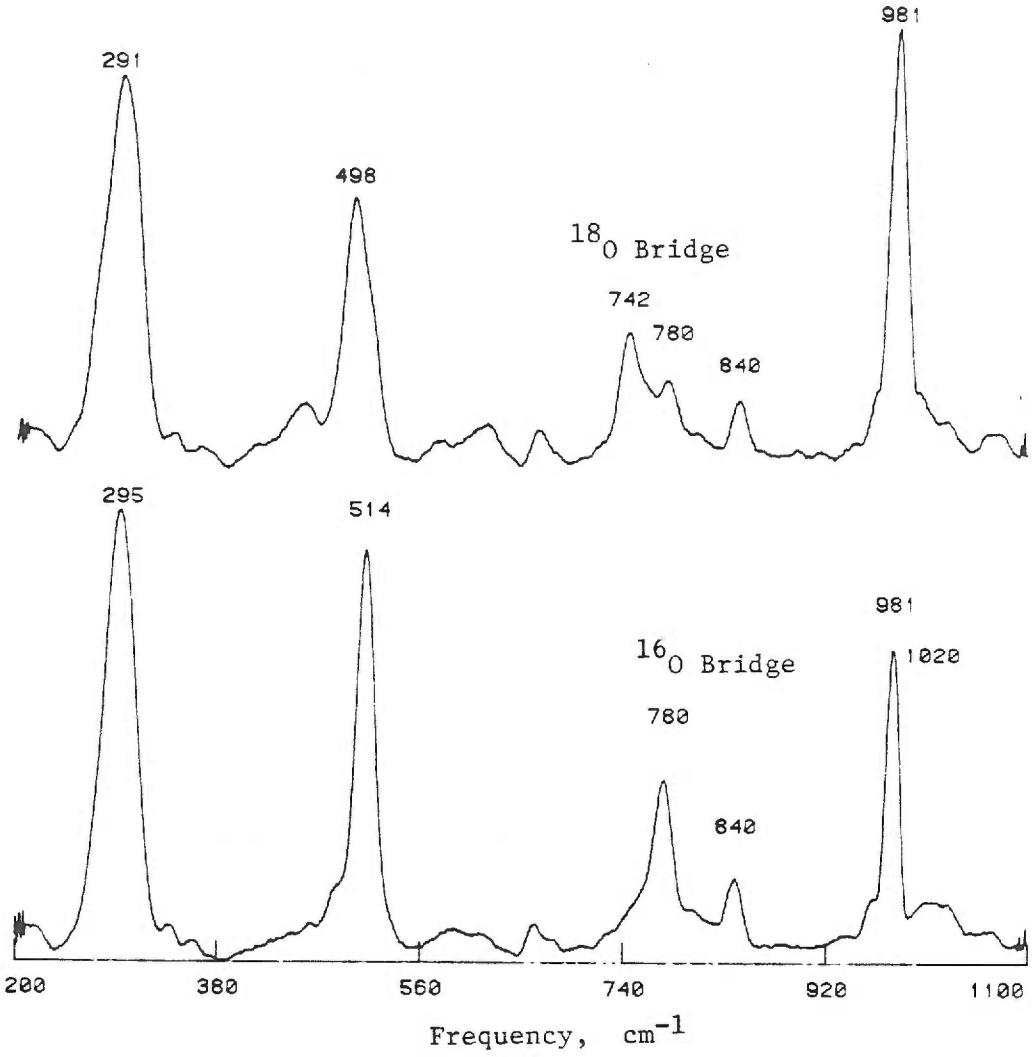

Figure 7. Thiocyanatomethemerythrin

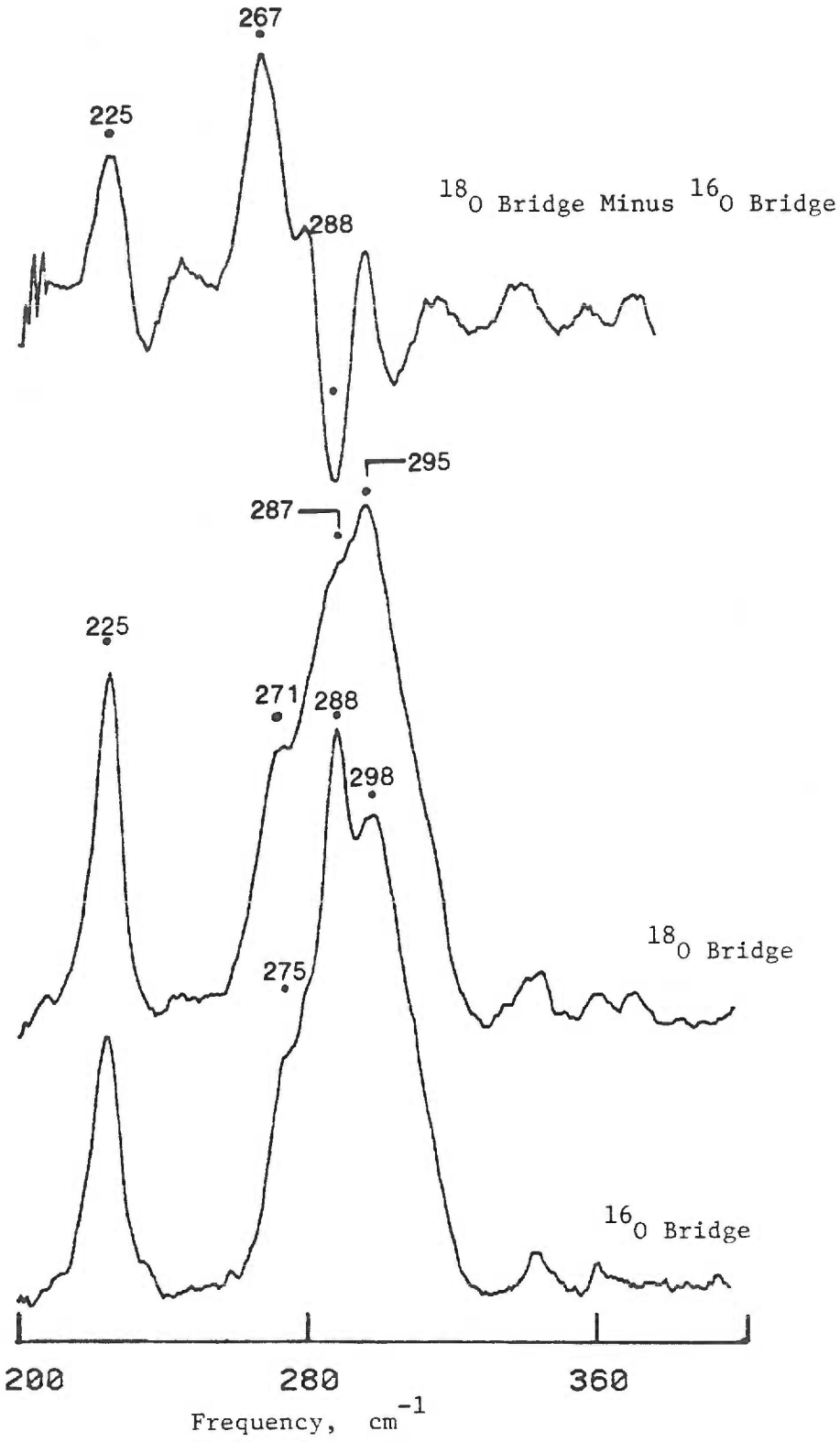

Figure 8. Thiocyanatomethemerythrin

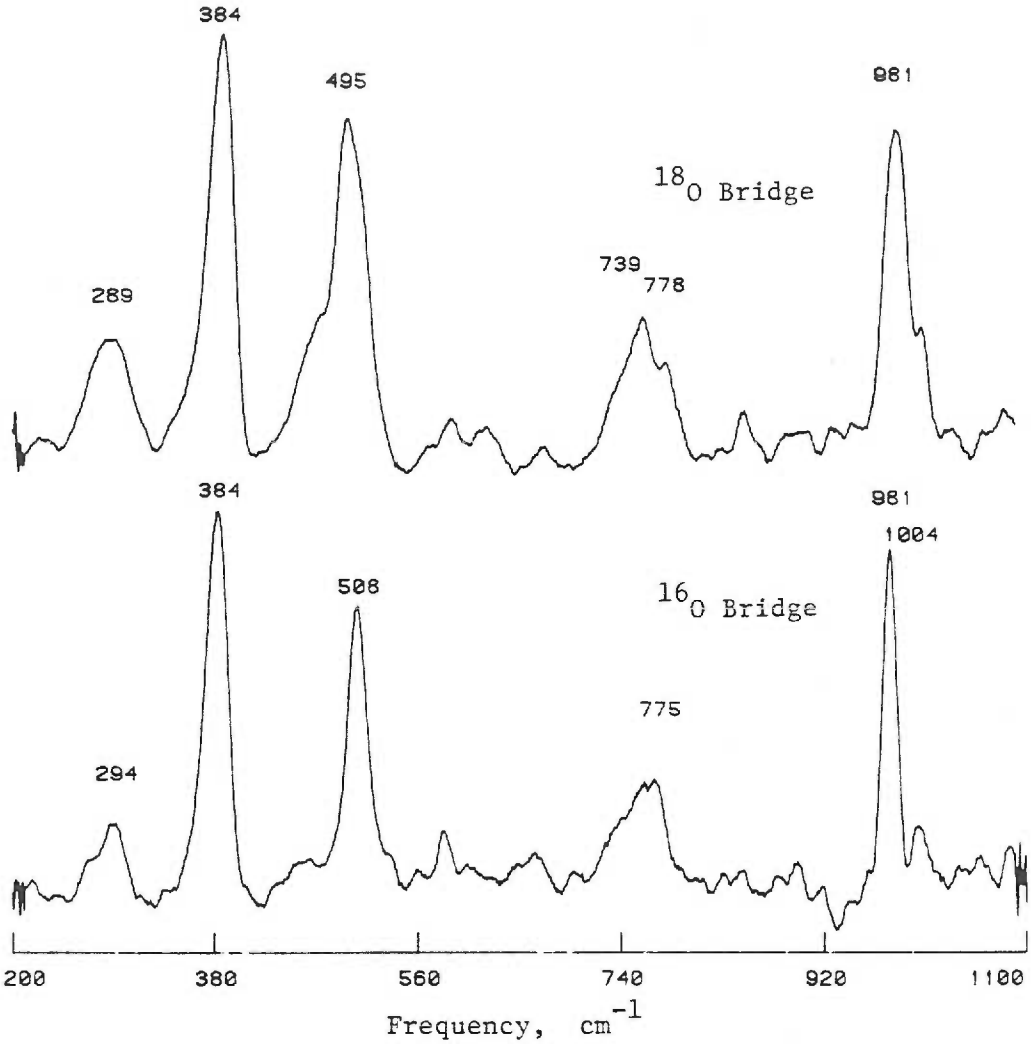

Figure 9. Cyanamidomethemerythrin

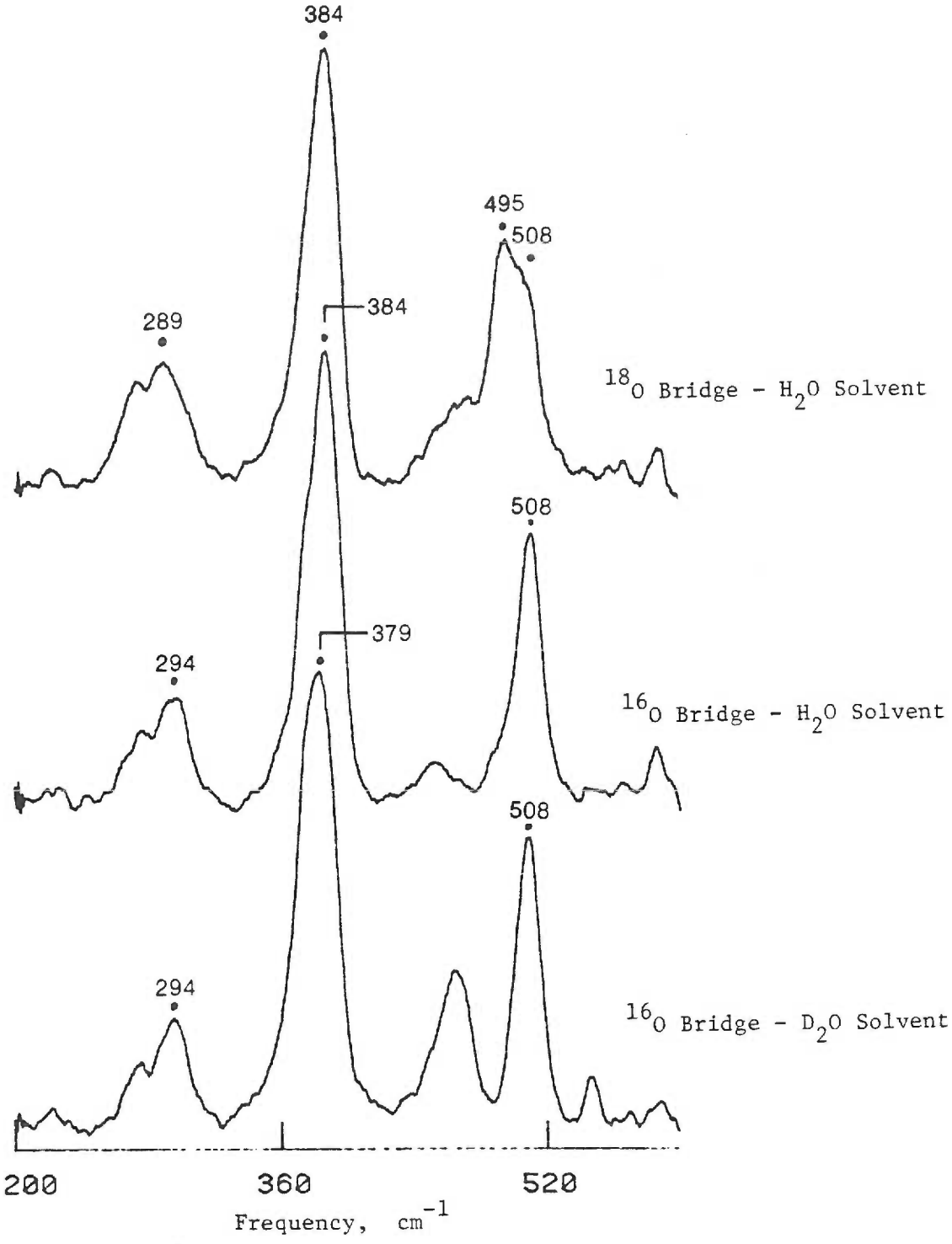

Figure 10. Cyanamidomethemerythrin

BIOGRAPHICAL NOTE

The author was born March 6, 1958 in Detroit, Michigan, the second child and first son of Andrew John and Gertrude Helen Shiemke. He attended Adlai Stevenson high school in Sterling Heights, Michigan, where he won varsity letters in football and basketball, and acquired a reputation for intellectual and athletic abilities, as well as the ability to consume massive amounts of beer. Directly after high school graduation the author entered Kalamazoo College. He majored in chemistry, receiving a B.A. in June, 1980. Highlights of his college career include intramural softball and basketball championships, honors on his Senior Thesis, and three months spent in Hannover, West Germany where he developed a taste for European beer. Nine months of indentured servitude in the immunology department of the Wayne State University Medical School followed graduation from Kalamazoo College. Besides murdering mice at Wayne State University, the author met Kim Kathleen Martin, whom he eventually married on August 27, 1983. The author entered the Oregon Graduate Center in September, 1981, promptly becoming the first baseman on the school softball team. Besides chapters 1, 3, and 4 of this thesis the authors other publications include:

"The Synthesis, Redox Properties and Ligand Binding Of Heterobinuclear Transition-Metal Macrocyclic Ligand Complexes. Measurement of an Apparent Delocalization Energy in a Mixed Valent Cu(I)-Cu(II) Complex." R. R. Gagne, C. L. Spiro, T. J. Smith, C. A. Hamann, W. R. Thies, and A. K. Shiemke. 1981, J. Am. Chem. Soc. **103**, 4073-4081.

"Resonance Raman Spectroscopic Characterization of the Nickel Cofactor F-430, from Methanogenic Bacteria." Andrew K. Shiemke, L. Dudley Eirich, and Thomas M. Loehr. 1983, Biochim. Biophys. Acta **748**, 143-149.

"Hydroxide Ion Binding to Methemerythrin. An Investigation by Resonance Raman and Difference Spectroscopy." John D. McCallum, Andrew K. Shiemke, and Joann Sanders-Loehr. 1984, Biochemistry **23**, 2819.

"Sulfide Bridged Derivatives of the Binuclear Iron Site of Hemerythrin at Both Met and Semi-Met Oxidation Levels." Gudrun S. Lukat, Donald M. Kurtz, Andrew K. Shiemke, Thomas M. Loehr, and Joann Sanders-Loehr. 1984, Biochemistry **23**, 6416.